

TECHNISCHE UNIVERSITÄT MÜNCHEN

Lehrstuhl für Grundwasserökologie

Pathway dependent isotope fractionation in triazine degradation

Armin Meyer

Vollständiger Abdruck der von der Fakultät Wissenschaftszentrum Weihenstephan für Ernährung, Landnutzung und Umwelt der Technischen Universität München zur Erlangung des akademischen Grades eines

Doktors der Naturwissenschaften

genehmigten Dissertation.

Vorsitzender:

Univ.-Prof. Dr. J. Schnyder

Prüfer der Dissertation:

1. Univ.-Prof. Dr. R. Meckenstock
2. Prof. Dr. P. Paneth
(Technical University of Lodz, Poland)
3. Univ.-Prof. Dr. R. Niessner

Die Dissertation wurde am 08.02.2010 bei der Technischen Universität München eingereicht und durch die Fakultät Wissenschaftszentrum Weihenstephan für Ernährung, Landnutzung und Umwelt am 29.06.2010 angenommen.

Summary

Atrazine, a triazine herbicide, has been used worldwide to control growth of annual grass and broadleaf weeds during crop production. Even after the use of atrazine was discontinued in many countries, atrazine and its metabolites have still been frequently detected in aquifers posing a potential hazard to aquatic ecosystems and human life. Over the last two decades, the fate of atrazine in the environment has therefore been of considerable environmental concern. Adequate assessments are made difficult by the fact that metabolites of the two main degradative processes – oxidative dealkylation and hydrolysis – show a different behaviour in the subsurface matrix. The mobile, and still herbicidal products desethylatrazine and desisopropylatrazine are frequently detected alongside with atrazine in groundwater, whereas the non herbicidal hydroxyatrazine tends to form bound residues to the soil matrix. Current analytical methods which rely on metabolite analysis, therefore, pick up only part of the degradative processes. On the other hand, a decrease in atrazine concentrations alone is not proof that real elimination is going on, since besides degradation, also physical processes like sorption or dilution lead to decreasing concentrations.

The need for new analytical approaches for a better risk assessment of atrazine in the environment motivated this work to assess for the first time the potential of compound specific isotope analysis (CSIA) to provide additional lines of evidence. Our goal was to measure carbon and nitrogen isotope fractionation associated with the different biotransformation reactions of this compound, to evaluate whether this approach can be used as an alternative way of qualitatively detecting, and possibly even quantitatively determining natural atrazine degradation, and to use the stable isotope fractionation, in combination with metabolite analysis to probe for underlying biochemical transformation mechanisms.

Chapter 2 developed and validated CSIA by GC-IRMS (gas chromatography isotope ratio mass spectrometry) for carbon and nitrogen isotope analysis of atrazine. Combustion was tested with reactors containing (i) CuO/NiO/Pt operating at 940°C; (ii) CuO operating at 800°C; (iii) Ni/NiO operating at 1150°C and being reoxidized for 2 minutes during each gas chromatographic run. Accurate and precise carbon isotope measurements were only obtained with Ni/NiO reactors giving a mean deviation $\Delta\delta^{13}\text{C}$ from dual inlet measurements of -0.1‰ to 0.2‰ and a standard deviation (s.d.) of $\pm 0.4\%$. CuO at 800°C gave precise, but inaccurate values ($\Delta\delta^{13}\text{C} = -1.3\%$, s.d. $\pm 0.4\%$), whereas commercial CuO/NiO/Pt reactors operated at the recommended temperature of 940°C gave inaccurate and imprecise data. Accurate ($\Delta\delta^{15}\text{N} = 0.2\%$) and precise (s.d. $\pm 0.3\%$) nitrogen isotope analysis was accomplished with a Ni/NiO-reactor previously used for carbon isotope analysis. The applicability of the method was demonstrated for alkaline hydrolysis of atrazine at 20°C and pH 12 (nucleophilic aromatic substitution) giving $\epsilon_{\text{carbon}} = -5.6\% \pm 0.1\%$ (s.d.) and $\epsilon_{\text{nitrogen}} = -1.2\% \pm 0.1\%$ (s.d.).

Chapter 3 reports significant C and N isotope fractionation of atrazine in transformation to hydroxyatrazine by *Chelatobacter heintzii*, *Pseudomonas* sp. ADP, and *Arthrobacter aurescens* TC1 highlighting an alternative approach for detecting this natural transformation pathway. Indistinguishable dual isotope slopes Δ for *Chelatobacter heintzii* (-0.65 ± 0.08) and *Arthrobacter aurescens* TC1 (-0.61 ± 0.02) suggest the same biochemical transformation mechanism despite different hydrolyzing enzymes (AtzA versus TrzN). With *Pseudomonas* sp. ADP (also AtzA) significantly smaller fractionation indicates masking effects by steps prior to enzyme catalysis, while a distinguishable $\Delta = -0.32 \pm 0.06$ suggests that some of these steps showed slight isotope fractionation. Abiotic reference experiments reproduced the pattern of biotic transformation at pH 3 (enrichment of ^{13}C , depletion of ^{15}N in atrazine), but showed enrichment of both ^{13}C and ^{15}N at pH 12. This indicates that the organisms activated atrazine by a similar Lewis acid complexation (e.g., with H^+) prior to nucleophilic aromatic substitution, giving the first detailed mechanistic insight into this important enzymatic reaction.

In chapter 4 CSIA was used to investigate the alternative biotic degradation pathway of atrazine and simazine, leading to the formation of the dealkylated metabolites desethyl- and desisopropylatrazine. Degradation experiments with the model organism *Rhodococcus* sp. NI86/21 led to a significant enrichment of ^{13}C and ^{15}N , reflected by the enrichment factors of $\epsilon_{\text{carbon}} = -4.0\text{‰} \pm 0.2\text{‰}$ and $\epsilon_{\text{nitrogen}} = -1.4\text{‰} \pm 0.3\text{‰}$ for atrazine and $\epsilon_{\text{carbon}} = -4.0\text{‰} \pm 0.2\text{‰}$ and $\epsilon_{\text{nitrogen}} = -1.9\text{‰} \pm 0.3\text{‰}$ for simazine. Slopes of dual isotope plots ($\Delta = 0.36 \pm 0.06$) were significantly different from the slopes obtained for biotic hydrolysis (see chapter 3) demonstrating that CSIA can indeed be a valuable tool to identify the oxidative desalkylation pathway of triazines. In addition, stable isotope fractionation was used in combination with analysis of metabolites by LC-MS/MS (liquid chromatography - tandem mass spectrometry) for mechanistic elucidation. Previous studies reported that oxidative transformation by *Rhodococcus* sp. NI86/21 is catalysed by a cytochrome P450 system. Single electron transfer (SET) and H atom abstraction (HAT) are debated as alternative mechanisms for this reaction. SET involves the nitrogen atom so that pronounced N isotope fractionation and selective oxidation in α -position are expected. Experiments were also conducted with permanganate as abiotic reference oxidant which is highly selective and gives rise to C, but not to N isotope fractionation. Biodegradation with *Rhodococcus* sp. NI86/21 showed that metabolites were oxidized in α - and β -position of the alkyl side chain demonstrating that oxidation was not selective and suggesting an unselective H atom abstraction. On the other hand, significant N isotope fractionation demonstrates that bond changes at the N atom were involved suggesting an initial SET. The combined results therefore indicate that oxidation by *Rhodococcus* sp. NI86/21 involved both SET as well as HAT. This surprising result demonstrates the power of dual isotope fractionation (C and N) not only to detect natural transformation pathways, but also for mechanistic studies in biochemistry.

Zusammenfassung

Das Triazinherbizid Atrazin wird und wurde weltweit in großem Maßstab in der Landwirtschaft eingesetzt, um den Unkrautbewuchs in der landwirtschaftlichen Produktion unter Kontrolle zu halten. In den Jahren der Anwendung und auch danach wurden Atrazin und seine Abbauprodukte häufig in Aquiferen detektiert und stellen deshalb sowohl eine Gefahr für aquatische Ökosysteme als auch für den Menschen dar. Aus diesem Grund rückte das Prozessverständnis bzgl. des Verhaltens von Atrazin in der Umwelt in den letzten beiden Jahrzehnten immer mehr in den Fokus der Umweltwissenschaften. Eine umfassende Risikoabschätzung gestaltet sich jedoch noch immer schwierig, da die Metaboliten der beiden wichtigsten Abbauewege (oxidative Dealkylierung und Hydrolyse) ein unterschiedliches Verhalten in der Bodenmatrix zeigen. Während die mobilen und immer noch herbizidal wirksamen Abbauprodukte Desethylatrazin und Desisopropylatrazin oft zusammen mit Atrazin im Grundwasser nachgewiesen werden, wird das nicht herbizidale Hydroxyatrazin verstärkt im Boden sorbiert und kann dort durch so genannte „bound residues“ immobilisiert werden. Mit den momentan eingesetzten analytischen Methoden, die auf dem Nachweis von Atrazin und seinen Metaboliten basieren, können nur bedingt Abbauprozesse erfasst werden. Ein Hauptgrund ist, dass die Messung von Schadstoffkonzentrationen allein keinen Aufschluss darüber geben, ob tatsächlich eine Eliminierung stattfindet, da neben Abbau auch physikalische Prozesse, wie Adsorption oder Verdünnung zu abnehmenden Konzentrationen führen können.

Die Notwendigkeit einer neuen analytischen Herangehensweise zum Zwecke einer besseren Risikoabschätzung für Atrazin in der Umwelt, motivierte diese Arbeit erstmals das Potential substanzspezifische Isotopenanalytik (CSIA), als zusätzliches Nachweisverfahren, abzuschätzen. Ziel dabei war, die Kohlenstoff- und Stickstoffisotopenfraktionierung von Atrazin in Folge von verschiedenen biotischen Abbauprozessen zu analysieren und zu evaluieren, ob dieser Ansatz eine Alternative darstellt, um Abbau von Atrazin im Feld, sowohl qualitativ als auch, wenn möglich, quantitativ bestimmen zu können. Des Weiteren sollte in Kombination mit Metabolitenaufklärung Einblicke in unterliegende biochemische Transformationsmechanismen gewonnen werden.

Im zweiten Kapitel dieser Arbeit wurde CSIA unter der Benutzung von GC-IRMS (Gaschromatographie Isotopenverhältnis-Massenspektrometrie) für die Kohlenstoff- und Stickstoffisotopenanalyse von Atrazin entwickelt und validiert. Für die Isotopenanalytik von Kohlenstoff wurden verschiedene Verbrennungsreaktoren getestet. Diese Reaktoren enthielten entweder (i) CuO/NiO/Pt (Betriebstemperatur: 940 °C), (ii) CuO (Betriebstemperatur 800°C) oder (iii) Ni/NiO (Betriebstemperatur: 1150°C, 2 Minuten oxidative Regeneration während jeder analytischer Messung) als Reaktanden. Akkurate und präzise Kohlenstoffisotopenmessungen wurden im Vergleich zu Dual-inlet-Messungen nur für Ni/NiO-Reaktoren erhalten. Sie zeigten im Vergleich zu Dual-inlet-Messungen eine mittlere Abweichung $\Delta\delta^{13}\text{C}$ von $-0.1 - 0.2 \text{ ‰}$ und einer Standardabweichung (SD) von $\pm 0.4\%$. Messungen mit

CuO-Reaktoren bei 800°C ergaben zwar ähnlich präzise Werte (SD: $\pm 0.4\%$), waren aber durchschnittlich um -1.3% vom richtigen Wert entfernt. Messungen mit CuO/NiO/Pt-Reaktoren produzierten sowohl unpräzise als auch unrichtige Werte. Für die substanz-spezifische Stickstoffisotopenanalytik von Atrazin, wurden Ni/NiO-Reaktoren eingesetzt, die bereits für die Analyse der Kohlenstoffisotope genutzt worden waren. Mit einer mittleren Abweichung von $\Delta\delta^{15}\text{N} = 0.2\%$ und einer Präzision von $\pm 0.3\%$ zeigte sich auch dieser Ansatz als robust und zuverlässig. Die erfolgreiche Anwendbarkeit der Methode wurde in einem alkalischen Hydrolyseversuch bei $T = 20^\circ\text{C}$ und pH 12 (nukleophile aromatische Substitution) demonstriert. Es wurden dabei Anreicherungsfaktoren von $\epsilon_{\text{carbon}} = -5.6\% \pm 0.1\%$ (s.d.) und $\epsilon_{\text{nitrogen}} = -1.2\% \pm 0.1\%$ (s.d.) bestimmt.

Das dritte Kapitel zeigt, dass signifikante Isotopenfraktionierung in C und N des Atrazines während der Transformation zu Hydroxyatrazin durch *Chelatobacter heintzii*, *Pseudomonas* sp. ADP und *Arthrobacter aurescens* TC1 eine vielversprechende Alternative darstellt, um diesen natürlichen Abbauweg nachzuweisen. Gleiche Steigungen Δ in den zweidimensionalen Isotopenplots von Kohlenstoff und Stickstoff zeigen an, dass der Reaktionsmechanismus, der zur Transformation von Atrazin führt, für *Chelatobacter heintzii* ($\Delta = -0.65 \pm 0.08$) und für *Arthrobacter aurescens* TC1 wahrscheinlich identisch ist, obwohl beide Mikroorganismen mit unterschiedlichen hydrolysierenden Enzymen (AtzA versus TrzN) ausgestattet sind. *Pseudomonas* sp. ADP (auch AtzA) zeigte insgesamt eine signifikant schwächer ausgeprägte Fraktionierung, was darauf hindeutet, dass maskierende Schritte vor der Enzymkatalyse auftraten. Da die Steigung des zweidimensionalen Isotopenplots mit $\Delta = -0.32 \pm 0.06$ auch verschieden zu den anderen war, müssen einige dieser Schritte eine leichte Isotopenfraktionierung gezeigt haben. Abiotische Referenzexperimente bei pH 3 spiegelten das Muster der biotischen Transformation wider (Anreicherung an ^{13}C , Abreicherung an ^{15}N in Atrazin), zeigten aber bei pH 12 eine Anreicherung sowohl an ^{13}C und ^{15}N . Dies deutet darauf hin, dass die Organismen mit Hilfe einer ähnlichen Lewis Säure Komplexierung die eigentliche nukleophile aromatische Substitution von Atrazin initiieren. Diese Ergebnisse bieten erstmals einen mechanistischen Einblick in diese wichtige Enzymreaktion.

In Kapitel 4 wurde mit Hilfe von CSIA der in der Natur alternativ auftretende oxidative Abbauweg von Atrazin und Simazin, der zu der Bildung der Abbauprodukte Desethyl- und Desisopropylatrazin führt, untersucht. In Abbaustudien mit dem Modellorganismus *Rhodococcus* sp. NI86/21 kam es zu einer Anreicherung an ^{13}C und ^{15}N , die einem $\epsilon_{\text{Kohlenstoff}} = -4.6\% \pm 0.6\%$ und $\epsilon_{\text{Stickstoff}} = -1.4\% \pm 0.3\%$ für Atrazin und einem $\epsilon_{\text{Kohlenstoff}} = -4.4\% \pm 0.5\%$ und einem $\epsilon_{\text{Stickstoff}} = -1.9\% \pm 0.3\%$ für Simazin entsprachen. Die Steigung des zweidimensionalen Isotopenplots für Kohlenstoff und Stickstoff von Atrazin waren ($\Delta = 0.36 \pm 0.06$) signifikant verschieden von den Steigungen, die für die biotische Hydrolyse beobachtet wurden (Kapitel 3) und bringen somit erstmals den Nachweis, dass oxidative Dealkylierung von Triazinen mittels CSIA nachgewiesen werden kann. Zusätzlich wurde die

Fraktionierung stabiler Isotopen in Kombination mit der Metabolitenaufklärung mittels LC-MS/MS (Flüssigkeitschromatographie - Tandem Massenspektrometrie) dazu genutzt, um mechanistische Einblicke in die ablaufende Reaktion zu gewinnen. Frühere Studien zeigten, dass die Transformationsreaktion im *Rhodococcus* sp. NI86/21 mittels eines Cytochrom P450 Systems katalysiert wird. Elektronentransfer (SET) und Wasserstoffabstraktion (HAT) werden in der Literatur als initiale Mechanismen für diese Reaktion diskutiert. Beim SET ist ein N-Atom in der Reaktion beteiligt, was eine ausgeprägte Stickstofffraktionierung und eine selektive Oxidation an der α -Position erwarten lässt. Es wurden abiotische Referenzexperimente mit Permanganat als Oxidans durchgeführt, welches sehr selektiv reagiert und C-, aber keine N-Fraktionierung zur Folge hat. Beim biotischen Abbau durch *Rhodococcus* sp. NI86/21 entstanden Metabolite, die in α - und β -Position der Alkylkette oxidiert gewesen waren. Diese Ergebnisse zeigten, dass die Reaktion nicht selektiv ablief und daher auf eine unselektive Wasserstoffabstraktion schließen lässt. Jedoch deutet signifikante N-Isotopenfraktionierung darauf hin, dass Bindungsänderungen am N-Atom auftraten, die einen SET vermuten lassen. Die Verknüpfung der Ergebnisse zeigen daher an, dass Oxidation mittels *Rhodococcus* sp. NI86/21 sowohl über SET als auch HAT ablief.

Table of contents

	Summary	i
	Zusammenfassung	iii
1.	General Introduction	1
1.1	PESTICIDES	2
1.1.1	Atrazine - a triazine herbicide	2
1.1.2	Fate of atrazine in the environment	3
1.2	CSIA – AN NEW APPROACH FOR RISK ASSESSMENT OF CONTAMINANTS IN THE ENVIRONMENT	6
1.2.1	CSIA – Concept and application	6
1.2.2	Factor influencing the isotopic fractionation	12
1.2.3	Dual isotope plots	13
1.3	OBJECTIVES	13
1.4	REFERENCES	14
2.	Precise and Accurate Compound Specific Carbon and Nitrogen Isotope Analysis of Atrazine: Critical Role of Combustion Oven Conditions	23
2.1	INTRODUCTION	24
2.2	EXPERIMENTAL SECTION	26
2.2.1	Chemicals	26
2.2.2	Instrumentation	26
2.2.3	Combustion reactors	27
2.2.4	HPLC	28
2.2.5	Hydrolysis experiment	28
2.2.6	Carbon and nitrogen enrichment factors for hydrolysis of atrazine	28
2.3	RESULTS AND DISCUSSION	29
2.3.1	Carbon isotope analysis of atrazine	30
2.3.2	Nitrogen isotope analysis of atrazine	33
2.3.3	Hydrolysis experiment	35
2.3.4	Environmental significance	37
2.4	REFERENCES	37
3.	C and N Isotope Fractionation Suggests Similar Mechanisms of of Microbial Atrazine Transformation Despite Involvement of Different Enzymes (AtzA and TrzN)	43
3.1	INTRODUCTION	44
3.2	EXPERIMENTAL SECTION	46
3.2.1	Chemicals	46
3.2.2	Bacterial strains and cultivation media	46
3.2.3	Abiotic hydrolysis	46
3.2.4	Sampling and preparation for quantification and isotope analysis	46
3.2.5	Quantification of atrazine and its metabolites	47
3.2.6	Isotope analysis	47
3.2.7	Carbon and nitrogen enrichment factors for hydrolysis of atrazine	47

3.3	RESULTS AND DISCUSSION	48
3.3.1	Carbon and nitrogen isotope fractionation during biotic hydrolysis of atrazine	49
3.3.2	Insight into enzymatic transformation mechanism from abiotic reference experiments	51
3.3.3	Environmental significance	55
3.4	REFERENCES	56
4	Probing for Concurring Mechanisms of Oxidative Atrazine Dealkylation: A combined Approach with Metabolite Identification and Dual Isotope Fractionation (C and N) Measurements	61
4.1	INTRODUCTION	62
4.2	EXPERIMENTAL SECTION	65
4.2.1	Chemicals	65
4.2.2	Bacterial strain and cultivation media	66
4.2.3	Oxidative degradation with potassium permanganate	66
4.2.4	Sampling for concentration measurements, identification of metabolites and isotope analysis	66
4.2.5	Quantification and identification of atrazine, simazine and its metabolites	67
4.2.6	Isotope analysis	68
4.2.7	Evaluation of stable isotope fractionation	68
4.2.8	Dual isotope plots	69
4.3	RESULTS	69
4.3.1	Metabolite identification during biotic oxidation of simazine and atrazine	69
4.3.2	Quantitative estimates of concurring transformation reactions	74
4.3.3	Carbon and nitrogen isotope fractionation during biotic and abiotic oxidation of atrazine and simazine	76
4.4	DISCUSSION	78
4.4.1	Mechanistic elucidation	78
4.4.2	Environmental Significance	80
4.5	REFERENCES	80
5.	Conclusions and Outlook	85
5.1	REFERENCES	90
APPENDIX A1		I
APPENDIX A2		III
APPENDIX A3		VII
Clarifications		XX
Publications		XXI
Danksagung		XXII
Curriculum Vitae		

„Die Realität, die reale Welt wird also nur eine gewisse Zeit lang bestanden haben, so lange wie unsere Gattung brauchte, sie durch den Filter der materiellen Abstraktion der Codes und Berechnung zu pressen.“ (Jean Baudrillard)

1.

General Introduction

1.1 Pesticides

Pesticides have been widely used for agricultural, horticultural, forestry and road industries, domestic and hygienic applications. The use and the efficacy of pesticides for the protection of crops and human health is of great importance [1]. Although these compounds are designed for effective application with a short lifetime, the parent substance or its metabolites often persist for a long time period in the environment. As a consequence, pesticides exhibit a toxicological hazard for human and nature.

The widespread use of synthetic pesticides over the past half century has led to their detection in many hydrological systems of the European Community and other countries around the world [2-4]. Besides possible harmful effects to non-target organisms of the aquatic flora and fauna, the contamination of groundwater and surface waters is the greatest concern, as more than 90 % of water resources are used for the production of drinking water. The contamination of waters by pesticides is caused mainly at production sites, by improper application or inappropriate disposal. According to the German Environmental Protection Agency report (UBA, 2006) about 30 t/a of pesticides reach surface and groundwater in Germany, which corresponds to one permil of the annual use in Germany. The risk that these compounds find their way into the human food chain via drinking water has given rise to extensive research into the fate and behaviour of pesticides. In soil environments the fate and behaviour of pesticides is governed by various retention, transport and transformation processes [5]. These processes determine both the efficacy of pesticides in controlling target organisms and their potential to become hazardous to the environment.

1.1.1 Atrazine - a triazine herbicide

Atrazine (2-chloro-4-isopropylamino-6-ethylamino-s-triazine) is like simazine, terbuthylazine and propazine member of the triazine herbicides and has been extensively used as a pre- and post-emergence herbicide to control annual grass and broadleaf weeds in agriculture of corn, sorghum and other crops. Its herbicidal function is caused by binding to the quinone-binding protein in photosystem II, thus inhibiting photosynthetic electron transport [6]. Also other processes that depend on the energy generated during photosynthesis like the opening of stomatas, transport of ions [7] as well as the RNA, enzyme, and protein synthesis [8] are affected.

Leaching of atrazine and its metabolites has led worldwide to groundwater contamination in the years of application [9] and is continuing owing to mobilisation of a recalcitrant atrazine pool [10, 11] from the topsoil. Therefore even after legislative prohibition by the European Union in

the mid 90's, atrazine and its metabolites are still widely detected in surface water and groundwater [2, 4, 7], frequently, exceeding the European Union limit of drinking-water concentration (0,1 µg/L) [12, 13]. In Germany, 1998, 63 % of all detected pesticides in groundwater were attributed to the s-triazines atrazine, desethylatrazine, and simazine, making them the most abundant pesticides in groundwater according to the ranking list of the year 2002 by the UBA (Table 1_1) [7]. Since atrazine has a toxic potential to many aquatic organisms [9, 14, 15] and may have long-term adverse effects to the aquatic environment [16] it poses a risk to ecosystem and to human health by contaminated drinking water wells [17].

Table 1_1. Ranking list of positive findings of pesticides in Germany in near surface groundwater, in the year 2002 (UBA, taken from Tappe [7])

Agent/metabolite	Rank	Agent/metabolite	Rank
Desethylatrazine	1	Bentazone	9
Atrazine	2	Mecoprop	10
Bromacile	3	Isoproturone	11
Simazine	4	Metolachlorine	12
Hexazinone	5	Prometryne	13
Diurone	6	Terbutylazine	14
Propazine	7	Chlorotolurone	15
Desisopropylatrazine	8	Lindan (gamma-HCH)	16

1.1.2 Fate of atrazine in the environment

Atrazine enters the environment mainly by improper application for weed control and subsequent surface run-off into surface-water or penetration through soil into groundwater. Another input pathway is volatilization during application from treated areas and deposition of atrazine by atmospheric precipitation [18]. In comparison with direct application, however, the diffuse contamination by atrazine is of minor importance. The fate and behaviour of atrazine in the soil environment involve several different and often simultaneous processes including chemical, biological and photochemical degradation, transport, accumulation and sorption [19-23] which are influenced to various extents by a number of physical, physico-chemical, biochemical, pedological and climatic factors [9, 24]. Therefore, it is important to differentiate between an apparent removal rate, which may be simply caused by dilution and true elimination which reflects actual compound degradation. Transport of atrazine takes place through diffusion, mass flow, and even by adsorption to carrier substances such as dissolved organic matter or soil colloids [25, 26]. Adsorption to stationary phases such as clay-minerals or soil organic matter causes an accumulation of the herbicide in the pedosphere, which leads to a decrease in dissolved concentrations and may diminish bioavailability in the soil-solution, bringing about a

minor extent of biodegradation. This favours the retention of atrazine and its metabolites in the soil. On a larger time scale, however, continuous desorption from the recalcitrant pool may lead to remobilization which may explain the fact that despite of the prohibition in the 90's, atrazine can still be detected in environmental samples around Europe. It was shown that sorption to organic matter and clay minerals [27, 28] increased in the order desalkylatrazine < atrazine << hydroxyatrazine. In particular, dealkylated atrazine metabolites are characterized by their pronounced reversible sorption behaviour, whereas for hydroxyatrazine also irreversible sorption (bound residues) constitutes an important sorption mechanism in upper soil layers [21, 24, 29, 30].

As on the one hand, only degradation leads to a sustainable elimination, but on the other hand the different metabolites contain again a specific extent of toxicity [9] it is important to know the amount of degradation and the relevance of different degradation pathways to assess more reliably the fate of atrazine in the environment. Atrazine may be transformed in soil by abiotic [21] as well as by microbial transformation [22, 31], whereas in subsurfaces and water, biotransformation represents the main route of degradation [32]. Triazine biotransformation in the environment occurs by two main pathways which can be performed by fungi [33, 34] and bacteria [35-37]. One initial degradation pathway is hydrolytic [38-41] - catalysed by chlorohydrolasae - leading to dehalogenation of atrazine (Figure 1_1).

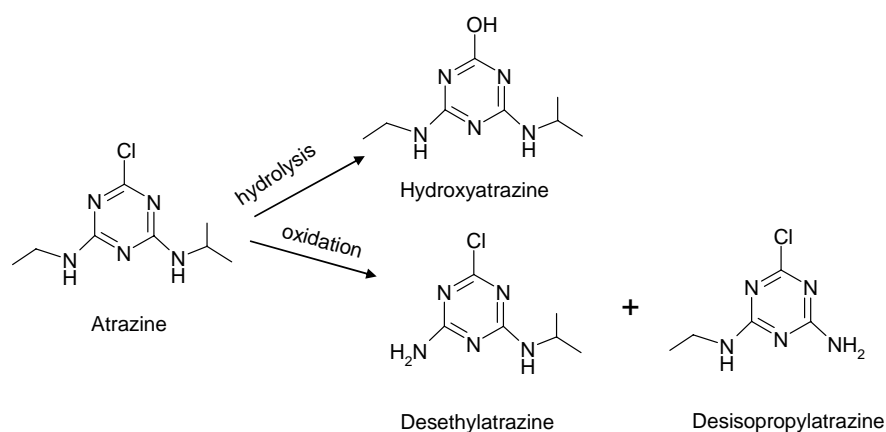


Figure 1_1. Biotic degradation pathways of atrazine modified from Wackett et al. [41]

The hydrolysis of atrazine at the C-Cl bond represents a formal a nucleophilic aromatic substitution (S_NAr), where the chlorine atom is substituted by an OH-group. Such hydrolysis of atrazine is known to be catalyzed by the enzymes AtzA and TrzN. Although these enzymes are both member of the amidohydrolase superfamily, amino acid sequence relatedness between them is only 27%, indicating that they have evolved independently from different ancestors [42]. In

environment [57-59]. Since hydroxyatrazine is not considered by this index, results sometimes can lead to an underestimation of the intrinsic degradation state [60]. Recent studies even suggest that hydroxyatrazine formation is in fact the dominating natural degradation pathway [41] implying that removal of atrazine from natural systems is presently not adequately assessed. Complete degradation of atrazine by biodegradation is rarely found in the field [61]. Accordingly, atrazine is considered to be a relative persistent chemical in the environment. Estimated half-lives in aquatic systems (surface water, groundwater) reported in different studies range around 26-253 days [61] and 1.5 to 4 years [8, 21], respectively. For soil it is estimated that the half-life is in a range between 41-146 days [61]. However, even despite much recent research on atrazine under controlled conditions, the difficulty of establishing complete mass balances in the subsurface makes it still a major challenge to address its origin and fate in the real environmental settings [1]. Furthermore, the assessment of metabolites is often difficult, due to their temporary or irreversible immobilisation. Therefore there is great interest in novel approaches to better assess the fate of atrazine in the environment.

1.2. CSIA - an new approach for risk assessment of contaminants in the environment

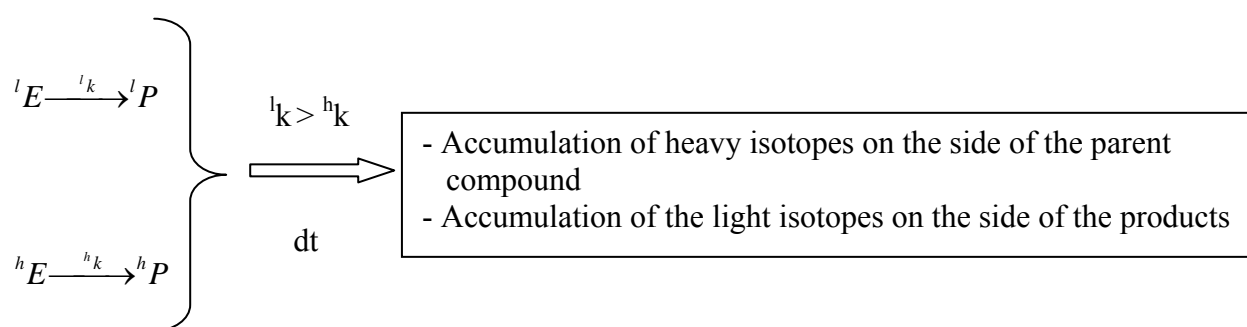
1.2.1 CSIA- Concept and application

In recent years CSIA has become a promising approach to identify and quantify transformation reactions of organic compounds in contaminant hydrology [62, 63]. It measures the isotopic composition of a compound at natural abundance. Such isotope signatures are often characteristic of a particular chemical product and are given by the ratio of the rare heavier isotope to the more abundant lighter isotope (e.g. $^{13}\text{C}/^{12}\text{C}$, $^2\text{H}/^1\text{H}$, $^{15}\text{N}/^{14}\text{N}$). Isotope ratios are generally expressed with respect to an international standard in the δ -notation in per mil (‰) according to eq. 1_1.

$$\delta_x = \left(\frac{R_x}{R_{reference}} - 1 \right) \times 1000 [\text{‰}] \quad (1_1)$$

where R_x and $R_{reference}$ are the ratios of the heavy isotope to the light isotope in compound x and in an international standard, respectively. Such an isotope signature may be considered like the fingerprint of an organic compound, and as such, it is frequently used in environmental forensics. Depending on the raw materials and the processes of synthesis, the same chemical substance may have different isotope signatures, which can make it possible to identify the original manufacturer and to allocate a source of contamination.

By characterizing changes in a compound's isotope ratio, this method is able to differentiate whether a decrease in concentrations is due to degradative or to non-degradative processes, like dilution, vaporization and sorption. As summarized in various current reviews [62-64], for different contaminants, such as toluene, benzene, chlorinated hydrocarbons, nitroaromates or MTBE (methyl t-butyl-ether), degradation is accompanied by an considerable enrichment of the heavier isotopes of carbon and hydrogen within the remaining substrate and an enrichment of the lighter isotope on the side of the products. In comparison, for non-degradative processes this phenomenon is less significant [65-67]. The reason for the enrichment of the heavier isotopes after chemical transformation of a compound is the kinetic isotope effect (KIE) occurring in the reacting bond. The KIE is a physical phenomenon caused by the fact that during a chemical reaction, molecules with the light isotope in the reacting bond will, in general, react slightly more faster than those with the heavy isotope (Scheme 1_2).



Scheme 1_2. Scheme for kinetic isotope effect occurring by different reaction rates for the light and heavy isotope of an element. E: parent compound of reaction; P: product of reaction; ${}^l k$: reaction constant of the light isotope; ${}^h k$: reaction rate of the heavy isotope; dt: time event

This is caused by differences in mass-dependent molecular energies, mainly by differences in vibrational but also by rotational and translational motions of the considered atoms. Most importantly, molecules with the heavy isotope will have a lower zero-point energy than the molecules of the light isotope [68, 69]. This means that the bonds formed by the light isotope are weaker than bonds involving the heavy isotope.

Thus, the kinetic isotope effect can be described as the ratio of the rate constant ${}^l k$ (light isotope) and ${}^h k$ (heavy isotope) (Equation 1_2).

$$KIE = \frac{{}^l k}{{}^h k} \quad (1_2)$$

KIEs depend on changes in bonding between reactant and transition state. Their accurate prediction is only possible through careful computational calculations [70-72]. The approximate

magnitude of KIEs, however, can already be predicted when knowing the type of reaction (e.g. S_N1 versus S_N2), and KIEs strongly depend on the type of bond being broken (e.g C-H vs C-Cl, see, e.g. [73]). It has therefore been found that different reaction pathways correspond to certain characteristic ranges of values ([74], Table 1_2).

Table 1_2. Experimentally determined kinetic isotope effects for important reactions (modified from Elsner et al., [74])

type of reaction	isotope	KIE	ref
reactions involving hydrogen (e.g., H-radical transfer in oxidation reactions)	$^{12}\text{C}/^{13}\text{C}$ $^1\text{H}/^2\text{H}$	1.015 (1 study) generally > 2, typically 3–8, up to 40–50	(47) (52–55)
nucleophilic substitution (S_N2 type) involving C–Cl, C–N, C–O bonds etc.	$^{12}\text{C}/^{13}\text{C}$ $^1\text{H}/^2\text{H}$ (secondary)	1.03–1.09 0.95–1.05 (next to reacting bond)	(56) (22), p 304 in ref 46
nucleophilic substitution (S_N1 type) involving C–Cl, C–N, C–O bonds etc.	$^{12}\text{C}/^{13}\text{C}$ $^1\text{H}/^2\text{H}$ (secondary)	1.00–1.03 1.1–1.2 (next to reacting bond) 1.05–1.15 (one bond apart)	(56) (22, 46)
oxidation of C=C bonds with permanganate (average over both C atoms)	$^{12}\text{C}/^{13}\text{C}$	1.024 (1 study)	(57, 58)
epoxidation of C=C bonds (average over both C atoms)	$^{12}\text{C}/^{13}\text{C}$	1.011 (1 study)	(50)

The isotope effect at the position at which chemical bonding changes during the reaction, is described as primary. An isotope effect is called secondary if it appears at an atomic position not directly involved in the reaction itself [75].

In biogeochemistry, isotopic fractionation between two compounds as a whole is expressed either by the fractionation factor α or the enrichment factor ϵ [76, 77]. One may attempt to link these parameters to the ratio of rate constants given in Equation 1_2. By assuming a first order kinetics for the reaction of each isotope (here in the case of ^{12}C and ^{13}C) the following rate law can be written

$$\frac{d[^{12}\text{C}]}{dt} = -^{12}k^{12}\text{C} \quad (1_3)$$

$$\frac{d[^{13}\text{C}]}{dt} = -^{13}k^{13}\text{C} \quad (1_4)$$

By integrating for the case of a closed system, and dividing eq.1_3 by eq.1_4 the following term is obtained,

$$\frac{^{13}\text{C}_t}{^{12}\text{C}_t} = \left(\frac{^{12}\text{C}_t}{^{12}\text{C}_0} \right)^{\frac{^{13}k}{^{12}k} - 1} = \left(\frac{^{12}\text{C}_t}{^{12}\text{C}_0} \right)^{\text{KIE}^{-1} - 1} \quad (1_5)$$

which is an expression analogous to the Rayleigh equation.

$$\frac{R_t}{R_0} = \frac{R_0 + \Delta R}{R_0} = f^{\alpha-1} \quad (1_6)$$

The Rayleigh equation describes the average isotope fractionation of a compound in terms of isotope fractionation factor α , where R_t and R_0 are the compound-specific isotope ratios of heavy versus light isotopes at a given time and at the beginning of the reaction. $\Delta R = (R - R_0)$ is the change in the isotope ratios, while C_t/C_0 is the fraction f of the remaining compound. Linearising this equation, α can be obtained by determination of the slope (Figure 1_2).

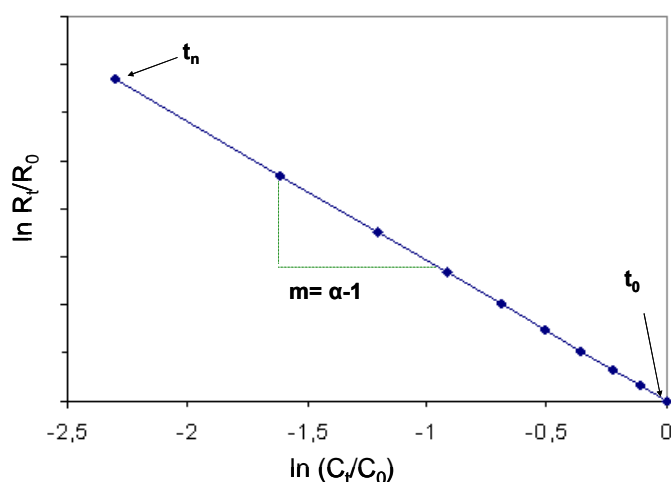


Figure 1_2. Simulated isotope fractionation in a residual substrate fraction during the process of degradation. m : slope of regression line with $\alpha-1$.

Isotopic-fractionation expressed in terms of the enrichment factor ε follows eq. 1_7 and is denoted in permil.

$$\frac{\varepsilon}{1000} = (\alpha - 1) = m \quad (1_7)$$

The significance of ε is most clearly visualized in Figure 1_3. During the reaction the average isotope ratio of all instantaneously formed products is always by the factor ε isotopically different than the ratio of the remaining substrate at that given time of conversion, as for example described for the reductive dechlorination of CCl_4 (Figure 1_3 [74]). The figure illustrates that in irreversible chemical reactions, both, the enrichment of the heavy isotope in the remaining substrate at a given time, as well as the depletion on the side of the products, can deliver suitable evidence that transformation is occurring in a given system. Such isotope fractionation for degradation of a chosen contaminant can be measured in laboratory experiments under controlled conditions (e.g. pure cultures or enrichments, known chemical reaction). Data of this experiment can then be evaluated as shown in Figure 1_2, to obtain fractionation factors α or enrichment factors ε . If these values of α or ε are robust for the respective chemical reaction

under different environmental conditions, these values can be used to quantify the extent of biodegradation B by the following equation (1_8), where B is denoted in percent.

$$B = 1 - f = \left[\frac{R_t}{R_0} \right]^{\frac{1}{\alpha-1}} \cdot 100\% \quad (1_8)$$

In a number of cases, such values were successfully used to derive estimates of biodegradation B from measured isotope ratios at contaminated field sites [78-82].

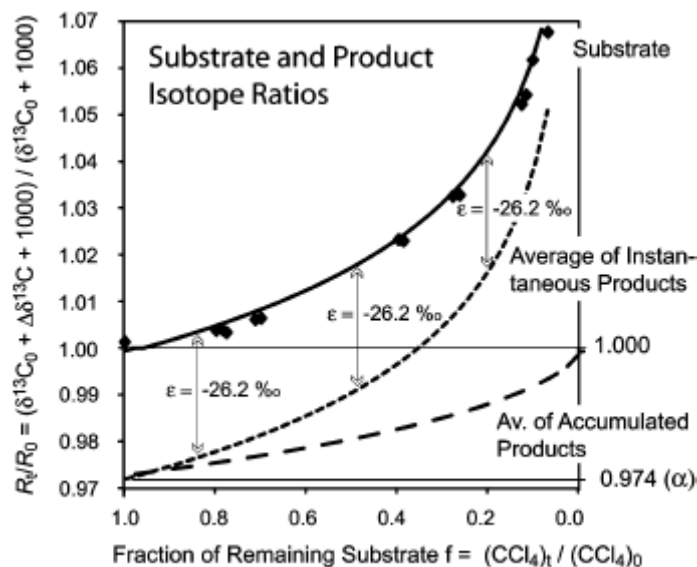


Figure 1_3. Carbon-isotope fractionation measured during reductive dehalogenation of carbon tetrachloride (CCl_4) [74].

Due to the fact that kinetic isotope effects strongly depend on the kind of reaction (Table 1_2), it was found that enrichment factors vary, according to the type of degradation pathway. For example, ϵ 's determined for the degradation of MTBE differed significantly between aerobic [83, 84] and anaerobic conditions [85]. Also Hirschhorn et al. [73] found varying enrichment factors for the oxidative and the hydrolytic degradation of 1,2-dichloroethane degradation. These studies demonstrated that the observable fractionation factors could indeed be used to decipher reaction mechanisms, as postulated by Elsner et al. [74]. As discussed in the following, through appropriate corrections, the obtained α or ϵ can even be related to the reaction specific KIEs. As should become clear from the derivation (eq. 1_3-1_5), the intrinsic KIE for an element corresponds to α^{-1} assuming that there are no masking effects (more detailed information see below) and that there is only one atom of the element of interest within the molecule. As CSIA measures the average bulk isotopic composition of a compound, however, for more complex molecules (more than one atom of the element in question, more reactive sites) this condition is

not fulfilled anymore. Specifically, if atoms of the element are located in non reactive positions, the bulk enrichment factor determined according to the Rayleigh equation (Equation 1_6) will be remarkably smaller than the value of $(KIE^{-1}-1)$ due to dilution of invariant isotope ratios in the non-reactive positions. The appearance of the concerning atom in non-reactive position, therefore, results in a remarkably. To obtain α 's and ε 's specifically in the reactive position, Elsner et al. [74] therefore proposed a re-evaluation of bulk enrichment factors by the following correction:

$$\ln \frac{R_{\text{reactive-position}}}{R_0} = \ln \frac{R_0 + n/x \cdot \Delta R}{R_0} = (\alpha_{\text{reactive-position}} - 1) \cdot \ln f = \frac{\varepsilon_{\text{reactive-position}}}{1000} \cdot \ln f \quad (1_9)$$

Assuming that isotopes are equally distributed over all molecules at natural isotopic abundance, changes in isotope-ratios over time, ΔR , must be multiplied by the factor n/x where n corresponds to the total positions of the atom and x is the number of reactive positions in the molecule (Eq.1_10). Thus the bulk enrichment factor can be interpreted in terms of apparent kinetic isotope effects, where the word “apparent” accounts again for cases in which masking cannot be excluded (see below).

$$AKIE = \frac{1}{(\varepsilon_{\text{reactive-position}} / 1000) + 1} \quad (1_{10})$$

Some molecules contain several atoms of the same element in the same reactive position of a molecule (e.g. three hydrogen atoms in a $-\text{CH}_3$ group). In such a case, an additionally correction must be carried out. Since only one of the competing bonds is broken in the initial reaction, there will be intramolecular isotopic competition between the isotopically heavier and lighter atoms. Neglecting secondary isotope effects (usually an order of magnitude smaller than primary effects [62], this competition can be taken into account according to

$$AKIE = \frac{1}{(z \cdot \varepsilon_{\text{reactive-position}} / 1000) + 1} = \frac{1}{(z \cdot \frac{n}{x} \cdot \varepsilon_{\text{bulk}} / 1000) + 1} \approx \frac{1}{(n \cdot \varepsilon_{\text{bulk}} / 1000) + 1} \quad (1_{11})$$

where z is the number of indistinguishable competing atoms in the reactive position. The last approximation is valid for all elements except for hydrogen. Therefore, the observed fractionation becomes smaller with increasing number of atoms within the molecule, limiting the

application of CSIA for larger molecules. A more detailed mathematical derivation and examples are given in Elsner et al. [74].

Converting bulk isotope fractionation factors into position specific apparent kinetic isotope effects gives on the one hand the opportunity to compare fractionation for the same reaction in different contaminants. On the other hand, it enables identification of transformation pathways, provided that a mechanistic hypothesis exists for which the agreement with observable isotope fractionation can be tested.

1.2.2 Factor influencing the isotopic fractionation

Although it was shown that this concept is appropriate to identify degradation processes, even the same transformation pathways may not always show the same fractionation when expressed in terms of α and ϵ . The reason for this are so called masking effects.

Masking-Effects

Masking effects cause a deviation of the observed apparent kinetic isotope effect (AKIE) from the expected intrinsic kinetic isotope effect ($KIE_{intrinsic}$) (see above). Masking appears when the bond-changing step of a reaction is not the slow one. In particular, if the reverse step of the preceding process is slow, every substrate molecule that reaches the reactive site will be converted, irrespective of its isotopic composition [74] and the observed isotopic fractionation will not correspond to the chemical transformation. Such preceding steps may be uptake, transport to reactive sites, adsorption to reactive surfaces or formation of enzyme-substrate complexes [86, 87]. Elucidation of masking effects can be carried out by comparison of the obtained AKIE with the $KIE_{intrinsic}$ described for several reactions in the biochemical literature. In the case of an unknown KIE of a given bio-transformation, the AKIE of the biotic reaction may be compared with the one of the corresponding abiotic reaction. Since abiotic transformations in homogeneous solutions are seldomly associated with rate-determining steps other than the intrinsic bond conversion agreement of biotic and abiotic AKIE can be a strong indicator that masking effects do not play a major role during bio-transformation.

1.2.3 Dual isotope plots

Masking can make the identification of transformation pathways difficult, since the sheer magnitude of observable ϵ values may no longer be indicative of the prevailing reaction mechanism. In addition, different degradation pathways may occur simultaneously in the environment bringing about, the difficulty of choosing the “correct” fractionation factor when estimating biodegradation. In such cases, dual isotope plots can be very helpful provided that the isotopic signature can be measured for two elements involved in the chemical conversion. Since

both elements undergo the same reaction mechanism and are affected by the same masking effects, the data may be considered relative to each other [74]. Plotting the $\epsilon_{\text{reactive-position}}$ or respectively the isotopic signatures of both elements against each other in dual isotope plots, gives a linear correlation, as it was demonstrated by Zwank et al. [88]. Comparison of such dual isotope plots, from the laboratory with those obtained in the field can give the evidence which degradation process takes place [89-91].

1.3 Objectives

This Ph.D. thesis therefore aims at developing Compound Specific Isotope Analysis (CSIA) for atrazine. On the one hand, the goal is to use the measurable isotope fractionation associated with biotransformation reactions of this compound as an alternative way to qualitatively detect, and possibly even to quantitatively determine the natural degradation of atrazine. On the other hand, stable isotope fractionation is being used to learn more about underlying transformation mechanisms. For that purpose carbon and nitrogen isotope fractionation associated with biotic degradation processes were evaluated in laboratory studies. In addition, observable stable isotope fractionations was linked to position-specific kinetic isotope effects, and dual isotope plots were constructed to decipher the different initial biotic transformation pathways of atrazine. This approach is particularly powerful, since it relies on isotope analysis of the substrate and would even work if the actual degradation products are not directly detectable in natural systems (e.g. because of further transformation or binding to soil matrix).

The three specific objectives of this dissertation were, therefore:

- a) To develop a sensitive and accurate method for the compound specific isotope analysis of atrazine by GC-IRMS (gas chromatography-isotope ratio mass spectrometry) and to investigate if alkaline hydrolysis of atrazine is associated with observable C and N isotope fractionation (Chapter 2).
- b) To evaluate the potential of isotope fractionation as an alternative way to quantify biotic hydrolysis and to identify the underlying enzymatic reaction mechanism of atrazine hydrolysis (Chapter 3).
- c) Likewise to evaluate the potential of C and N isotope fractionation to trace biotic oxidative dealkylation when catalysed by a cytochrome P450 system-containing microorganisms and in

combination with metabolite analysis to decipher the mechanism of the initial step in this biotic oxidation of atrazine (Chapter 4).

Chapter 2 [92] and Chapter 3[93] as well as studies addressing isotope fractionation of atrazine during photolysis [94] and alkaline hydrolysis [95], were recently published in peer-reviewed environmental journals giving a telling indication of its environmental relevance.

1.4 References

1. Rice, P. J.; Arthur, E. L.; Barefoot, A. C., Advances in pesticide environmental fate and exposure assessments. *J. Agric. Food Chem.* 2007, 55, (14), 5367-5376.
2. Baran, N.; Mouvet, C.; Negrel, P., Hydrodynamic and geochemical constraints on pesticide concentrations in the groundwater of an agricultural catchment (Brevilles, France). *Environ. Pollut.* 2007, 148, (3), 729-738.
3. Dalton, M. S.; Frick, E. A., Fate and transport of pesticides in the ground water systems of southwest Georgia, 1993-2005. *J. Environ. Qual.* 2008, 37, (5), S264-S272.
4. Sagratini, G.; Ametisti, M.; Canella, M.; Cristalli, G.; Francoletti, E.; Giardina, D.; Luminari, M. C.; Paparelli, G.; Pico, Y.; Volpini, R.; Vittori, S., Well water in central Italy: Analysis of herbicide residues as potential pollutants of untreated crops. *Fresen. Environ. Bull.* 2007, 16, (8), 973-979.
5. Barbash, J. E.; Heinrich, D. H.; Karl, K. T., The geochemistry of pesticides. In *Treatise on geochemistry*, Pergamon: Oxford, 2007; pp 1-43.
6. Trebst, A., The mode of action of triazine herbicides in plants. In *The triazine herbicides*, 1 ed.; Le Baron, H. M.; McFarland, J. E.; Burnside, O. C., Eds. Elsevier: Amsterdam, 2008; pp 101-110.
7. Tappe, W.; Groeneweg, J.; Jantsch, B., Diffuse atrazine pollution in German aquifers. *Biodegradation* 2002, 13, (1), 3-10.
8. Huber, W., Ecotoxicological relevance of atrazine in aquatic systems. *Environ. Toxicol. Chem.* 1993, 12, 1865-1881.
9. Graymore, M.; Stagnitti, F.; Allinson, G., Impacts of atrazine in aquatic ecosystems. *Environ. Int.* 2001, 26, (7-8), 483-495.
10. Pignatello, J. J.; Huang, L. Q., Sorptive reversibility of atrazine and metolachlor residues in field soil samples. *J Environ Qual* 1991, 20, (1), 222-228.
11. Ying, G. G.; Kookana, R. S.; Mallavarpu, M., Release behavior of triazine residues in stabilised contaminated soils. *Environmental Pollution* 2005, 134, (1), 71-77.

12. Claver, A.; Ormad, P.; Rodriguez, L.; Ovelleiro, J. L., Study of the presence of pesticides in surface waters in the Ebro river basin (Spain). *Chemosphere* 2006, *64*, (9), 1437-1443.
13. Kersante, A.; Martin-Laurent, F.; Soulas, G.; Binet, F., Interactions of earthworms with atrazine-degrading bacteria in an agricultural soil. *FEMS Microbiol. Ecol.* 2006, *57*, (2), 192-205.
14. Suzawa, M.; Ingraham, H. A., The herbicide atrazine activates endocrine gene networks via non-steroidal NR5A nuclear receptors in fish and mammalian cells. *PLoS One* 2008, *3*, (5).
15. Rohr, J. R.; Schotthoefer, A. M.; Raffel, T. R.; Carrick, H. J.; Halstead, N.; Hoverman, J. T.; Johnson, C. M.; Johnson, L. B.; Lieske, C.; Piwoni, M. D.; Schoff, P. K.; Beasley, V. R., Agrochemicals increase trematode infections in a declining amphibian species. *Nature* 2008, *455*, 1235-1239.
16. Pang, L.; Close, M.; Flintoft, M., Degradation and sorption of atrazine, hexazinone and procymidone in coastal sand aquifer media. *Pest. Manag. Sci.* 2005, *61*, 133-143.
17. Gammon, D. W.; Aldous, A. C.; Carr, W.; Sanborn, J. R.; Pfeifer, K. F., A risk assessment of atrazine use in California: human health and ecological aspects. *Pest. Manag. Sci.* 2005, *61*, (25), 331-355.
18. Alvord, H. H.; Kadlec, R. H., Atrazine fate and transport in the Des Plaines Wetlands. *Ecol. Model.* 1996, *90*, (1), 97-107.
19. Mandelbaum, R. T.; Sadowsky, M. J.; Wackett, L. P., Microbial degradation of s-triazines herbicides. In *The triazine herbicides*, Le Baron, H. M.; McFarland, J. E.; Burnside, O. C., Eds. Elsevier: Amsterdam, 2008; pp 301-328.
20. Cessna, A. J., Nonbiological degradation of triazine herbicides: photolysis and hydrolysis. In *The triazine herbicides*, Le Baron, H. M.; McFarland, J. E.; Burnside, O. C., Eds. Elsevier: Amsterdam, 2008; pp 329-354.
21. Ma, L.; Selim, H. M., Atrazine retention and transport in soils. *Rev. Environ. Contam. T.* 1996, *145*, 129-162.
22. Erickson, L. E., Degradation of atrazine and related s-triazines. *Crit. Rev. Env. Con.* 1989, *19*, 1-14.
23. Laird, D. A.; Koskinen, W. C., Triazine soil interactions. In *The triazine herbicide*, Le Baron, H. M.; McFarland, J. E.; Burnside, O. C., Eds. Elsevier: Amsterdam, 2008; pp 275-300.
24. Senesi, N.; D'Orazio, V.; Miano, T. M., Adsorption mechanisms of s-triazine and bipyridylum herbicides on humic acids from hop field soils. *Geoderma* 1995, *66*, (3-4), 273-283.
25. Barton, C. D.; Karathanasis, A. D., Influence of Soil Colloids on the Migration of Atrazine and Zinc Through Large Soil Monoliths. *Water, Air, & Soil Pollution* 2003, *VI43*, (1), 3-21.

26. Seta, A.; Karathanasis, A. D., Atrazine adsorption by soil colloids and co-transport through subsurface environments. *Soil. Sci. Soc. Am. J.* 1997, *61*, 612-617.
27. Brouwer, W. W. M.; Boesten, J. J. T. I.; Siegers, W. G., Adsorption of transformation products of atrazine by soil. *Weed Res.* 1990, *30*, (2), 123-128.
28. Xie, H.; Guetzloff, T. F.; Rice, J. A., Fractionation of pesticide residues bound to humin. *Soil Sci.* 1997, *162*, 421-429.
29. Moreau-Kervevan, C.; Mouvet, C., Adsorption and desorption of atrazine, deethylatrazine, and hydroxyatrazine by soil components. *J. Environ. Qual.* 1998, *27*, 46-53.
30. Loiseau, L.; Barriuso, E., Characterization of the atrazine's bound (nonextractable) residues using fractionation techniques for soil organic matter. *Environ. Sci. Technol.* 2002.
31. Burkhard, N.; Guth, J. A., Chemical hydrolysis of 2-Chloro-4,6-bis(alkylamino)-1,3,5-triazine herbicides and their breakdown in soil under the influence of adsorption. *Pesticide Science* 1981, *12*, 45-52.
32. Rodriguez, C. J., Harkin, J.M., Degradation of Atrazine in Subsoils, and Groundwater Mixed with Aquifer Sediments. *Bull. Environ. Contam. Toxicol.* 1997, *59*, 728-735.
33. Hickey, W. J.; Fuster, D. J.; Lamar, R. T., Transformation of atrazine in soil by *Phanerochaete chrysosporium*. *Soil Biol. Biochem.* 1994, *26*, (12), 1665-1671.
34. Mougin, C.; Laugero, C.; Asther, M.; Dubroca, J.; Frasse, P.; Asther, M., Biotransformation of the herbicide atrazine by the white rot fungus *Phanerochaete chrysosporium*. *Appl. Environ. Microbiol.* 1994, *60*, (2), 705-708.
35. Behki, R.; Khan, S., Degradation of Atrazine, propazine, and simazine by *Rhodococcus* Strain B-30. *J. Agric. Food Chem.* 1994, *42*, 1237-1241.
36. Mandelbaum, R. T.; Wackett, L. P.; Allan, D. L., Mineralization of the s-triazine ring of atrazine by stable bacterial mixed cultures. *Applied Environmental Microbiology* 1993, *59*, (6), 1695-1701.
37. Ralebitso, K. T.; Senior, E.; Verseveld van, H. W., Microbial aspects of atrazine degradation in natural environments. *Biodegradation* 2002, *13*, 11-19.
38. Ellis, L.; Wackett, L.; Li, C.; Gao, J.; Turnbull, M., Biocatalysis/Biodegradation Database. In University of Minnesota: 2006.
39. Mandelbaum, R. T.; Allan, D. L.; Wackett, L. P., Isolation and characterization of a *Pseudomonas* sp. that mineralizes the s-triazine herbicide atrazine. *Appl. Environ. Microbiol.* 1995, *61*, (4), 1451-1457.
40. Radosevich, M.; Traina, S. J.; Hao, Y. L.; Tuovinen, O. H., Degradation and mineralization of atrazine by a soil bacterial isolate. *Appl. Environ. Microbiol.* 1995, *61*, (1), 297-302.

41. Wackett, L.; Sadowsky, M.; Martinez, B.; Shapir, N., Biodegradation of atrazine and related s-triazine compounds: from enzymes to field studies. *Appl. Microbiol. Biotechnol* 2002, *V58*, (1), 39-45.
42. Shapir, N.; Mongodin, E. F.; Sadowsky, M. J.; Daugherty, S. C.; Nelson, K. E.; Wackett, L. P., Evolution of catabolic pathways: Genomic insights into microbial s-triazine metabolism. *J. Bacteriol.* 2007, *189*, (3), 674-682.
43. Scott, C.; Jackson, C. J.; Coppin, C. W.; Mourant, R. G.; Hilton, M. E.; Sutherland, T. D.; Russell, R. J.; Oakeshott, J. G., Atrazine chlorohydrolase: catalytic improvement and evolution. *Appl. Environ. Microbiol.* 2009, *75*, 2184-2191.
44. Guengerich, F. P., Common and uncommon cytochrome P450 reactions related to metabolism and chemical toxicity. *Chem. Res. Toxicol.* 2001, *14*, (6), 611-650.
45. Sono, M.; Roach, M. P.; Coulter, E. D.; Dawson, J. H., Heme-containing oxygenases. *Chem. Rev.* 1996, *96*, (7), 2841-2888.
46. Miwa, G. T.; Walsh, J. S.; Kedderis, G. L.; Hollenberg, P. F., The use of intramolecular isotope effects to distinguish between deprotonation and hydrogen atom abstraction mechanisms in cytochrome P-450- and peroxidase-catalyzed N-demethylation reactions. *J. Biol. Chem.* 1983, *258*, (23), 14445-14449.
47. Dinnocenzo, J. P.; Karki, S. B.; Jones, J. P., On isotope effects for the cytochrome P-450 oxidation of substituted N,N-dimethylanilines. *J. Am. Chem. Soc.* 1993, *115*, (16), 7111-7116.
48. Karki, S. B.; Dinnocenzo, J. P.; Jones, J. P.; Korzekwa, K. R., Mechanism of oxidative amine dealkylation of substituted N,N-dimethylanilines by cytochrome P-450: application of isotope effect profiles. *J. Am. Chem. Soc.* 1995, *117*, (13), 3657-3664.
49. Hall, L. R.; Hanzlik, R. P., Kinetic deuterium isotope effects on the N-demethylation of tertiary amides by cytochrome P-450. *J. Biol. Chem.* 1990, *265*, (21), 12349-12355.
50. Wang, Y.; Kumar, D.; Yang, C.; Han, K.; Shaik, S., Theoretical study of N-demethylation of substituted N,N-dimethylanilines by cytochrome P450: the mechanistic significance of kinetic isotope effect profiles. *J. Phys. Chem. B* 2007, *111*, (26), 7700-7710.
51. Guengerich, F. P.; Okazaki, O.; Seto, Y.; Macdonald, T. L., Radical cation intermediates in N-dealkylation reactions. *Xenobiotica* 1995, *25*, (7), 689-709.
52. Brown, C. M.; Reisfeld, B.; Mayeno, A. N., Cytochromes P450: a structure-based summary of biotransformations using representative substrates. *Drug Metab. Rev.* 2008, *40*, (1), 1-100.
53. Solomon, K. R.; Baker, D. B.; Richards, R. P.; Dixon, K. R.; Klaine, S. J.; La Point, T. W.; Kendall, R. J.; Weisskopf, C. P.; Giddings, J. M.; Giesy, P.; Hall, L. W., Jr.; Williams, W. M., Ecological risk assessment of atrazine in North American surface waters. *Environ. Toxicol. Chem.* 1996, *15*, (1), 31-76.
54. Wallnöfer, P. R.; Engelhardt, G., *Microbial degradation of pesticides*. Springer: Berlin, 1989; Vol. 2, p 1-115.

55. Clay, S. A.; Koskinen, W. C., Adsorption and desorption of atrazine, hydroxyatrazine, and S-glutathione atrazine on two soils. *Weed Res.* 1990, 38, 262-266.
56. Martin-Neto, L.; Traghetta, D. G.; Vaz, C. M. P.; Crestana, S.; Sposito, G., On the interaction mechanisms of atrazine and hydroxyatrazine with humic substances. *J. Environ. Qual.* 2001, 30, (2), 520-525.
57. Spalding, R. F.; Snow, D. D.; Cassada, D. A.; Burbach, M. E., Study of pesticide occurrence in two closely spaced lakes in northeastern Nebraska. *J. Environ. Qual.* 1994, 23, 571-578.
58. Thurman, E. M.; Ferrer, I.; Barcelo, D., Choosing between atmospheric pressure chemical ionization and electrospray ionization interfaces for the HPLC/MS analysis of pesticides. *Anal. Chem.* 2001, 73, (22), 5441-5449.
59. Paschke, S. S.; Schaffrath, K. R.; Mashburn, S. L., Near-decadal changes in nitrate and pesticide concentrations in the South Platte River alluvial aquifer, 1993-2004. *J. Environ. Qual.* 2008, 37, (5), S281-S295.
60. Krutz, L. J.; Shaner, D. L.; Accinelli, C.; Zablutowicz, R. M.; Henry, W. B., Atrazine dissipation in s-triazine-adapted and nonadapted soil from Colorado and Mississippi: Implications of enhanced degradation on atrazine fate and transport parameters. *J. Environ. Qual.* 2008, 37, (3), 848-857.
61. Norhede, P.; Nielsen, E.; Ladefoged, O.; Meyer, O. *Evaluation of health hazards by exposure to triazines and degradation products*; The Institute of Food Safety and Nutrition and Danish Veterinary and Food Administration, Danish EPA, Miljoministeriet, p. 1-106 2004.
62. Schmidt, T. C.; Zwank, L.; Elsner, M.; Berg, M.; Meckenstock, R. U.; Haderlein, S. B., Compound-specific stable isotope analysis of organic contaminants in natural environments: a critical review of the state of the art, prospects, and future challenges. *Anal. Bioanal. Chem.* 2004, 378, (2), 283-300.
63. Hofstetter, T. B.; Schwarzenbach, R. P.; Bernasconi, S. M., Assessing transformation processes of organic compounds using stable isotope fractionation. *Environ. Sci. Technol.* 2008, 42, (21), 7737-7743.
64. Meckenstock, R. U.; Morasch, B.; Griebler, C.; Richnow, H. H., Stable isotope fractionation analysis as a tool to monitor biodegradation in contaminated aquifers. *J. Contam. Hydrol.* 2004, 75, (3-4), 215-255.
65. Dempster, H. S.; Sherwood Lollar, B.; Feenstra, S., Tracing organic contaminants in groundwater: A new methodology using compound specific isotopic analysis. *Environ. Sci. Technol.* 1997, 31, (11), 3193-3197.
66. Harrington, R. R.; Poulson, S. R.; Drever, J. I.; Colberg, P. J. S.; Kelly, E. F., Carbon isotope systematics of monoaromatic hydrocarbons: vaporization and adsorption experiments. *Org. Geochem.* 1999, 30, 765-775.

67. Slater, G.; Sherwood Lollar, B.; Allen King, R.; O'Hannesin, S. F., Isotopic fractionation during reductive dechlorination of trichloroethene by zero-valent iron: influence of surface treatment. *Chemosphere* 2002, 49, 587-596.
68. Hoefs, J., *Stable Isotope Geochemistry*. Springer-Verlag: Berlin, 1997.
69. Mariotti, A.; Germon, J. C.; Hubert, P.; Kaiser, P.; Letolle, R.; Tardieux, A.; Tardieux, P., Experimental determination of nitrogen kinetic isotope fractionation - Some principles - Illustration for the denitrification and nitrification processes. *Plant and Soil* 1981, 62, (3), 413-430.
70. Gawlita, E.; Szyllabel-Godala, A.; Paneth, P., Kinetic isotope effects on the Menshutkin reaction: theory versus experiment. *J. Phys. Orga. Chem.* 1996, 9, (1), 41-49.
71. Paneth, P., Theoretical calculations of heavy-atom isotope effects. *Comput. Chem.* 1995, 19, (3), 231-240.
72. Roberto-Neto, O.; Coitino, E. L.; Truhlar, D. G., Dual-level direct dynamics calculations of deuterium and carbon-¹³ kinetic isotope effects for the reaction Cl + CH₄. *J. Phys. Chem. A* 1998, 102, (24), 4568-4578.
73. Hirschorn, S. K.; Dinglasan, M. J.; Elsner, M.; Mancini, S. A.; Lacrampe-Couloume, G.; Edwards, E. A.; Sherwood Lollar, B., Pathway dependent isotopic fractionation during aerobic biodegradation of 1,2-dichloroethane. *Environ. Sci. Technol.* 2004, 38, (18), 4775 - 4781.
74. Elsner, M.; Zwank, L.; Hunkeler, D.; Schwarzenbach, R. P., A new concept linking observable stable isotope fractionation to transformation pathways of organic pollutants. *Environ. Sci. Technol.* 2005, 39, (18), 6896-6916.
75. Melander, L.; Saunders, W. H., *Reaction rates of isotopic molecules*. John Wiley: New York, 1980; p 331.
76. Mariotti, A.; Germon, J. C.; Hubert, P.; Kaiser, P.; Letolle, R.; Tardieux, A.; Tardieux, P., Experimental determination of nitrogen kinetic isotope fractionation: some principles; illustration for the denitrification and nitrification processes. *Plant and Soil* 1981, 62, 413-430.
77. Hayes, J. M., Fractionation of carbon and hydrogen isotopes in biosynthetic processes. *Rev. Mineral. Geochem.* 2001, 43, 225-277.
78. Griebler, C.; Safinowski, M.; Vieth, A.; Richnow, H. H.; Meckenstock, R. U., Combined application of stable carbon isotope analysis and specific metabolites determination for assessing in situ degradation of aromatic hydrocarbons in a tar oil-contaminated aquifer. *Environ. Sci. Technol.* 2004, 38, (2), 617-631.
79. Hunkeler, D.; Aravena, R.; Butler, B. J., Monitoring microbial dechlorination of tetrachloroethene (PCE) using compound-specific carbon isotope ratios: Microcosms and field experiments. *Environ. Sci. Technol.* 1999, 33, (16), 2733-2738.
80. Sherwood Lollar, B.; Slater, G. F.; Sleep, B.; Witt, M.; Klecka, G. M.; Harkness, M.; Spivack, J., Stable carbon isotope evidence for intrinsic bioremediation of tetrachloroethene and trichloroethene at Area 6, Dover Air Force Base. *Environ. Sci. Technol.* 2001, 35, 261-269.

81. Richnow, H. H.; Meckenstock, R. U.; Reitzel, L. A.; Baun, A.; Ledin, A.; Christensen, T. H., In situ biodegradation determined by carbon isotope fractionation of aromatic hydrocarbons in an anaerobic landfill leachate plume (Vejen, Denmark). *J. Contam. Hydrol.* 2003, *64*, (1-2), 59-72.
82. Meckenstock, R. U.; Morasch, B.; Matthias, K., M.; Vieth, A.; Richnow, H. H., Assessment of bacterial degradation of aromatic hydrocarbons in the environment by analysis of stable carbon isotope fractionation. *Water, Air, & Soil Pollution: Focus* 2002, *V2*, (3), 141-152.
83. Gray, J. R.; Lacrampe-Couloume, G.; Gandhi, D.; Scow, K. M.; Wilson, R. D.; Mackay, D. M.; Sherwood Lollar, B., Carbon and hydrogen isotopic fractionation during biodegradation of methyl *tert*-butyl ether. *Environ. Sci. Technol.* 2002, *36*, (9), 1931-1938.
84. McKelvie, J. R.; Hyman, M. R.; Elsner, M.; Smith, C.; Aslett, D. M.; Lacrampe-Couloume, G.; Sherwood Lollar, B., Isotopic fractionation of methyl *tert*-butyl ether suggests different initial reaction mechanisms during aerobic biodegradation. *Environ. Sci. Technol.* 2009, *43*, (8), 2793-2799.
85. Kuder, T.; Wilson, J. T.; Kaiser, P.; Kolhatkar, R.; Philp, P.; Allen, J., Enrichment of stable carbon and hydrogen isotopes during anaerobic biodegradation of MTBE: Microcosm and field evidence. *Environ. Sci. Technol.* 2005, *39*, (1), 213-220.
86. Northrop, D. B., The expression of isotope effects on enzyme-catalyzed reactions. *Ann. Rev. of Biochem.* 1981, *50*, 103-131.
87. Paneth, P., Heavy atom isotope effects on enzymatic reactions. *J. Mol. Struct.* 1994, *321*, 35-44.
88. Zwank, L.; Berg, M.; Elsner, M.; Schmidt, T. C.; Schwarzenbach, R. P.; Haderlein, S. B., New evaluation scheme for two-dimensional isotope analysis to decipher biodegradation processes: Application to groundwater contamination by MTBE. *Environ. Sci. Technol.* 2005, *39*, (4), 1018-1029.
89. Vogt, C.; Cyrus, E.; Herklotz, I.; Schlosser, D.; Bahr, A.; Herrmann, S.; Richnow, H.-H.; Fischer, A., Evaluation of toluene degradation pathways by two-dimensional stable isotope fractionation. *Environ. Sci. Technol.* 2008, *42*, (21), 7793-7800.
90. Fischer, A.; Herklotz, I.; Herrmann, S.; Thullner, M.; Weelink, S. A. B.; Stams, A. J. M.; Schlömann, M.; Richnow, H.-H.; Vogt, C., Combined carbon and hydrogen isotope fractionation investigations for elucidating benzene biodegradation pathways. *Environ. Sci. Technol.* 2008, *42*, (12), 4356-4363.
91. Elsner, M.; McKelvie, J.; LacrampeCouloume, G.; SherwoodLollar, B., Insight into methyl *tert*-butyl ether (MTBE) stable isotope fractionation from abiotic reference experiments. *Environ. Sci. Technol.* 2007, *41*, (16), 5693-5700.
92. Meyer, A. H.; Penning, H.; Lowag, H.; Elsner, M., Precise and accurate compound specific carbon and nitrogen isotope analysis of atrazine: critical role of combustion oven conditions. *Environ. Sci. Technol.* 2008, *42*, (21), 7757-7763.

93. Meyer, A. H.; Penning, H.; Elsner, M., C and N isotope fractionation suggests similar mechanisms of microbial atrazine transformation despite involvement of different Enzymes (AtzA and TrzN). *Environ. Sci. Technol.* 2009, 43, (21), 8079-8085.
94. Hartenbach, A. E.; Hofstetter, T. B.; Tentscher, P. R.; Canonica, S.; Berg, M.; Schwarzenbach, R. P., Carbon, hydrogen, and nitrogen isotope fractionation during light-Induced transformations of atrazine. *Environ. Sci. Technol.* 2008, 42, (21), 7751-7756.
95. Dybala-Defratyka, A.; Szatkowski, L.; Kaminski, R.; Wujec, M.; Siwek, A.; Paneth, P., Kinetic isotope effects on dehalogenations at an aromatic carbon. *Environ. Sci. Technol.* 2008, 42, (21), 7744-7750.

2.

Precise and Accurate Compound Specific Carbon and Nitrogen Isotope Analysis of Atrazine: Critical Role of Combustion Oven Conditions

Armin H. Meyer, Holger Penning, Harald Lowag, Martin Elsner

published in

Environmental Science & Technology, 42, 7757-7763, 2008

2.1 Introduction

Compound-specific stable isotope analysis (CSIA) by gas chromatography - isotope ratio mass spectrometry (GC -IRMS) allows determination of the isotope composition of organic substances in environmental samples. Over recent years, the method has become an increasingly valuable tool to assess the origin and fate of organic contaminants in the environment. On the one hand, isotope signatures may be considered like the fingerprint of an organic compound. Depending on the raw materials and the processes of synthesis, the same chemical substance may have different isotope signatures, which can make it possible to identify the original manufacturer and to allocate a source of contamination [1, 2]. On the other hand, CSIA may identify [3-6] and quantify [7, 8] transformation reactions of organic contaminants. A body of recent literature comprising such different contaminants as toluene [9, 10], benzene [11, 12], methyl *tert.*-butyl ether (MTBE) [6, 13, 14], chlorinated alkanes [3, 15] and ethenes [16-19] as well as nitroaromatic compounds [20, 21] has shown that degradation, due to the kinetic isotope effect associated with biotic and abiotic contaminant transformation, is generally accompanied by a significant enrichment of the heavier isotopes in the remaining contaminant, which may be characteristic of specific degradation pathways [5, 6]. Furthermore as summarized in [22], such values have been successfully used to derive estimates of degradation at contaminated field sites. Such applications, however, depend critically on a reliable instrumental method providing precise and accurate isotope data [23]. Commercially available GC-IRMS instruments, which analyze compounds in low amounts from complex samples in an automated on-line process, have found increasingly entrance into analytical laboratories [24]. As in conventional quantitative analysis, instruments separate individual compounds on a gas chromatography column. To prepare them for C and N isotope analysis, the analytes subsequently enter an interface and are combusted to CO₂, N₂, H₂O, NO_x etc. in a ceramic tube filled with CuO/NiO/Pt operating at 900-940°C [25, 26]. An adjacent reduction reactor converts NO_x species to N₂ providing the gas quantitatively for nitrogen isotope analysis and scavenging NO_x which would interfere with carbon isotope analysis [27]. Further treatment includes removal of water in a Nafion-membrane [28], trapping of CO₂ prior to N isotope analysis [27] and adjusting the He flow to the mass spectrometer using an open split [29].

Such a continuous flow setup is more complex and harbors more potential sources of bias than conventional dual inlet analysis which has traditionally been used to determine isotope values in

2. Precise and Accurate Compound Specific Carbon and Nitrogen Isotope Analysis of Atrazine

organic compounds. Also here, analytes are first combusted over CuO and then reduced with Cu giving CO₂ and N₂. Subsequently the gases are isolated, however, and introduced separately into the ion source of the IRMS so that they can be analyzed in repeated measurements against a reference gas of the same signal amplitude [30]. Accuracy is validated by bracketing these measurements with gases from standards prepared in the same way.

In contrast, GC-IRMS samples enter the MS as transient peaks in a He carrier stream so that time-dependent or instrument-specific mass discriminating effects prevent a similar reliability of the measurement [23]. Specifically, reference gas peaks do not always have the same amplitude as analyte peaks [31] and repeated comparative measurements of the same sample are not possible. Also, if isotopic fractionation occurs during sample injection, due to lack of baseline separation, peak distortion, incomplete combustion / reduction, or changing flow conditions at the open split [32, 33], these systematic errors cannot be corrected for by the reference gas, because it is introduced subsequent to the interface [32]. Whereas dual inlet measurements give a precision of better than 0.1‰ [31], standard deviations of GC-IRMS measurements are therefore about 0.3‰ and 0.7‰ for C and N, respectively, [24], and the total error incorporating both reproducibility and accuracy for C is reported as 0.5‰ [31]. Since discriminating parameters may change from compound to compound, it is mandatory to validate instrumental method GC-IRMS methods for every new substance, preferably in comparison to dual inlet measurements.

This study focuses on such a method validation for carbon isotope analysis of atrazine, a herbicide which has been widely used to control broadleaf weeds in agriculture. Leaching of atrazine and its metabolites has led to serious groundwater contamination so that its origin and fate in the environment is of major concern [34, 35]. Owing to the inability of conventional methods to establish complete mass balances and to assess all metabolites in natural systems, it is the aim of this study to establish CSIA for atrazine as a new method to assess the compound's fate in the subsurface.

Our objective was to test the right conditions for measurement of accurate and precise isotope values of atrazine compared to values determined by dual inlet measurements. The following different combustion reactor tube fillings were tested for carbon isotope analysis: (i) CuO, NiO, and Pt, operating at 940°C, as advertised by the manufacturer Thermo Fisher Scientific; (ii) CuO operating at 800°C, according to Merritt [36] and Matthews [37]; (iii) Ni/NiO, operating at 1150°C, according to Merritt [36]. Secondly, it was tested whether accurate and precise N isotope data can be obtained from pyrolytic conversion of atrazine in a Ni/NiO-furnace previously used for C carbon analysis. Finally, it was our objective to demonstrate the

2. Precise and Accurate Compound Specific Carbon and Nitrogen Isotope Analysis of Atrazine

applicability of the developed method by measuring isotope fractionation in an actual transformation experiment, hydrolysis of atrazine at 20°C and pH 12.

2.2 Experimental Section

2.2.1 Chemicals

Atrazine (1-chloro-3-ethylamino-5-isopropylamino-2,4,6-triazine, CAS: 1912-24-9) batches were from Chem Service (98%; West Chester, UK), Tropitzsch (97.7 %) and Riedel-de Haën (97.4%; supplied by Sigma Aldrich (Seelze, Germany). Ethyl acetate (CAS-Nr.: 141-78-6, 99.8% Riedel-de Haën, supplied by Sigma Aldrich, Taufkirchen, Germany) was used as solvent for standard solutions (GC-IRMS). Atrazine standards for GC-IRMS were adjusted to a carbon content of 1.9, 3.7, 7.4, 9.3 and 11.2 nmol and to a nitrogen content of 2.3, 4.7, 7.0, 9.3, 14.0, 18.6 and 23.3 nmol. Aqueous HPLC standards contained atrazine, hydroxyatrazine (CAS: 2163-68-0), desethylatrazine (CAS: 6190-65-4), and desisopropylatrazine (CAS: 1007-28-9) (96.0%, 99.9%, and 96.3%, respectively; all Riedel de Haën, supplied by Sigma Aldrich, Seelze, Germany) and had concentrations of 1, 2.5, 5, 7.5, 10 and 20 mg/L of the analytes. Acetonitrile (CAS.: 75-05-8) used as HPLC eluent was from Roth (Karlsruhe, Germany), Na₃PO₄ · 12H₂O (CAS: 10101-89-0) and Na₂HPO₄ · 2H₂O (CAS: 10028-24-7), and dichloromethane (CAS: 75-09-2) were purchased from Merck (Darmstadt, Germany).

2.2.2 Instrumentation

The GC-IRMS system consisted of a TRACE GC Ultra gas chromatograph (GC) (Thermo Fisher Scientific, Milan, Italy), which was coupled to a FinniganTM MAT 253 isotope ratio mass spectrometer (IRMS) (Thermo Fisher Scientific, Bremen, Germany) via a FinniganTM GC Combustion III Interface. The mass spectrometer was operated at an accelerating potential of 10 kV. Ions were generated by an electron impact of 70 eV. Emission energy for C isotope analyses was 1.5 mA and 2.0 mA for N isotope analyses. He of grade 5.0 was used as carrier gas. Samples were injected with a GC Pal autosampler (CTC, Zwingen, Switzerland). The split/splitless injector was operated for 1 min in splitless and then in split mode (split ratio 1:10) held at 250°C, with a flow rate of 1.4 mL min⁻¹. The analytical column was a DB-5 (30 m x 0,25 mm; 1 µm film; J&W Scientific, Folsom; CA, USA). The GC oven was programmed from 65 °C (hold: 1min), ramp 20 °C to 180 °C (hold: 10 min), ramp 15 °C/min to 230 °C (hold: 8 min).

2.2.3 Combustion reactors

Three different combustion reactors were used to oxidize atrazine for carbon isotope analyses. The first was a commercial ceramic tube filled with CuO/NiO/Pt-wire (Thermo Fisher Scientific, Bremen, Germany) operated at 940°C. The second and the third were self-made reactors consisting of a ceramic tube (inner diameter 0.8 mm, outer diameter 1.5 mm, length 33 cm, Friatec, Mannheim, Germany) containing three copper wires (diameter 0.1mm, length 26 cm, purity 99.99 %, Alfa Aesar, Karlsruhe, Germany), or three nickel wires (diameter 0.1 mm, length 15 cm, purity 99.99 %, Alfa Aesar, Karlsruhe, Germany) operating at 800°C and 1150°C, respectively. Prior to analyses the CuO/NiO/Pt and the Cu/CuO reactor were oxidized for 8h at 600°C in a continuous stream of O₂ passing through the reactor tube. The Ni/NiO reactor was reoxidized for two minutes during each gas chromatographic run, six minutes before the analyte peak appeared. Nitrogen isotope analyses were carried out with a Ni/NiO reactor which had been used for carbon isotope analysis before (287 injections). In contrast to carbon isotope analysis, the combustion reactor was not reoxidized. For reduction of nitrogen oxides in the He carrier stream of carbon and nitrogen analysis, a standard reduction reactor from Thermo Fisher Scientific (Bremen, Germany) was operated at 640°C subsequent to the combustion process, which contained in all setups three wires of copper.

The carbon isotopic composition of atrazine standards was determined in separate measurements by dual inlet analysis on a Delta S isotope ratio mass spectrometer (Finnigan MAT). For carbon isotope analysis 3 mg of atrazine were combusted at 960°C in the presence of CuO and O₂ in an automated system (CHN-O-Rapid, Heraeus) and were carried in a He stream through a Cu reduction reactor at 600°C. Combustion gases were separated in an automated cryotrapping system (CN-Version CT Box, Finnigan MAT) on traps operated at -80°C (H₂O) and -180°C (CO₂). CO₂ analyte gas was measured against reference gas calibrated with the international standards RM 8562, RM 8563, RM 8564. The precision of analysis was about ±0.1‰. CO₂ measurements were validated by bracketing with international (IAEA CH6) as well as laboratory standards (coffein, acetanilide).

The carbon and nitrogen isotopic composition of atrazine standards was also determined by elemental analyzer – isotope ratio mass spectrometry (EA-IRMS) consisting of EuroEA (EuroVector, Milano, Italy) coupled to a FinniganTM MAT 253 IRMS (Thermo Fisher Scientific, Bremen, Germany) by a FinniganTM ConFlo III Interface (Thermo Fisher Scientific, Bremen, Germany) and calibration against organic reference materials (USGS 40, USGS 41, IAEA 600)

2. Precise and Accurate Compound Specific Carbon and Nitrogen Isotope Analysis of Atrazine

provided by the International Atomic Agency (IAEA, Vienna). $\delta^{13}\text{C}$ - and $\delta^{15}\text{N}$ -values are reported in permil relative to Vienna PeeDee Belemnite (VPDB) and air respectively:

$$\delta^{13}\text{C} = \left[\left(\frac{{}^{13}\text{C}/{}^{12}\text{C}_{\text{Sample}} - {}^{13}\text{C}/{}^{12}\text{C}_{\text{Standard}}}{{}^{13}\text{C}/{}^{12}\text{C}_{\text{Standard}}} \right) \times 1000 \right] \text{ in } \text{‰} \quad (2_1)$$

$$\delta^{15}\text{N} = \left[\left(\frac{{}^{15}\text{N}/{}^{14}\text{N}_{\text{Sample}} - {}^{15}\text{N}/{}^{14}\text{N}_{\text{Standard}}}{{}^{15}\text{N}/{}^{14}\text{N}_{\text{Standard}}} \right) \times 1000 \right] \text{ in } \text{‰} \quad (2_2)$$

During carbon analysis by GC-IRMS, analytes were measured against a laboratory CO_2 standard gas that was introduced at the beginning and the end of each run. The laboratory standard was calibrated to V- PDB by reference CO_2 standards (RM 8562, RM 8563, RM 8564). In a similar way, an N_2 laboratory standard gas was used for nitrogen GC-IRMS analysis, which had been calibrated to air by reference materials (USGS 40, USGS 41, IAEA 601, USGS 34, and IAEA N-2). All reference standards were provided by the IAEA.

2.2.4 HPLC

Concentrations of atrazine and its degradation products were analyzed using a Shimadzu LC-10A series HPLC system. The column used was an ODS (30) (Ultracarb 5, 150 x 4.6 mm, Phenomenex, Aschaffenburg). Eluents and measuring conditions were the same as described in Berg et al. [38]. Oven-temperature was set to 45°C. Compounds were detected by UV absorbance at 220 nm and quantified by CLASS-VP V6.10 software (Shimadzu).

2.2.5 Hydrolysis experiment

Triplicate experiments were conducted at 20°C and pH 12 with phosphate-buffered (50 mM) aqueous (deionized water) atrazine solutions (1 L). Concentrations of atrazine were approximately 20 mg L⁻¹. Samples for quantification (150 µL) and isotope analysis (15 – 200 mL) were taken at each sampling event. For HPLC analysis, aqueous samples were used directly. For isotope analysis, aqueous samples were extracted with 5-10 mL dichloromethane, and afterwards dried at room temperature under the hood. Dried extracts were redissolved in ethyl acetate to a final atrazine concentration of about 100 mg L⁻¹. Tests with standards showed that fractionation introduced by the preparation steps was smaller than the analytical uncertainty of the method.

2.2.6 Carbon and nitrogen enrichment factors for hydrolysis of atrazine

Bulk isotope enrichment factors for carbon and nitrogen were determined as the slope of a linear regression according to the Rayleigh-equation :

2. Precise and Accurate Compound Specific Carbon and Nitrogen Isotope Analysis of Atrazine

$$\ln \frac{R_t}{R_0} = \varepsilon_{bulk} / 1000 \cdot \ln f \quad (2_3)$$

where the enrichment factor ε_{bulk} is a measure for the isotopic enrichment as average over all positions in a molecule, and R_t and R_0 are the compound-specific isotope ratios of heavy versus light isotopes at a given time and at the beginning of the reaction. C_t/C_0 is the fraction f of the remaining compound. The primary isotope effect of a given element present in a reacting bond (e.g., carbon in a C-Cl bond of atrazine) is position-specific. The corresponding primary position-specific apparent kinetic isotope effects (AKIE) can be calculated from bulk enrichment factors ε according to

$$AKIE \approx \frac{1}{(n \cdot \varepsilon_{bulk} / 1000 + 1)} \quad (2_4),$$

where n corresponds to the number of atoms of the element present in the molecule. In the case that atoms of the element of interest are located only in proximity to, or within a conjugated π -system next to the reacting bond (e.g., all nitrogen atoms present in atrazine), they contribute together to observable fractionation. In such a case secondary position-specific apparent kinetic isotope effects (AKIE) can be calculated according to

$$AKIE \approx \frac{1}{(n/x \cdot \varepsilon_{bulk} / 1000 + 1)} \quad (2_5),$$

where x is the number of atoms located in positions affected by the reaction [5]. As in atrazine all nitrogen atoms are located within the conjugated π -system, $x = n$ is assumed.

2.3 Results and Discussion

Method validation was performed with three different commercial products of atrazine spanning a $\delta^{13}\text{C}$ range of $-28.90\text{‰} \pm 0.10\text{‰}$ to $-27.95\text{‰} \pm 0.10\text{‰}$, as determined by dual inlet analysis and a $\delta^{15}\text{N}$ range of $-0.3\text{‰} \pm 0.2\text{‰}$ to $-1.5\text{‰} \pm 0.2\text{‰}$, as determined by continuous flow elemental analyzer - IRMS. For better comparability, all carbon isotope data measurements in this study are reported as deviations from these values (see Appendix A1, Table A1_1), $\Delta\delta^{13}\text{C}$ and $\Delta\delta^{15}\text{N}$.

2.3.1 Carbon isotope analysis of atrazine

Combustion conditions recommended by the manufacturer Thermo Fisher Scientific are commercially available ceramic tubes filled with CuO/NiO/Pt-wire that are operated at 940°C. As discussed in the introduction, this setup has served in the isotope analysis of a range of different organic chemicals, and no cases have been reported to date in which these conditions have been unsuccessful. In the case of atrazine, however, $\Delta\delta^{13}\text{C}$ data were obtained that scattered over a range of -5.8‰ to +1.1‰ (Figure 2_1a) resulting in an accuracy and precision prohibitory for reliable isotope analysis of atrazine.

Merritt et al. [36] report alternative combustion conditions that allowed accurate and precise carbon isotope analysis for different n-alkanes and aromatic compounds (mean $\Delta\delta^{13}\text{C}$: 0.01 - 0.22 ‰; s.d.: 0.20-0.28‰). They used a self-made combustion furnace containing three oxidized Cu wires which was operated at 800°C. We tested the same setup for analysis of atrazine and obtained precise, but inaccurate data with $\Delta\delta^{13}\text{C}$ values that were systematically depleted in ^{13}C with a mean of -1.3‰ (Figure 2_1b). Similarly, Hartenbach et al. observed a systematic bias of -1.2‰ when using a commercial CuO/NiO/Pt reactor operated at 800°C [39]. If such data is reported without accuracy check, it would lead to erroneous results illustrating the necessity to always bracket samples with standards of the same substance and known isotopic composition. Such practice makes it possible to correct in principle also for the systematic inaccuracy of $\Delta\delta^{13}\text{C} = -1.3‰$. Moreover, the offset cancels out in degradation studies where the focus is on isotopic differences to the beginning of a reaction. Nonetheless, systematically inaccurate values indicate incomplete conversion in the GC-IRMS system suggesting substance losses by a non-controlled process. If atrazine is analyzed in natural samples and data is compared to values from other laboratories, a truly accurate method is therefore overall preferable. A second alternative reported by Merritt et al. [36] is the use of a self-made Ni/NiO oven, operating at 1150 °C. In contrast to their approach, where oxidation of the nickel oven took place prior to a bulk of measurements, or where alternatively a trickling stream of oxygen was applied during each run, we carried out a reoxidation for two minutes during each analytical run. Figure 2_1c shows data for analysis of atrazine according to this oxidation setup from a total of two different self-made Ni/NiO ovens. It illustrates that, after a reproducible conditioning phase of about 60 injections, precise and accurate data were obtained, with an overall mean $\Delta\delta^{13}\text{C}$ of -0.1‰ to 0.2 ‰ and a standard deviation of $\pm 0.4‰$ (Figure 2_1c, see also Table A1_1 in

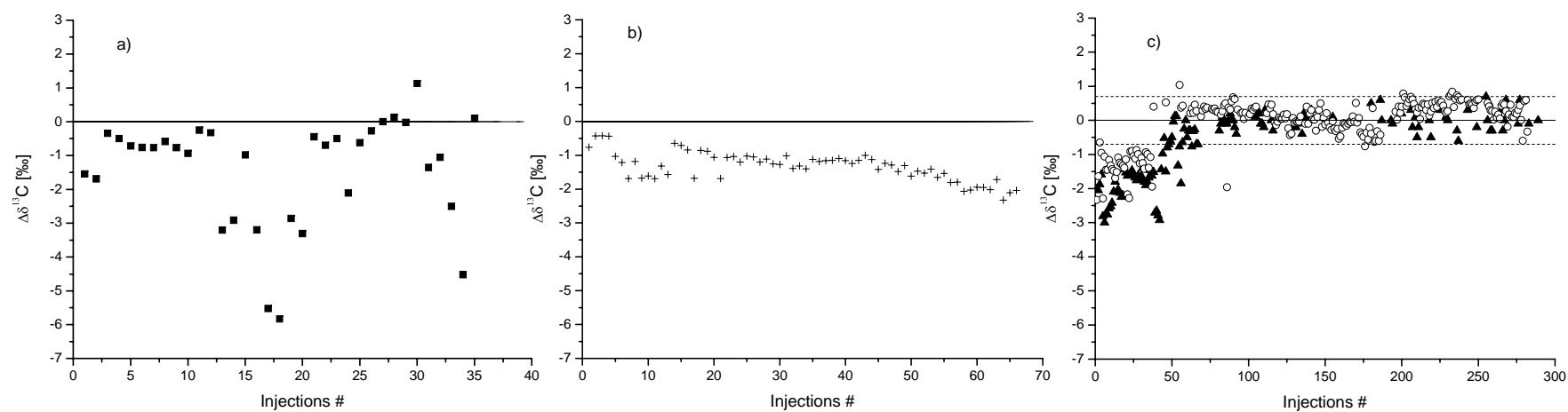


Figure 2_1. $\Delta\delta^{13}\text{C}$ values of different atrazine standards using different combustion reagents. a) CuO/NiO/Pt operating at 940°C (35 injections); b) CuO operating at 800°C (65 injections); c) Ni/NiO operating at 1150°C, different symbols (triangle and circles) represent two different Ni/NiO ovens (289 and 287 injections, respectively). $\Delta\delta^{13}\text{C}$ data represent deviations from the values of the different atrazine standards measured by dual inlet analysis. Dashed lines in panel c) indicate the total uncertainty of measurements with the Ni/NiO oven ($\pm 0.7\text{‰}$) after an initial conditioning period of about 60 runs.

2. Precise and Accurate Compound Specific Carbon and Nitrogen Isotope Analysis of Atrazine

Appendix A1). Importantly, greater amplitudes (Figure 2_2a) were obtained compared to the CuO and CuO/NiO/Pt ovens indicating a more efficient conversion. The conditioning for about 60 injections (of 7.4 nmol C each) needed to obtain accurate values corresponded to a week-end of automated injections (Figure 2_1c). After that the first Ni/NiO oven lasted for 230 measurements and the second was used equally long and could afterwards even be employed for nitrogen isotope analysis (see below). The linearity plot of Figure 2_2b illustrates that after conditioning a minimum amplitude (m/z 44) of 1300 mV was required for precise and accurate data corresponding to an amount of 2 nmol carbon. For signal sizes up to 8120 mV (corresponding to 7.5 nmol C) isotope measurements were consistent. We note that we observed one outlier after about 90 injections (Figure 1c, 2b) which can not be discarded on the basis of chromatographic peak shape or peak separation. Since it was not reproduced, however, any similar outliers would be identified by routine duplicate analysis of samples so that we conclude the overall validity of our method was not affected.

Also Merritt et al. [36] observed that conditioning of Ni/NiO reactors was necessary for accurate analyses of n-alkanes, albeit with fewer runs, when an oven operating temperature below 1050°C was used. In contrast to their observations, conditioning could not even be avoided at an operating temperature of 1150°C in our study. However, no memory effects were observed if different atrazine products were analyzed in sequence, and there was no difference in the signal area between the conditioning phase and afterwards indicating that a constant amount of C reached the analyzer over time. We hypothesize that conditioning leads to Ni-C compounds forming a coating on the nickel wires that results in improved combustion conditions and greater accuracy after the initial conditioning phase. In conclusion, we found that the conversion of atrazine needs high temperature conditions to obtain accurate and precise C isotope data (Figure 2_1). In comparison to CuO/NiO/Pt and CuO combustion ovens, the Ni/NiO combustion reactor showed the most reproducible performance with precise and accurate data compared to the values measured by EA-IRMS.

2. Precise and Accurate Compound Specific Carbon and Nitrogen Isotope Analysis of Atrazine

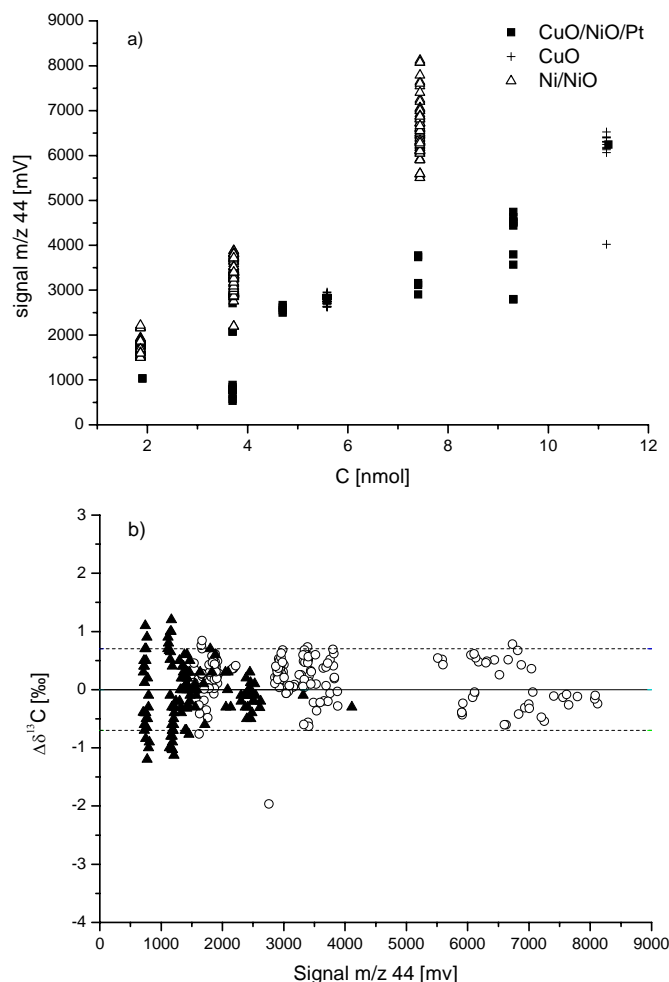


Figure 2_2. a) Peak amplitudes of m/z 44 for different amounts of injected carbon shown for three different ovens. b) Linearity of $\Delta\delta^{13}\text{C}$ values of atrazine as a function of signal size. Different symbols (triangle and circles) represent two different Ni/NiO ovens. Dashed lines in panel b) indicate the total uncertainty of measurements with the Ni/NiO oven ($\pm 0.7\text{‰}$) for peak amplitudes (m/z 44) greater than 1300 mV.

2.3.2 Nitrogen isotope analysis of atrazine

The nickel reactor setup used for successful carbon isotope analysis was also tested for nitrogen isotope analysis of atrazine, however, without reoxidation during each analysis. Nitrogen isotope data of atrazine were accurate and precise showing an average off-set of 0.2‰ compared to elemental analyzer measurements and a standard deviation of $\pm 0.3\text{‰}$ (Figure 2_3a, see also Table A1_1 in A1), which is in good agreement with results of Merritt and Hayes [27] using an comparable setup. Linearity was excellent giving good precision down to N signals (m/z 28) of

2. Precise and Accurate Compound Specific Carbon and Nitrogen Isotope Analysis of Atrazine

270 mV, corresponding to an amount of 2.3 nmol N (Figure 2_3b). Unlike in nitrogen analysis using oxidative conversion by common

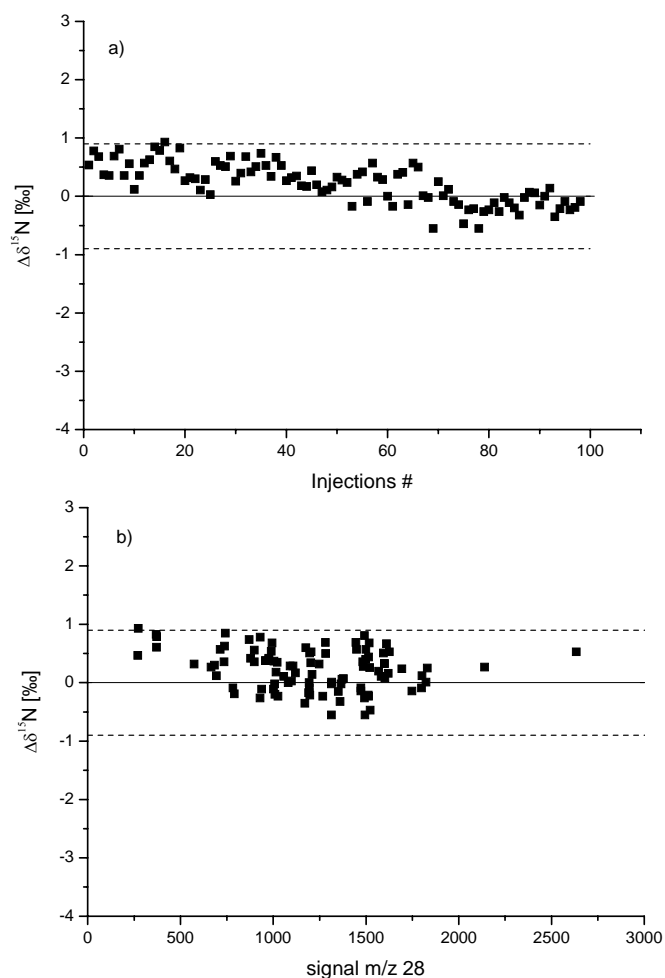


Figure 2_3. $\Delta\delta^{15}\text{N}$ values of atrazine obtained with a Ni/NiO oven which had previously been used for carbon measurements. Oven was operated at 1150°C and was not reoxidized (99 injections). $\Delta\delta^{15}\text{N}$ values are given as deviations from the values of the different atrazine standards measured by dual inlet analysis. Dashed lines indicate the total uncertainty of $\pm 0.9\text{‰}$ associated with measurements. a) Results as a function of injection number. b) Results as a function of signal size m/z 28.

CuO/NiO/Pt ovens, formation of NO was of minor concern. This is indicated by the signal of mass 30 (300 times amplified compared to mass 28) which was about 10 times smaller compared to the signal of mass 28, irrespective of the amount of N (2,3 – 23 nmol) passing the furnace. If

2. Precise and Accurate Compound Specific Carbon and Nitrogen Isotope Analysis of Atrazine

trace amounts were formed, they were, therefore, successfully removed by subsequent conversion in the reduction reactor. Reoxidation of the Ni/NiO reactor for 2 minutes was tested, but led to a significant increase in the signal of mass 30 resulting in enriched nitrogen isotope signatures. Nitrogen isotope analysis was therefore consistently conducted without reoxidation of the Ni reactor. Also CO may potentially be formed from carbon and traces of NiO leading to artifacts on the mass 28. We, therefore, tested toluene (38 nmol C/toluene) – a nitrogen free compound – as negative control. No detectable signal for the mass 28 was observed indicating the absence of significant interferences from CO. In conclusion, we obtained reliable N isotope measurements with a Ni oven setup which, in the case of atrazine, provides an expedient alternative to the common oxidative method.

2.3.3 Hydrolysis experiment

To test the applicability of our method in an experimental system, we carried out a hydrolysis experiment at pH 12 and 20°C. Hydroxylatrazine was the only detectable product. The observed pseudo-first order rate constant of hydrolysis was $2.5 \times 10^{-7} \pm 8.3 \times 10^{-9} \text{ s}^{-1}$ (Figure 2_4a). Evaluation according to the Rayleigh equation (Figure 4b) yielded excellent regression data demonstrating that our validated method was indeed robust and reliable (see also plot of standards bracketing the sample measurements in Figure A1_1 in the A1). Bulk isotope enrichment factors for carbon and nitrogen were derived from the slopes of the Rayleigh plots (Figure 4b) giving $\epsilon_{\text{carbon}} = -5.6 \pm 0.1\text{‰}$ and $\epsilon_{\text{nitrogen}} = -1.2 \pm 0.1 \text{‰}$, respectively. Assuming that the carbon isotope effect is primary – i.e., that it is predominantly expressed at the position where Cl is replaced by OH - an apparent kinetic isotope effect of 1.047 can be calculated according to equation 4. In contrast, nitrogen isotope effects in this reaction are secondary, since all the nitrogen atoms are embedded in the aromatic π -system that is disturbed by reaction at the C-Cl position. This is in analogy to computational calculations for the acid-catalyzed hydrolysis of triazines [40], a nucleophilic aromatic substitution via Meisenheimer complexes. All nitrogen atoms experience a small, but non-negligible isotope fractionation which cannot be deconvolved with our method so that an average AKIE value over all nitrogen atoms of 1.001 is calculated. To our knowledge, these are the first isotope effects reported for a nucleophilic aromatic substitution.

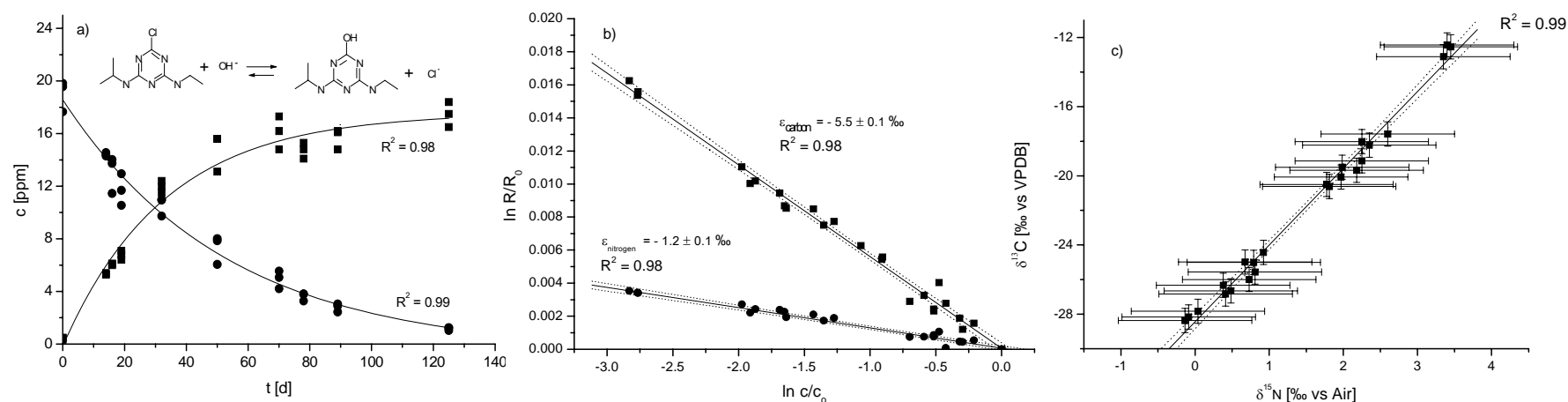


Figure 2_4. Hydrolysis of atrazine at pH 12 and 20°C. a) Concentrations of atrazine (circles) and of the only degradation product hydroxyatrazine (squares) over time. b) Logarithmic plot of isotope ratios according to the Rayleigh equation for carbon (squares) and nitrogen (circles) (Equation 3). c) Two dimensional isotope plot of carbon and nitrogen atrazine isotope ratios. Error bars indicate the total uncertainty of carbon isotope ($\pm 0.7\text{‰}$) and nitrogen isotope measurements ($\pm 0.9\text{‰}$) corresponding to the ranges indicated in Figures 1 to 3. Dotted lines represent 95 % confidence intervals of linear regressions.

2.3.4 Environmental significance

The significance of this study is two fold. On the one hand, we caution that the conditions advertised for commercially available GC-IRMS systems may not always give accurate isotope values, but always require validation and, in some cases like atrazine, further optimization. This has important consequences for trace compounds. For example if metabolites in natural samples cannot be obtained in sufficient quantities for independent dual-inlet characterization, isotope measurements via GC-IRMS must be communicated with great caution.

On the other hand, this study has successfully identified conditions that allow accurate and precise compound specific isotope analysis of carbon and nitrogen in atrazine. In the case of carbon, a self-made Ni/NiO reactor led to efficient conversion to CO₂ if it was operated at elevated temperature (1150°C), and shortly (2 min) reoxidized in each chromatographic run. We thereby provide a method that allows two-dimensional isotopic characterization of atrazine (Figure 4c) giving superb resolution for fingerprinting in environmental forensics [1] as well as to obtain mechanistic elucidation in transformation studies [4, 5, 14, 41]. Our first data on isotope fractionation associated with alkaline hydrolysis of atrazine shows very different trends compared to a parallel study on atrazine photo-transformation [39]. This demonstrates the potential of the method to provide two-dimensional isotopic patterns which help assess the fate of atrazine in natural transformation reactions.

Supporting Information Available in Appendix A1

2.4 References

1. Shouakar-Stash, O.; Frappe, S. K.; Drimmie, R. J., Stable hydrogen, carbon and chlorine isotope measurements of selected chlorinated organic solvents. *J. Contam. Hydrol.* 2003, 60, (3-4), 211-228.
2. Schmidt, T. C.; Zwank, L.; Elsner, M.; Berg, M.; Meckenstock, R. U.; Haderlein, S. B., Compound-specific stable isotope analysis of organic contaminants in natural environments: a critical review of the state of the art, prospects, and future challenges. *Anal. Bioanal. Chem.* 2004, 378, (2), 283-300.

2. Precise and Accurate Compound Specific Carbon and Nitrogen Isotope Analysis of Atrazine

3. Hirschorn, S. K.; Dinglasan, M. J.; Elsner, M.; Mancini, S. A.; Lacrampe-Couloume, G.; Edwards, E. A.; Sherwood Lollar, B., Pathway dependent isotopic fractionation during aerobic biodegradation of 1,2-dichloroethane. *Environ. Sci. Technol.* 2004, 38, (18), 4775 - 4781.
4. Zwank, L.; Berg, M.; Elsner, M.; Schmidt, T. C.; Schwarzenbach, R. P.; Haderlein, S. B., New evaluation scheme for two-dimensional isotope analysis to decipher biodegradation processes: Application to groundwater contamination by MTBE. *Environ. Sci. Technol.* 2005, 39, (4), 1018-1029.
5. Elsner, M.; Zwank, L.; Hunkeler, D.; Schwarzenbach, R. P., A new concept linking observable stable isotope fractionation to transformation pathways of organic pollutants. *Environ. Sci. Technol.* 2005, 39, (18), 6896-6916.
6. Elsner, M.; McKelvie, J.; LacrampeCouloume, G.; SherwoodLollar, B., Insight into methyl tert-butyl ether (MTBE) stable isotope fractionation from abiotic reference experiments. *Environ. Sci. Technol.* 2007, 41, (16), 5693-5700.
7. Sherwood Lollar, B.; Slater, G. F.; Sleep, B.; Witt, M.; Klecka, G. M.; Harkness, M.; Spivack, J., Stable carbon isotope evidence for intrinsic bioremediation of tetrachloroethene and trichloroethene at Area 6, Dover Air Force Base. *Environ. Sci. Technol.* 2001, 35, 261-269.
8. Abe, Y.; Hunkeler, D., Does the Rayleigh equation apply to evaluate field isotope data in contaminant hydrogeology? *Environ. Sci. Technol.* 2006, 40, (5), 1588-1596.
9. Mancini, S. A.; Hirschorn, S. K.; Elsner, M.; Lacrampe-Couloume, G.; Sleep, B. E.; Edwards, E. A.; SherwoodLollar, B., Effects of trace element concentration on enzyme controlled stable isotope fractionation during aerobic biodegradation of toluene. *Environ. Sci. Technol.* 2006, 40, (24), 7675-7681.
10. Morasch, B.; Richnow, H. H.; Vieth, A.; Schink, B.; Meckenstock, R. U., Stable isotope fractionation caused by glyxyl radical enzymes during bacterial degradation of aromatic compounds. *Appl. Environ.l Microbiol.* 2004, 70, (5), 2935-2940.
11. Mancini, S. A.; Ulrich, A. E.; Lacrampe-Couloume, G.; Sleep, B.; Edwards, E. A.; Sherwood Lollar, B., Carbon and hydrogen isotopic fractionation during anaerobic biodegradation of benzene. *Appl. Environ.l Microbiol.* 2003, 69, (1), 191-198.
12. Hunkeler, D.; Andersen, N.; Aravena, R.; Bernasconi, S. M.; Butler, B. J., Hydrogen and carbon isotope fractionation during aerobic biodegradation of benzene. *Environ. Sci. Technol.* 2001, 35, 3462-3467.
13. Kuder, T.; Wilson, J. T.; Kaiser, P.; Kolhatkar, R.; Philp, P.; Allen, J., Enrichment of stable carbon and hydrogen isotopes during anaerobic biodegradation of MTBE: microcosm and field evidence. *Environ. Sci. Technol.* 2005, 39, (1), 213-220.

2. Precise and Accurate Compound Specific Carbon and Nitrogen Isotope Analysis of Atrazine

14. Rosell, M.; Barcelo, D.; Rohwerder, T.; Breuer, U.; Gehre, M.; Richnow, H. H., Variations in $^{13}\text{C}/^{12}\text{C}$ and D/H enrichment factors of aerobic bacterial fuel oxygenate degradation. *Environ. Sci. Technol.* 2007, *41*, (6), 2036-2043.
15. Elsner, M.; Cwiertny, D. M.; Roberts, A. L.; SherwoodLollar, B., 1,1,2,2-Tetrachloroethane reactions with OH-, Cr(II), granular iron, and a copper-iron bimetal: insights from product formation and associated carbon isotope fractionation. *Environ. Sci. Technol.* 2007, *41*, (11), 4111-4117.
16. Nijenhuis, I.; Andert, J.; Beck, K.; Kastner, M.; Diekert, G.; Richnow, H. H., Stable isotope fractionation of tetrachloroethene during reductive dechlorination by *Sulfurospirillum multivorans* and *Desulfitobacterium* sp. Strain PCE-S and abiotic reactions with cyanocobalamin. *Appl. Environ. Microbiol.* 2005, *71*, (7), 3413-3419.
17. Lee, P. K. H.; Conrad, M. E.; Alvarez-Cohen, L., Stable carbon isotope fractionation of chloroethenes by dehalorespiring isolates. *Environ. Sci. Technol.* 2007, *41*, (12), 4277-4285.
18. Slater, G. F.; Sherwood Lollar, B.; Sleep, B. E.; Edwards, E. A., Variability in carbon isotopic fractionation during biodegradation of chlorinated ethenes: implications for field applications. *Environ. Sci. Technol.* 2001, *35*, (5), 901-907.
19. Hunkeler, D.; Aravena, R.; Cox, E., Carbon isotopes as a tool to evaluate the origin and fate of vinyl chloride: laboratory experiments and modeling of isotope evolution. *Environ. Sci. Technol.* 2002, *36*, 3378-3384.
20. Hartenbach, A.; Hofstetter, T. B.; Berg, M.; Bolotin, J.; Schwarzenbach, R. P., Using nitrogen isotope fractionation to assess abiotic Reduction of nitroaromatic compounds. *Environ. Sci. Technol.* 2006, *40*, (24), 7710-7716.
21. Tobler, N. B.; Hofstetter, T. B.; Schwarzenbach, R. P., Assessing iron-mediated oxidation of toluene and reduction of nitroaromatic contaminants in anoxic environments using compound-specific isotope analysis. *Environ. Sci. Technol.* 2007, *41*, (22), 7773-7780.
22. Meckenstock, R. U.; Morasch, B.; Griebler, C.; Richnow, H. H., Stable isotope fractionation analysis as a tool to monitor biodegradation in contaminated aquifers. *J. Contam. Hydrol.* 2004, *75*, (3-4), 215-255.
23. Werner, R. A.; Brand, W. A., Referencing strategies and techniques in stable isotope ratio analysis. *Rapid Commun. Mass Spectrom.* 2001, *15*, 501-519.
24. Sessions, A. L., Isotope-ratio detection for gas chromatography. *J. Sep. Sci.* 2006, *29*, 1946-1961.
25. Brand, W. A., High precision isotope ratio monitoring techniques in mass spectrometry. *J. Am. Soc. Mass Spectr.* 1996, *31*, (3), 225-235.

2. Precise and Accurate Compound Specific Carbon and Nitrogen Isotope Analysis of Atrazine

26. Meier-Augenstein, W., Applied gas chromatography coupled to isotope ratio mass spectrometry. *J. Chromatogr. A* 1999, *842*, 351–371.
27. Merritt, D. A.; Hayes, J. M., Nitrogen isotopic analyses by isotope-ratio-monitoring gas chromatography / mass Spectrometry. *Journal of the American Society for Mass Spectrometry* 1994, *5*, 387-397.
28. Brand, W. A., Mass spectrometer hardware for analyzing stable isotope ratios. In *Handbook of Stable Isotope Analytical Techniques, Volume-I*, Groot, P. A. d., Ed. Elsevier B.V.: 2004; pp 835-857.
29. Merritt, D. A.; Brand, W. A.; Hayes, J. M., Isotope-ratio-monitoring gas chromatography mass-spectrometry: methods for isotopic calibration. *Org. Geochem.* 1994, *21*, 573-583.
30. McKinney, C. R.; McCrea, J. M.; Epstein, S.; Allen, H. A.; Urey, H. C., Improvements in mass spectrometers for the measurement of small differences in isotopic abundance ratios. *Rev. Sci. Instrum.* 1950, *21*, 724-730.
31. SherwoodLollar, B.; Hirschorn, S. K.; Chartrand, M. M. G.; Lacrampe-Couloume, G., An approach for assessing total instrumental uncertainty in compound-specific carbon isotope analysis: implications for environmental remediation studies. *Anal. Chem.* 2007, *79*, (9), 3469-3475.
32. Meier-Augenstein, W., A reference gas inlet module for internal isotopic calibration in high precision gas chromatography/combustion-isotope ratio mass spectrometry. *Rapid Commun. Mass Spectrom.* 1997, *11*, 1775-1780.
33. Blessing, M.; Jochmann, M.; Schmidt, T., Pitfalls in compound-specific isotope analysis of environmental samples. *Analytical and Bioanalytical Chemistry* 2008, *390*, (2), 591-603.
34. Tappe, W.; Groeneweg, J.; Jantsch, B., Diffuse atrazine pollution in German aquifers. *Biodegradation* 2002, *13*, (1), 3-10.
35. Graziano, N.; McGuire, M. J.; Roberson, A.; Adams, C.; Jiang, H.; Blute, N., 2004 National atrazine occurrence monitoring program using the abraxaxis ELISA method. *Environ. Sci. Technol.* 2006, *40*, (4), 1163-1171.
36. Merritt, D. A.; Freeman, K. H.; Ricci, M. P.; Studley, S. A.; Hayes, J. M., Performance and optimization of a combustion interface for isotope ratio monitoring gas-chromatography mass-spectrometry. *Analytical Chemistry* 1995, *67*, (14), 2461-2473.
37. Matthews, D. E.; Hayes, J. M., Isotope-ratio-monitoring gas chromatography-mass spectrometry. *Analytical Chemistry* 1978, *50*, (11), 1465-1473.

2. Precise and Accurate Compound Specific Carbon and Nitrogen Isotope Analysis of Atrazine

38. Berg, M.; Mueller, S. R.; Schwarzenbach, R. P., Simultaneous determination of triazines including atrazine and their major metabolites hydroxyatrazine, desethylatrazine, and deisopropylatrazine in natural waters. *Anal. Chem.* 1995, *67*, (11), 1860-1865.
39. Hartenbach, A. E.; Hofstetter, T. B.; Tentscher, P. R.; Canonica, S.; Berg, M.; Schwarzenbach, R. P., Carbon, hydrogen, and nitrogen isotope fractionation during light-induced transformations of Atrazine. *Environ. Sci. Technol.* 2008, *42*,(21), 7751-7756.
40. Sawunyama, P.; Bailey, G. W., Computational chemistry study of the environmentally important acid-catalyzed hydrolysis of atrazine and related 2-chloro-s-triazines. *Pest. Manag. Sci* 2002, *58*, (8), 759-768.
41. Whiticar, M. J., Carbon and hydrogen isotope systematics of bacterial formation and oxidation of methane. *Chem.Geol.* 1999, *161*, (1-3), 291-314.

3.

C and N Isotope Fractionation Suggests Similar Mechanisms of Microbial Atrazine Transformation despite Involvement of Different Enzymes (AtzA and TrzN)

Armin H. Meyer, Holger Penning, Martin Elsner

published in

Environmental Science & Technology, 43, 8079-8085, 2009

3. C and N Isotope Fractionation Suggests Similar Mechanism of Microbial Atrazine Transformation despite Involvement of Different Enzymes (AtzA and TrzN)

3.1 Introduction

Atrazine has been widely used for broadleaf and grassy weed control in the agricultural production of corn, sugarcane, sorghum and others [1]. Due to its high persistence atrazine and its primary metabolites have become frequent pollutants of surface and groundwater and therefore their fate is of considerable environmental concern [2]. Biotransformation of atrazine in the environment may occur by two alternative initial transformation mechanisms: either by oxidative dealkylation leading to formation of desethyl- and desisopropylatrazine, or by hydrolysis, leading to the formation of the dehalogenated product hydroxyatrazine [3, 4]. While the dealkylated products retain their herbicidal mode of action, the hydroxylated compound is not herbicidal anymore representing a more direct route of detoxification (1), and evidence for the importance of this pathway has been increasing over recent years (5). Such hydrolysis of atrazine may be catalyzed by the enzymes AtzA and TrzN. Although these enzymes are both member of the amidohydrolase superfamily, amino acid sequence relatedness between them is only 27%, indicating that they have evolved independently from different ancestors [5].

Two scientific questions are of particular aspect in this context. (i) In order to address the great interest in the evolutionary history of such catabolic enzymes [6], it is very interesting to know whether AtzA and TrzN catalyze the hydrolysis reaction in the same way. (ii) In order to assess the fate of atrazine in the environment, new tools are needed whose insight is complementary to existing approaches. Specifically, hydroxyatrazine may be immobilised by sorption, possibly through bound residues, in the pedosphere [7-11] so that concentrations of hydroxyatrazine in natural water samples are often below detection limit. The common practice of using desethylatrazine-to-atrazine or desisopropylatrazine-to-atrazine ratios as indicators for degradation and mobility in the environment [12-14] may therefore considerably underestimate the total extent of degradation. Owing to the difficulty of establishing complete mass balances in the subsurface, assessing the origin and fate of atrazine and its metabolite hydroxyatrazine is therefore still of major concern.

Compound specific isotope analysis (CSIA) is a promising alternative to identify [15-17] and quantify [18, 19] transformation reactions of organic compounds in aqueous environments. This approach traces the isotopic shift during transformation reactions in the remaining substance even without the need of metabolite detection. The pattern of isotope fractionation depends on the kinetic isotope effect (KIE), which is distinct for different types of reaction mechanism [20, 21]. The observable amount of isotopic enrichment in an organic compound can be expressed by the isotope enrichment factor ϵ , derived from the Rayleigh equation, and has to be determined experimentally in

3. C and N Isotope Fractionation Suggests Similar Mechanism of Microbial Atrazine Transformation despite Involvement of Different Enzymes (AtzA and TrzN)

lab experiments. Although this concept has been successfully used to identify and even to quantify degradation processes, enrichment factors ϵ may nonetheless show considerable variability even for the same compound and the same transformation pathway [22, 23]. The reason is that biotic transformation processes involve preceding steps such as uptake, transport to reactive sites or formation of enzyme-substrate complexes [24]. If such preceding processes are slow and the intrinsic chemical reaction is fast in comparison, the biotransformation is committed. Almost every substrate molecule that reaches the reactive site is then converted, irrespective of its isotopic composition [20]. Consequently, observable isotope fractionation reflects only to a small part the intrinsic isotope effect KIE of the actual bond cleavage and to a great part that of the preceding steps [25]. The KIE is then generally masked and a smaller apparent kinetic isotope effect (AKIE) is observed. Fortunately, slopes in dual isotope plots (i.e., diagrams plotting changes in isotope ratios of one element relative to another) are much less affected than the isotope effects. In the case of non-fractionating steps they remain the same, since KIE of both elements are masked to the same degree. In the case of slight fractionation, slopes represent an additional isotope effect from preceding steps that may differ slightly between elements. In recent studies, dual isotope plots provided essential lines of evidence to distinguish different transformation mechanisms [17, 20, 26], as shown for MTBE, toluene and isoproturon [16, 22, 27].

Recent studies in environmental and computational chemistry have already demonstrated that the transformation of atrazine in abiotic reactions is accompanied by significant carbon and nitrogen isotope fractionation [28-30]. In this work we determine for the first time isotope fractionation of carbon and nitrogen associated with biotic hydrolytic degradation of atrazine. A first major aim of our study was to test isotope fractionation as an alternative way of qualitatively detecting, and possibly even quantifying natural transformation of atrazine to hydroxyatrazine. A second major aim was to address the question whether AtzA and TrzN catalyze the hydrolysis reaction in the same way. To this end we used in our experiments the two bacterial strains *Chelatobacter heintzii* [31] and *Pseudomonas* sp. ADP [32] containing the AtzA [33] enzyme and the strain *Arthrobacter aureescens* TC1 [34] containing the TrzN enzyme [35]. As a reference system for a better understanding of the underlying hydrolytic reaction mechanism, carbon and nitrogen isotope fractionation was also determined in abiotic hydrolysis experiments under alkaline and acidic conditions.

3. C and N Isotope Fractionation Suggests Similar Mechanism of Microbial Atrazine Transformation despite Involvement of Different Enzymes (AtzA and TrzN)

3.2 EXPERIMENTAL SECTION

3.2.1 Chemicals

Atrazine (1-chloro-3-ethylamino-5-isopropylamino-2,4,6-triazine, CAS: 1912-24-9) was purchased from Tropitzsch (97.7 %). Ethyl acetate (99.8% Riedel-de Haën, supplied by Sigma Aldrich, Taufkirchen, Germany) was used as a solvent for standard solutions (GC-IRMS). Atrazine standards for GC-IRMS were adjusted to 200, 300, 400 mg/L. Aqueous HPLC standards contained atrazine, hydroxyatrazine (CAS: 2163-68-0), desethylatrazine (CAS: 6190-65-4), and desisopropylatrazine (CAS: 1007-28-9) (96.0%, 99.9%, and 96.3%, respectively; all Riedel de Haën, supplied by Sigma Aldrich, Seelze, Germany) and had concentrations of 1, 2.5, 5, 7.5, 10 and 20 mg/L of the analytes. Acetonitrile used as HPLC eluent was from Roth (Karlsruhe, Germany), $\text{Na}_3\text{PO}_4 \cdot 12\text{H}_2\text{O}$ and $\text{Na}_2\text{HPO}_4 \cdot 2\text{H}_2\text{O}$, and dichloromethane were purchased from Merck (Darmstadt, Germany).

3.2.2 Bacterial strains and cultivation media

Chelatobacter heintzii and *Pseudomonas* sp. ADP were kindly provided by S. R. Sørensen (GEUS, Denmark). *Arthrobacter aurescens* TC1 was kindly provided by L. P. Wackett (The BioTechnology Institute, University of Minnesota). All strains were grown in mineral salt medium (MSM, see Appendix A2), supplemented with 100 mg L⁻¹ of glucose and 100 mg/L sodium citrate (Roth, Karlsruhe, Germany) and 20 mg L⁻¹ atrazine. The strains were harvested in the late-exponential growth phase and washed twice in sterile 50 mM phosphate buffer. For the degradation experiments, cell pellets of each strain were dissolved in 1 mL of 50 mM sterile phosphate buffer and added to MSM supplemented with 12-20 mg L⁻¹ atrazine (resting cell experiment). All experiments were performed in triplicate at 21°C.

3.2.3 Abiotic hydrolysis

Triplicate experiments were carried out for pH 3 and pH 12 with phosphate-buffered (50 mM) aqueous (deionized water) atrazine solutions (500 mL) at 60°C. The elevated temperature was chosen because an ongoing pH 3 experiment conducted at 20°C had a reaction time longer than two years. Initial concentrations of atrazine were approximately 20 mg L⁻¹.

3.2.4 Sampling and preparation for quantification and isotope analysis

At each sampling event, samples were taken for quantification (150 µL) and isotope analysis (15 – 200 mL) of atrazine. For quantification of atrazine and hydroxyatrazine concentrations by HPLC

3. C and N Isotope Fractionation Suggests Similar Mechanism of Microbial Atrazine Transformation despite Involvement of Different Enzymes (AtzA and TrzN)

analysis, aqueous samples were used directly. For isotope analysis, aqueous samples were extracted with 5-10 mL dichloromethane, which was subsequently dried at room temperature under the hood. Dried extracts were redissolved in ethyl acetate to a final atrazine concentration of about 200 mg L⁻¹. Tests with standards showed that fractionation introduced by the preparation steps was smaller than the analytical uncertainty of the method [30].

3.2.5 Quantification of atrazine and its metabolites

Concentrations of atrazine and its degradation products were analyzed using a Shimadzu LC-10A series HPLC system. The column used was an ODS (30) (Ultrasorb 5, 150 x 4.6 mm, Phenomenex, Aschaffenburg). Eluents and measuring conditions were the same as described in Berg et al. [36]. Oven-temperature was set to 45°C. Compounds were detected by UV absorbance at 220 nm and quantified by CLASS-VP V6.10 software (Shimadzu).

3.2.6 Isotope analysis

Isotope analyses were performed on a GC-C-IRMS (Thermo Fisher Scientific) with the method described in detail by Meyer et al.[30]. Briefly, samples were injected with a GC Pal autosampler (CTC, Zwingen, Switzerland). The split/splitless injector was operated for 1 min in splitless and then in split mode (split ratio 1:10) held at 250°C, with a flow rate of 1.4 mL min⁻¹. The analytical column was a DB-5 (30 m x 0,25 mm; 1 µm film; J&W Scientific, Folsom; CA, USA). The GC oven was programmed from 65 °C (hold: 1min), ramp 20 °C/min to 180 °C (hold: 10 min), ramp 15 °C/min to 230 °C (hold: 8 min).

The δ¹⁵N- and δ¹³C-values are reported in per mil relative to Vienna PeeDee Belemnite (VPDB) and air respectively:

$$\delta^{13}\text{C} = [({}^{13}\text{C}/{}^{12}\text{C}_{\text{Sample}} - {}^{13}\text{C}/{}^{12}\text{C}_{\text{Standard}}) / {}^{13}\text{C}/{}^{12}\text{C}_{\text{Standard}}]. \quad (3_1)$$

$$\delta^{15}\text{N} = [({}^{15}\text{N}/{}^{14}\text{N}_{\text{Sample}} - {}^{15}\text{N}/{}^{14}\text{N}_{\text{Standard}}) / {}^{15}\text{N}/{}^{14}\text{N}_{\text{Standard}}]. \quad (3_2)$$

CO₂ and N₂ reference gas were calibrated to VPDB and air, respectively, as described in Meyer et al. [30].

3.2.7 Carbon and nitrogen enrichment factors for hydrolysis of atrazine

Bulk isotope enrichment factors for carbon and nitrogen were determined as the slope of a linear regression according to the Rayleigh-equation:

3. C and N Isotope Fractionation Suggests Similar Mechanism of Microbial Atrazine Transformation despite Involvement of Different Enzymes (AtzA and TrzN)

$$\ln \frac{R_t}{R_0} = \ln \left(\frac{1 + \delta^h E}{1 + \delta^h E_0} \right) = \varepsilon \cdot \ln f \quad (3_3)$$

where R_t and R_0 are the compound-specific isotope ratios of heavy versus light isotopes at a given time and at the beginning of the reaction. $\delta^h E$ and $\delta^h E_0$ are the isotopic signatures of the compound for the element E at times t and zero, respectively, while C_t/C_0 is the fraction f of the remaining compound. The enrichment factor ε is a measure for the isotopic enrichment as average over all positions in a molecule. ε has a negative value for normal kinetic isotope effects and is positive for inverse isotope effects. A primary isotope effect of a given element present in a reacting bond (e.g., carbon in a C-Cl bond of atrazine) is highly position-specific. To derive such primary position-specific apparent kinetic isotope effects (AKIE) from bulk enrichment factors ε , the approximate formula

$$AKIE \approx \frac{1}{((n \cdot \varepsilon_{bulk})/1000 + 1)} \quad (3_4),$$

was used, where n corresponds to the number of atoms of the element present in the molecule. In the case that atoms of the element of interest are located only in proximity to, or within a conjugated π -system next to the reacting bond (e.g., all nitrogen atoms present in atrazine), these atoms may contribute simultaneously with a secondary isotope effect to observable fractionation. In such a case an average secondary position-specific apparent kinetic isotope effect (AKIE) can be calculated according to

$$AKIE \approx \frac{1}{(n/x \cdot \varepsilon_{bulk} + 1)} \quad (3_5),$$

where x is the number of atoms located in positions affected by the reaction [20].

3.3 RESULTS AND DISCUSSION

3.3.1 Carbon and nitrogen isotope fractionation during biotic hydrolysis of atrazine

All three strains converted atrazine to hydroxyatrazine and the metabolite was subsequently further degraded (Figure A3_1 in Appendix 2A), consistent with the well-documented pathways established

3. C and N Isotope Fractionation Suggests Similar Mechanism of Microbial Atrazine Transformation despite Involvement of Different Enzymes (AtzA and TrzN)

for *Chelatobacter heintzii*, *Pseudomonas* sp. ADP and *Arthrobacter aurescens* TC1 [31, 32, 37]. Figure 3_1 further shows that transformation by all three strains was associated with significant enrichment of ^{13}C and depletion of ^{15}N in the remaining atrazine; no atrazine degradation and no

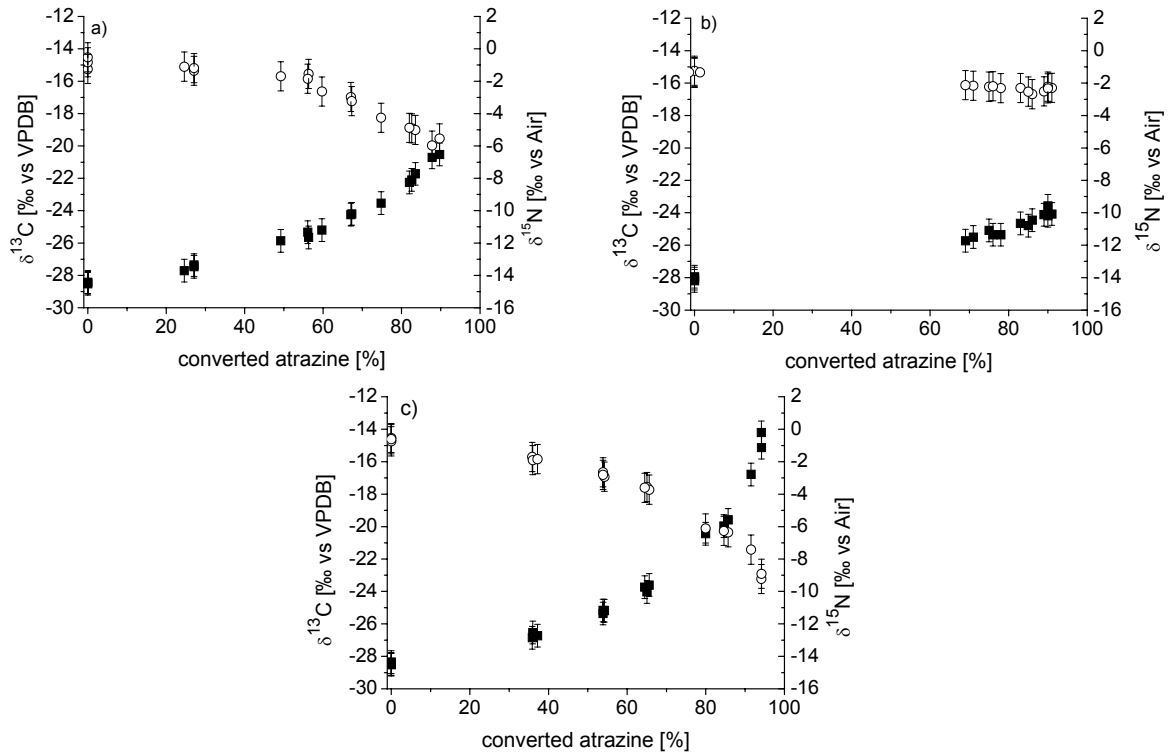


Figure 3_1. Changes in isotope ratios of carbon (left axis; filled squares) and nitrogen (right y-axis, open circles) during transformation of atrazine with (a) *Chelatobacter heintzii*, (b) *Pseudomonas* sp. ADP and (c) *Arthrobacter aurescens* TC1. Error bars indicate total uncertainty of carbon isotope (± 0.7 ‰) and nitrogen isotopes measurements according to Meyer et al. [30].

isotope fractionation was observed in sterile controls (data not shown). Our results therefore demonstrate that CSIA bears potential to qualitatively detect biotic transformation of atrazine to hydroxyatrazine in the field. While clearly demonstrating isotope fractionation, Figure 3_1 also shows that the extent of isotopic changes differed significantly between the cultures, being greatest with *Arthrobacter aurescens* TC1 and smallest with *Pseudomonas* sp. ADP. This observation is reflected in significantly different C and N enrichment factors for the three bacterial strains (Figure 3_2a and 3_2b, Table 1). Our results therefore indicate that an adequate enrichment factor ϵ to quantify natural atrazine degradation is not easily chosen. If a small $\epsilon_{\text{C}} = -1.8\text{‰} \pm 0.2\text{‰}$ is inserted into the Rayleigh equation to evaluate shifts in atrazine isotope ratios of natural samples, the actual

3. C and N Isotope Fractionation Suggests Similar Mechanism of Microbial Atrazine Transformation despite Involvement of Different Enzymes (AtzA and TrzN)

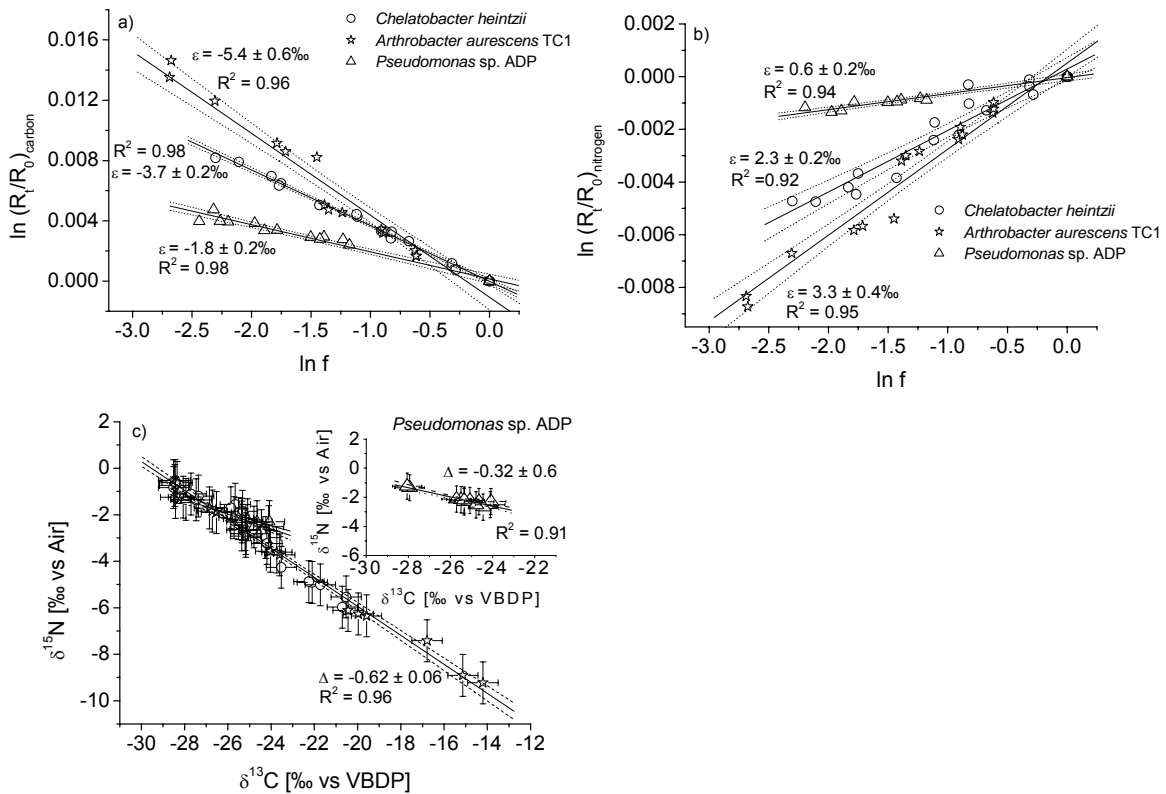


Figure 3_2. Logarithmic plots of isotope ratios according to the Rayleigh equation (eq. 1) (a) for carbon and (b) for nitrogen. (c) Two dimensional isotope plot of carbon and nitrogen atrazine isotope ratios for *Pseudomonas* sp. ADP (open triangle) (see also isolated sketch) and average regression for *Chelatobacter heintzii* (open circles), and *Arthrobacter aurescens* TC1 (open stars). The slope of regression is determined using bulk data of all strains and is given as Δ . Error bars indicate total uncertainty of carbon isotope ($\pm 0.7\text{‰}$) and nitrogen isotopes measurements according to Meyer et al. [30]. Dotted lines represent 95% confidence interval of linear regression.

transformation may be overestimated. Vice versa, if the largest $\epsilon_C = -5.4\text{‰} \pm 0.6\text{‰}$ is chosen, degradation is likely to be underestimated [38]. For conservative estimates, the latter choice is therefore preferable. Figure 3_2c plots values of $\delta^{15}\text{N}$ against $\delta^{13}\text{C}$ showing that the slope ($\Delta \approx \epsilon_{\text{nitrogen}} / \epsilon_{\text{carbon}}$) of the regression lines coincided well for *Chelatobacter heintzii* and *Arthrobacter aurescens* TC1 (Table 3_1).

This gives evidence that the same reaction mechanism was responsible for the conversion of atrazine into hydroxyatrazine, irrespective of the type of enzyme present (AtzA vs. TrzN). With *Pseudomonas* sp. ADP, the dual isotope slope showed the same qualitative trend of normal isotope fractionation in C and inverse isotope fractionation in N, however with a distinguishable value of

3. C and N Isotope Fractionation Suggests Similar Mechanism of Microbial Atrazine Transformation despite Involvement of Different Enzymes (AtzA and TrzN)

Δ. Since also isotope fractionation of both elements decreased drastically with *Pseudomonas* sp. ADP, it can be concluded that some other, only slightly fractionating step contributed in addition to overall isotope fractionation. Steps of the actual AtzA enzyme catalysis such as formation of substrate-enzyme-complex or reaction with co-substrate [39] are unlikely causes, since *Pseudomonas* sp. ADP contains the same enzyme as *Chelatobacter heintzii*. More likely, a reversible process previous to the substrate-enzyme-complexation may be responsible. with pure enzymes. Since both organisms are phylogenetically diverse, differences in the physiology, possibly substrate specific uptake mechanisms [40] or atrazine binding to transporter-molecules could be potential reasons for the distinguishable dual isotope trend in the case of *Pseudomonas* sp. ADP. To substantiate such hypotheses, these aspects would have to be investigated in further research.

3.3.2 Insight into the enzymatic transformation mechanism from abiotic reference experiments

To our knowledge, the exact biochemical transformation mechanism of biotic atrazine hydrolysis by AtzA and TrzN is as yet unknown.

Table 1 shows that calculated AKIE values can give only limited mechanistic insight. They span a range between 1.015 and 1.045 for carbon and between 0.974 and 0.995 for nitrogen (Table 3_1). The normal carbon AKIE values are consistent with weakened carbon-containing bonds, whereas the inverse nitrogen AKIE values indicate increased bonding to one or several nitrogen atoms in the transition state. To obtain better mechanistic insight, we therefore investigated abiotic hydrolysis of atrazine under alkaline and acidic conditions as reference systems for the biotic hydrolysis. On the one hand, isotope fractionation in abiotic transformations often directly reflects the intrinsic conversion of the chemical bond so that masking effects may be eliminated. On the other hand, differences in isotope fractionation may give hints about differences in reaction mechanisms. Based on insight from computational chemistry of abiotic systems [29, 41], microbial hydrolysis of atrazine to hydroxyatrazine may be hypothesized to occur either by a direct substitution of the chlorine atom (hypothesis A, Figure 3_4), which would be in accordance to the hypothesis from Scott et al. [6] derived from enzymatic modeling. Alternatively, some kind of activation of the aromatic ring prior to the nucleophilic attack may occur [42] (hypothesis B, Figure 3_4). Carbon isotope fractionation during acidic hydrolysis was of the same order of magnitude as for *Arthrobacter aurescens* TC1 (Table 3_1, Figure 3_1 and 3_3). Carbon isotope shifts were slightly

Table 3_1. Bulk Carbon and Nitrogen Enrichment Factors (ϵ_{carbon} and $\epsilon_{\text{nitrogen}}$). Apparent Kinetic Isotope Effects ($\text{AKIE}_{\text{carbon}}$ and $\text{AKIE}_{\text{nitrogen}}$) and Δ Values for Biotic (Catalysed by Different Enzymes) and Abiotic Hydrolysis of Atrazine. Uncertainties given are 95% confidence interval.

		ϵ_{carbon} [‰]	$\epsilon_{\text{nitrogen}}$ [‰]	$\Delta = \delta^{15}\text{N} / \delta^{13}\text{C} =$ $\epsilon_{\text{nitrogen}} / \epsilon_{\text{carbon}}$	$\text{AKIE}_{\text{carbon}}$	$\text{AKIE}_{\text{nitrogen}}$
biotic hydrolysis	<i>Enzyme</i>					
<i>Chelatobacter heintzii</i>	AtzA	-3.7 ± 0.2	2.3 ± 0.4	$-0.65 \pm 0.08^{\text{a)}$	$1.031 \pm 0.002^{\text{c)}$	$0.982 \pm 0.003^{\text{d)}$
<i>Pseudomonas sp.</i> ADP	AtzA	-1.8 ± 0.2	0.6 ± 0.2	$-0.32 \pm 0.06^{\text{a)}$	$1.015 \pm 0.002^{\text{c)}$	$0.995 \pm 0.002^{\text{d)}$
<i>Arthrobacter aurescens</i> TC1	TrzN	-5.4 ± 0.6	3.3 ± 0.4	$-0.61 \pm 0.02^{\text{a)}$	$1.045 \pm 0.005^{\text{c)}$	$0.974 \pm 0.003^{\text{d)}$
abiotic hydrolysis	<i>Temperature</i>					
pH 3	60 °C	-4.8 ± 0.4	2.5 ± 0.2	-0.52 ± 0.04	$1.040 \pm 0.003^{\text{c)}$	$0.988 \pm 0.001^{\text{d)}$
pH 12	60 °C	-3.7 ± 0.4	-0.9 ± 0.2	0.26 ± 0.06	$1.031 \pm 0.003^{\text{c)}$	$1.001 \pm 0.000^{\text{e)}$
pH 12 ^{f)}	20 °C	-5.6 ± 0.2	-1.2 ± 0.2	$0.22 \pm 0.02^{\text{b)}$	$1.047 \pm 0.002^{\text{c)}$	$1.001 \pm 0.000^{\text{e)}$

^{a)} Δ obtained from each individual two dimensional isotope plot of each strain

^{b)} calculated with data from . Meyer et al., [30]

^{c)} $\text{AKIE}_{\text{carbon}}$ is calculated according to eq.(4) with $n = 8$.

^{d)} $\text{AKIE}_{\text{nitrogen}}$ is calculated according to eq(4)

^{e)} $\text{AKIE}_{\text{nitrogen}}$ is calculated according to eq(5) with $x = n$.

^{f)} from Meyer et al.[30]

3. C and N isotope fractionation suggests similar mechanism of microbial atrazine transformation despite involvement of different enzymes (AtzA and TrzN)

smaller in the alkaline hydrolysis at 60°C (Figure 3_3) but of comparable magnitude in the alkaline hydrolysis at 20°C [30]. The fact that isotope fractionation observed with *Arthrobacter aurescens* TC1 was similarly strong as in the “unmasked” abiotic experiments (meaning that uptake, transport or enzyme-substrate binding can be excluded) therefore suggests only a small commitment to catalysis in the enzymatic reaction involving TrzN. In contrast, smaller isotope

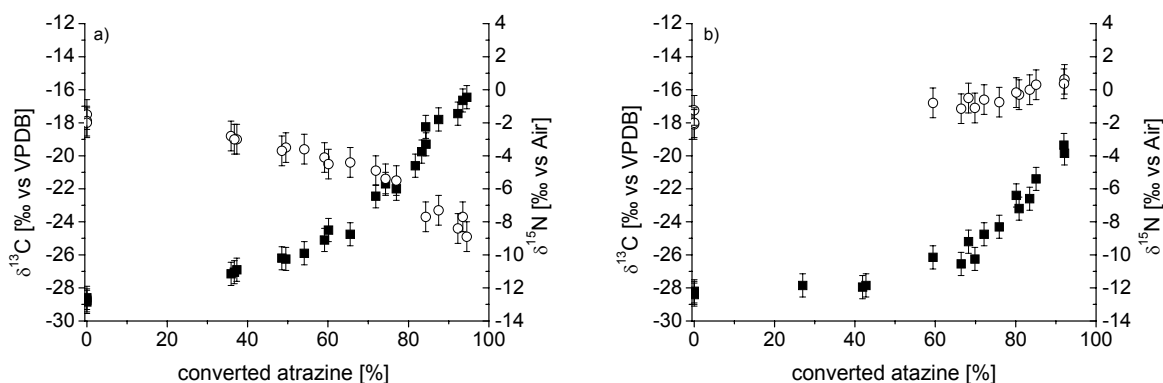


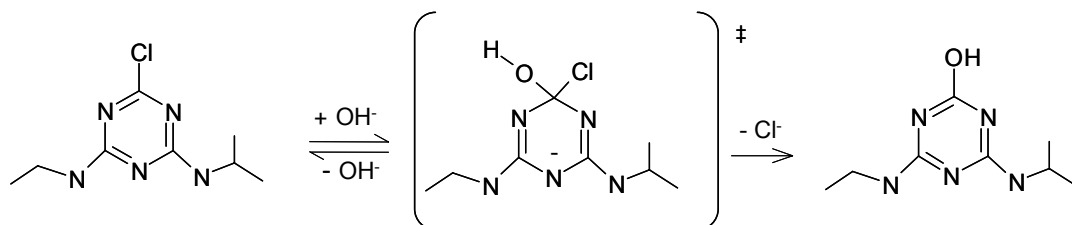
Figure 3_3. Changes in isotope ratios of carbon (left axis; filled squares) and nitrogen (right y-axis, open circles) during abiotic hydrolysis of atrazine at 60°C at (a) pH 3 and (b) pH 12. Error bars indicate total uncertainty of carbon isotope (± 0.7 ‰) and nitrogen isotopes measurements according to Meyer et al. [30].

fractionation with the other two strains suggests that isotope fractionation was masked by the presence of either isotope insensitive or slightly sensitive rate limiting steps other than the isotopically sensitive bond cleavage (see above). Regarding the chemical reaction mechanism, however, insight from C isotope analysis alone is not conclusive so that isotope information of other elements is important.

Most compelling evidence is therefore given by the nature of nitrogen isotope fractionation. The nitrogen isotope effects in the alkaline reaction at 20°C and 60°C were normal meaning that heavy isotopes became enriched in the reactant. Such a trend is predicted by computations of Dybala-Defratyka [29] who derived small, normal secondary nitrogen isotope effects for aromatic nitrogen atoms in the case of a tight S_N2Ar transition state as depicted in mechanism A of Figure 3_4. In contrast, pronounced *inverse* nitrogen isotope effects were observed in both acidic and biotic hydrolysis of atrazine meaning that heavy isotopes became depleted in the reactant.

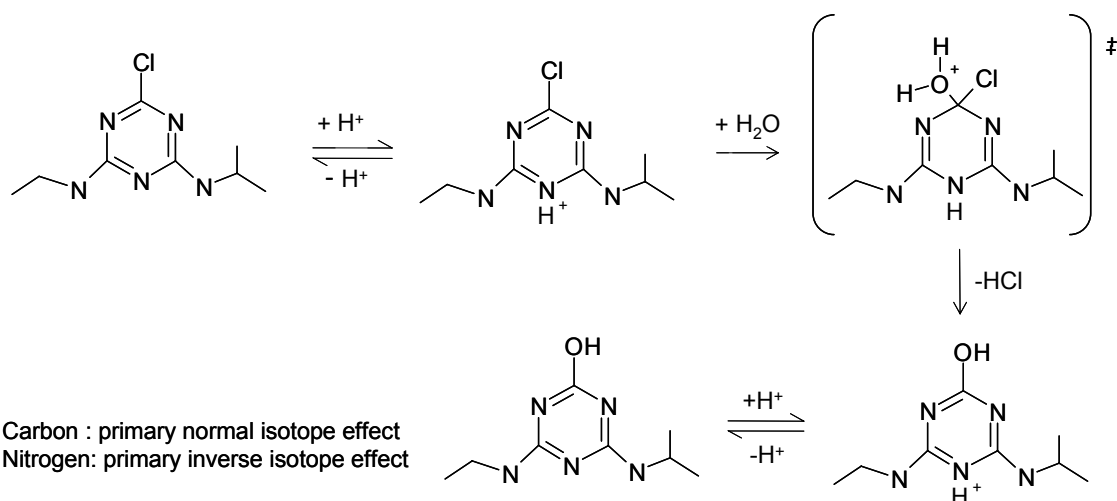
3. C and N Isotope Fractionation Suggests Similar Mechanism of Microbial Atrazine Transformation despite Involvement of Different Enzymes (AtzA and TrzN)

Hypothesis A



Carbon : primary normal isotope effect
Nitrogen: secondary isotope effect

Hypothesis B



Carbon : primary normal isotope effect
Nitrogen: primary inverse isotope effect

Figure 3_4. Schematic illustration of possible hydrolysis of atrazine.

Inverse isotope effects generally occur if the bonding environment in the transition state is tighter / more restricted than in the reactant [43], for example if the transition state involves an additional bond to the element of concern. For the acidic hydrolysis the most likely reason is protonation at one of the nitrogen atoms [44] of the heterocyclic ring [42]. Such protonation results in further polarization of the C-Cl bond, favoring the expulsion of the chloride via a S_NAr addition-elimination pathway [41] (mechanism B, Figure 3_4). To answer the question whether biotic hydrolysis of atrazine involves a similar reaction mechanism as acidic hydrolysis, we compared the two-dimensional isotope plots of both transformation pathways (Figure 3_4, Table 3_1). With 0.52 ± 0.4 the dual isotope slope Δ of the acidic hydrolysis was statistically indistinguishable from the average regression (calculated with the data of *Chelatobacter heintzii* and *Arthrobacter aureescens*

3. C and N Isotope Fractionation Suggests Similar Mechanism of Microbial Atrazine Transformation despite Involvement of Different Enzymes (AtzA and TrzN)

TC1) of the biotic hydrolysis ($\Delta = 0.62 \pm 0.6$) (Figure 3_5). For the enzymatic reaction, we therefore conclude that a Lewis acid binds to the nitrogen atoms of the atrazine ring in a similar way as H^+ during acid hydrolysis leading to an activation of the aromatic ring that facilitates the nucleophilic substitution reaction [45] of Cl by H_2O at the atrazine molecule. Further confirmation may be expected from Cl-isotope effect measurements, solvent isotope effects of ^{18}O and 2H as well as studies with pure enzymes indicated in grey color.

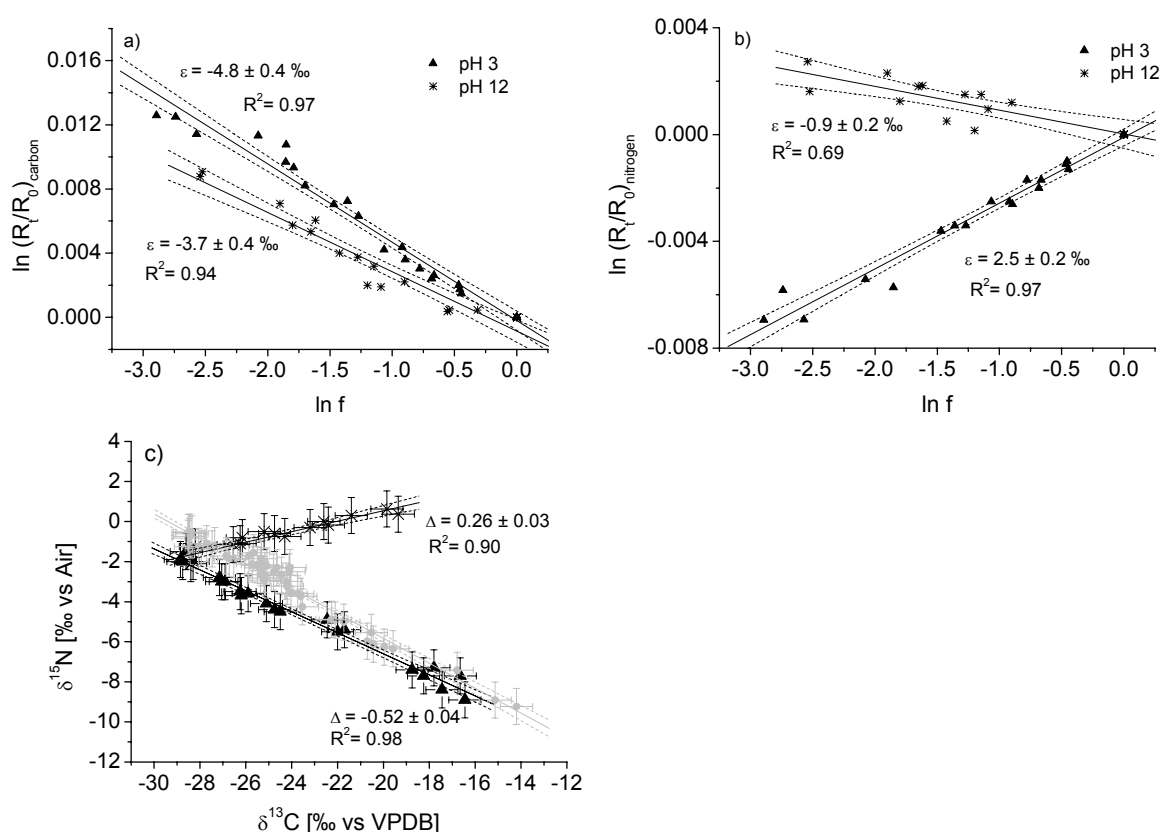


Figure 3_5. Logarithmic plot of isotope ratios according to the Rayleigh equation during abiotic hydrolysis of atrazine at $60^\circ C$ at pH 3 (filled triangles) and pH 12 (crosses) for (a) carbon and (b) nitrogen. (c) Two dimensional isotope plot of carbon and nitrogen atrazine isotope ratios for pH 3 (filled triangle) and pH 12 (stars). For comparison two dimensional isotope plot of the biotic hydrolysis (indicated regression is associated to data of *Chelatobacter heintzii* and *Arthrobacter aurescens* TC1) is The slope of regression is given as Δ . Error bars indicate the total uncertainty of carbon isotope ($\pm 0.7\text{‰}$) and nitrogen isotopes measurements according to Meyer et al. [30]. Dotted lines represent 95% confidence interval of linear regression.

3. C and N Isotope Fractionation Suggests Similar Mechanism of Microbial Atrazine Transformation despite Involvement of Different Enzymes (AtzA and TrzN)

3.3.3 Environmental Significance

Our evidence from carbon and nitrogen isotope fractionation allows a first glimpse on the reaction chemistry of enzymatic atrazine transformation and shows that the enzymes TrzN and AtzA, which are thought to have independent evolution histories, seem to have evolved towards catalysis of similar biochemical transformation mechanisms. Our work also shows that changes in isotope ratios may be used to qualitatively detect natural biotic transformation of atrazine to hydroxyatrazine. In principle, also the extent of atrazine degradation may be estimated from isotope data. However, since isotope fractionation varies between bacterial strains, for conservative estimates we recommend using the greatest enrichment factor observed ($\epsilon_C = -5.4\% \pm 0.6\%$). Further, the characteristic dual isotope slope $\Delta = \epsilon_{\text{nitrogen}} / \epsilon_{\text{carbon}}$ of our study may be compared with data from Hartenbach et al. [28] for direct and indirect photolysis of atrazine. Their values of $\Delta = 0.24 \pm 0.15$ (indirect photooxidation mediated by OH-radicals), $\Delta = 0.4 \pm 0.04$ (indirect photooxidation mediated by 4-carboxybenzophenone) and $\Delta = 1.05 \pm 0.14$ (direct photolysis) are distinctly different from our values of Δ (Table 3_1). This demonstrates that such two dimensional isotope plots can be a new instrument to differentiate between these concurring environmental degradation reactions in natural samples.

Supporting Information Available in Appendix A2

3.4 References

1. Le Baron, H. M.; McFarland, J. E.; Burnside, O. C., *The triazine herbicides*. 1 ed.; Elsevier: Oxford, 2008; p 600.
2. Rohr, J. R.; Schotthoefer, A. M.; Raffel, T. R.; Carrick, H. J.; Halstead, N.; Hoverman, J. T.; Johnson, C. M.; Johnson, L. B.; Lieske, C.; Piwoni, M. D.; Schoff, P. K.; Beasley, V. R., Agrochemicals increase trematode infections in a declining amphibian species. *Nature* 2008, 455, 1235-1239.
3. Ellis, L.; Wackett, L.; Li, C.; Gao, J.; Turnbull, M., Biocatalysis/Biodegradation Database. In University of Minnesota: 2006.
4. Erickson, L. E., Degradation of atrazine and related s-triazines. *Crit. Rev. Env. Con.* 1989, 19, 1-14.

3. C and N Isotope Fractionation Suggests Similar Mechanism of Microbial Atrazine Transformation despite Involvement of Different Enzymes (AtzA and TrzN)

5. Shapir, N.; Mongodin, E. F.; Sadowsky, M. J.; Daugherty, S. C.; Nelson, K. E.; Wackett, L. P., Evolution of catabolic pathways: Genomic insights into microbial s-triazine metabolism. *J. Bacteriol.* 2007, 189, (3), 674-682.
6. Scott, C.; Jackson, C. J.; Coppin, C. W.; Mourant, R. G.; Hilton, M. E.; Sutherland, T. D.; Russell, R. J.; Oakeshott, J. G., Atrazine chlorohydrolase: catalytic improvement and evolution. *Appl. Environ. Microbiol.* 2009, 75, 2184-2191.
7. Clay, S. A.; Koskinen, W. C., Adsorption and desorption of atrazine, hydroxyatrazine, and S-glutathione atrazine on two soils. *Weed Res.* 1990, 38, 262-266.
8. Moreau-Kervevan, C.; Mouvet, C., Adsorption and desorption of atrazine, deethylatrazine, and hydroxyatrazine by soil components. *J. Environ. Qual.* 1998, 27, 46-53.
9. Lerch, R. N.; Thurman, M. E.; Kruger, E. L., Mixed-mode sorption of hydroxylated atrazine degradation products to soil: a mechanism for bound residue. *Environ. Sci. Technol.* 1997, 31, 1539-1546.
10. Martin-Neto, L.; Traghetta, D. G.; Vaz, C. M. P.; Crestana, S.; Sposito, G., On the interaction mechanisms of atrazine and hydroxyatrazine with humic substances. *J. Environ. Qual.* 2001, 30, (2), 520-525.
11. Ma, L.; Selim, H. M., Atrazine retention and transport in soils. *Rev. Environ. Contam. T.* 1996, 145, 129-162.
12. Spalding, R. F.; Snow, D. D.; Cassada, D. A.; Burbach, M. E., Study of pesticide occurrence in two closely spaced lakes in northeastern Nebraska. *J. Environ. Qual.* 1994, 23, 571-578.
13. Adams, C. D.; Thurmann, E. M., Formation and transport of deethylatrazine in the soil and vadose zone. *J. Environ. Qual.* 1991, 20, 540-547.
14. Tappe, W.; Groeneweg, J.; Jantsch, B., Diffuse atrazine pollution in German aquifers. *Biodegradation* 2002, 13, (1), 3-10.
15. Hirschorn, S. K.; Dinglasan, M. J.; Elsner, M.; Mancini, S. A.; Lacrampe-Couloume, G.; Edwards, E. A.; Sherwood Lollar, B., Pathway dependent isotopic fractionation during aerobic biodegradation of 1,2-dichloroethane. *Environ. Sci. Technol.* 2004, 38, (18), 4775 - 4781.
16. Elsner, M.; McKelvie, J.; LacrampeCouloume, G.; SherwoodLollar, B., Insight into methyl tert-butyl ether (MTBE) stable isotope fractionation from abiotic reference experiments. *Environ. Sci. Technol.* 2007, 41, (16), 5693-5700.
17. Fischer, A.; Herklotz, I.; Herrmann, S.; Thullner, M.; Weelink, S. A. B.; Stams, A. J. M.; Schlömann, M.; Richnow, H.-H.; Vogt, C., Combined carbon and hydrogen isotope fractionation investigations for elucidating benzene biodegradation pathways. *Environ. Sci. Technol.* 2008, 42, (12), 4356-4363.
18. Sherwood Lollar, B.; Slater, G. F.; Sleep, B.; Witt, M.; Klecka, G. M.; Harkness, M.; Spivack, J., Stable carbon isotope evidence for intrinsic bioremediation of tetrachloroethene and trichloroethene at Area 6, Dover Air Force Base. *Environ. Sci. Technol.* 2001, 35, 261-269.

3. C and N Isotope Fractionation Suggests Similar Mechanism of Microbial Atrazine Transformation despite Involvement of Different Enzymes (AtzA and TrzN)

19. Abe, Y.; Hunkeler, D., Does the Rayleigh equation apply to evaluate field isotope data in contaminant hydrogeology? *Environ. Sci. Technol.* 2006, 40, (5), 1588-1596.
20. Elsner, M.; Zwank, L.; Hunkeler, D.; Schwarzenbach, R. P., A new concept linking observable stable isotope fractionation to transformation pathways of organic pollutants. *Environ. Sci. Technol.* 2005, 39, (18), 6896-6916.
21. Schmidt, T. C.; Zwank, L.; Elsner, M.; Berg, M.; Meckenstock, R. U.; Haderlein, S. B., Compound-specific stable isotope analysis of organic contaminants in natural environments: a critical review of the state of the art, prospects, and future challenges. *Anal. Bioanal. Chem.* 2004, 378, (2), 283-300.
22. Vogt, C.; Cyrus, E.; Herklotz, I.; Schlosser, D.; Bahr, A.; Herrmann, S.; Richnow, H.-H.; Fischer, A., Evaluation of toluene degradation pathways by two-dimensional stable isotope fractionation. *Environ. Sci. Technol.* 2008, 42, (21), 7793-7800.
23. Nijenhuis, I.; Andert, J.; Beck, K.; Kastner, M.; Diekert, G.; Richnow, H. H., Stable isotope fractionation of tetrachloroethene during reductive dechlorination by *Sulfurospirillum multivorans* and *Desulfitobacterium* sp. Strain PCE-S and abiotic reactions with cyanocobalamin. *Appl. Environ. Microbiol.* 2005, 71, (7), 3413-3419.
24. Northrop, D. B., The expression of isotope effects on enzyme-catalyzed reactions. *Annual Review of Biochemistry* 1981, 50, 103-131.
25. Penning, H.; Cramer, C. J.; Elsner, M., Rate-Dependent carbon and nitrogen kinetic isotope fractionation in hydrolysis of isoproturon. *Environ. Sci. Technol.* 2008, 42, (21), 7764-7771.
26. Zwank, L.; Berg, M.; Elsner, M.; Schmidt, T. C.; Schwarzenbach, R. P.; Haderlein, S. B., New evaluation scheme for two-dimensional isotope analysis to decipher biodegradation processes: Application to groundwater contamination by MTBE. *Environ. Sci. Technol.* 2005, 39, (4), 1018-1029.
27. Penning, H.; Sørensen, S. R.; Amand, J.; Elsner, M., Isotope fractionation of the herbicide isoproturon in microbial transformation pathways is distinct from abiotic hydrolysis. *Environ. Sci. Technol.* 2008, *submitted*.
28. Hartenbach, A. E.; Hofstetter, T. B.; Tentscher, P. R.; Canonica, S.; Berg, M.; Schwarzenbach, R. P., Carbon, hydrogen, and nitrogen isotope fractionation during light-Induced transformations of atrazine. *Environ. Sci. Technol.* 2008, 42, (21), 7751-7756.
29. Dybala-Defratyka, A.; Szatkowski, L.; Kaminski, R.; Wujec, M.; Siwek, A.; Paneth, P., Kinetic isotope effects on dehalogenations at an aromatic carbon. *Environ. Sci. Technol.* 2008, 42, (21), 7744-7750.
30. Meyer, A. H.; Penning, H.; Lowag, H.; Elsner, M., Precise and accurate compound specific carbon and nitrogen isotope analysis of atrazine: critical role of combustion oven conditions. *Environ. Sci. Technol.* 2008, 42, (21), 7757-7763.

3. C and N Isotope Fractionation Suggests Similar Mechanism of Microbial Atrazine Transformation despite Involvement of Different Enzymes (AtzA and TrzN)

31. Rousseaux, S.; Hartmann, A.; Soulas, G., Isolation and characterisation of new Gram-negative and Gram-positive atrazine degrading bacteria from different French soils. *FEMS Microbiol. Ecol.* 2001, *36*, (2-3), 211-222.
32. Mandelbaum, R. T.; Allan, D. L.; Wackett, L. P., Isolation and characterization of a *Pseudomonas* sp. that mineralizes the s-triazine herbicide atrazine. *Appl. Environ. Microbiol.* 1995, *61*, (4), 1451-1457.
33. Devers, M.; Soulas, G.; Martin-Laurent, F., Real-time reverse transcription PCR analysis of expression of atrazine catabolism genes in two bacterial strains isolated from soil *J.Microbiol.l Meth.* 2004, *56*, (1), 3-15.
34. Strong, L. C.; Rosendahl, C.; Johnson, G.; Sadowsky, M. J.; Wackett, L. P., *Arthrobacter aurescens* TC1 metabolizes diverse s-triazine ring compounds. *Appl. Environ. Microbiol.* 2002, *68*, (12), 5973-5980.
35. Sajjaphan, K.; Shapir, N.; Wackett, L. P.; Palmer, M.; Blackmon, B.; Sadowsky, M. J., *Arthrobacter aurescens* TC1 atrazine catabolism genes trzN, atzB, and atzC are linked on a 160-kilobase region and are functional in *Escherichia coli*. . *Appl. Environ. Microbiol.* 2004, *70*, (7), 4402-4407.
36. Berg, M.; Mueller, S. R.; Schwarzenbach, R. P., Simultaneous determination of triazines including atrazine and their major metabolites hydroxyatrazine, desethylatrazine, and deisopropylatrazine in natural waters. *Anal. Chem.* 1995, *67*, (11), 1860-1865.
37. Shapir, N.; Pedersen, C.; Gil, O.; Strong, L.; Seffernick, J.; Sadowsky, M. J.; Wackett, L. P., TrzN from *Arthrobacter aurescens* TC1 Is a zinc amidohydrolase. *J. Bacteriol.* 2006, *188*, (16), 5859-5864.
38. Meckenstock, R. U.; Morasch, B.; Griebler, C.; Richnow, H. H., Stable isotope fractionation analysis as a tool to monitor biodegradation in contaminated aquifers. *J.Contam.Hydrol.* 2004, *75*, (3-4), 215-255.
39. Paneth, P., Heavy atom isotope effects on enzymatic reactions. *J. Mol. Struc.* 1994, *321*, 35-44.
40. Evans, R. D., Physiological mechanisms influencing plant nitrogen isotope composition. *Trends Plant. Sci.* 2001, *6*, (3),121-126.
41. Sawunyama, P.; Bailey, G. W., Computational chemistry study of the environmentally important acid-catalyzed hydrolysis of atrazine and related 2-chloro-s-triazines. *Pest. Manag. Sci* 2002, *58*, (8), 759-768.
42. Russell, J. D.; Cruz, M.; White, J. L.; Bailey, G. W.; Payne, W. R. J.; Pope, J. D. J.; Teasley, J. I., Mode of chemical degradation of s-triazines by montmorillonite. . *Science* 1968, *160*, 1340-1342.

3. C and N Isotope Fractionation Suggests Similar Mechanism of Microbial Atrazine Transformation despite Involvement of Different Enzymes (AtzA and TrzN)

43. Schramm, V. L., Enzymatic transition states and transition state analog design. *Annu. Rev. Biochem.* 1998, *67*, 693-720.

44. Plust, S. J.; Loehe, J. R.; Feher, F. J.; Benedict, J. H.; Herbrandson, H. F., Kinetics and mechanisms of hydrolysis of chloro-1,3,5-triazines. Atrazine. *J. Org. Chem.* 1981, *46*, 3661-3665.

45. Souza de, M. L.; Sadowsky, M. J.; Wackett, L. P., Atrazine chlorohydrolase from *Pseudomonas* sp. strain ADP: gene sequence, enzyme purification and protein characterization. *J. Bacteriol.* 1996, *178*, (16), 4894-4900.

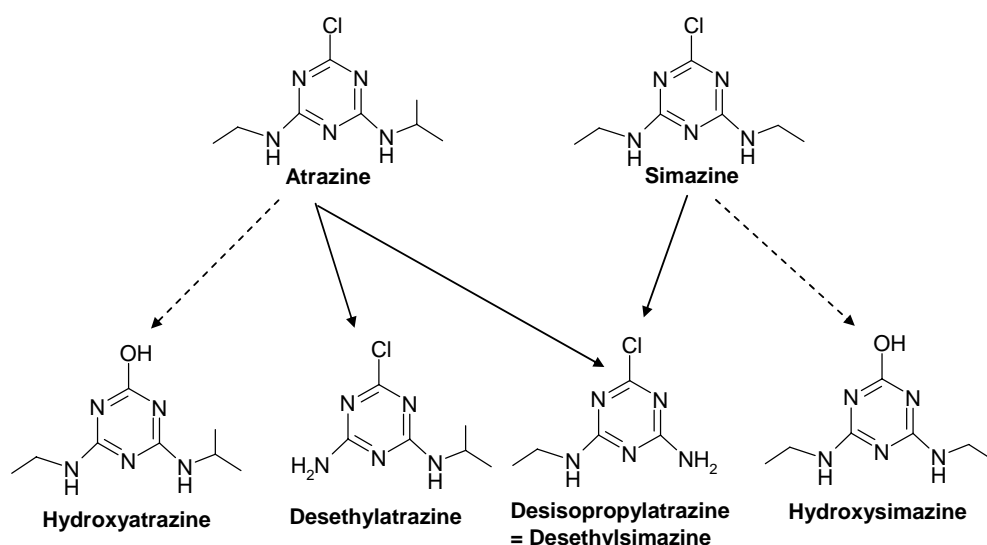
4.

Probing for Concurring Mechanisms of Oxidative Atrazine Dealkylation: A combined Approach with Metabolite Identification and Dual Isotope Fractionation (C and N) Measurements

Armin H. Meyer and Martin Elsner

4.1 Introduction

Triazine herbicides like atrazine and simazine are used as pre- and post-emergence herbicides mainly for broadleaf and grassy weed control in agricultural cultivation of corn, sugar cane sorghum and other crops. Atrazine has a toxic potential to aquatic organisms [1] and may have long-term adverse effects to the aquatic environment [2]. Due to its high persistence atrazine has become a frequent pollutant of surface and groundwater and may therefore pose a hazard to environment and human health. Elimination from the environment occurs primarily by two different biotic degradation pathways. These are either hydrolysis [3-6] giving non herbicidal hydroxyatrazine [7], or oxidative dealkylation [3, 6, 8] leading to products that still retain some phytotoxic effects: desethyl- and desisopropylatrazine from atrazine [7], and desethylsimazine (= desisopropylatrazine) from simazine [9] (Scheme 4_1).



Scheme 4_1. Proposed biotic degradation pathways of atrazine and simazine. Dashed lines indicate hydrolysis and solid lines oxidative dealkylation.

Due to their high mobility in the aquatic environment and due to their low degradability, also the dealkylated transformation products are frequently detected in groundwater systems, often in concentrations exceeding that of the parent compound. To assess degradation of atrazine in the environment it has therefore become common to use the ratio of desethylatrazine to atrazine, or desisopropylatrazine to atrazine as an indicator for degradation [10-12]. However, this practice neglects the alternative degradation product hydroxyatrazine and possible subsequent formation of bound residues. Recent studies even suggest that hydroxyatrazine formation is in fact the

4. Probing for Concurring Mechanisms of Oxidative Atrazine Dealkylation: A Combined Approach with Metabolite Identification and Dual Isotope (C and N) Fractionation Measurements

confirm or discard these alternative mechanisms, the nature of the initial step remains subject to controversial debate.

Compound specific isotope analysis (CSIA) by gas chromatography isotope ratio mass spectrometry (GC-IRMS) bears considerable potential to address both important research gaps: (1) to provide additional lines of evidence to assess degradation of atrazine in the environment, and (2) to complement information from metabolite analysis for elucidation of the underlying biochemical transformation mechanism.

For *assessment in the environment*, recent studies demonstrated that CSIA can help identifying and quantifying transformation reactions of organic contaminants [26-31]. To this end the method analyzes changes in isotopic ratios of the original contaminant during transformation reactions so that the approach is independent of metabolite detection. Such changes in isotope ratios are caused by underlying kinetic isotope effects (KIE). Even quantitative interpretations are possible when using the Rayleigh equation. This relationship provides the link between degradation-induced shifts in isotope ratios and the extent of degradation by which they have been caused. Both observables are linked by the enrichment factor ϵ , which can be determined in laboratory experiments and which enables estimating the extent of degradation from observed isotopic shifts.

To *identify in addition biochemical transformation pathways* it has been shown that enrichment factors ϵ can be used to estimate the underlying KIE, which typically varies for different types of reaction mechanisms [27, 32]. In addition, isotope analysis may be conducted for two elements, and isotope data of both elements can be plotted relative to each other. Such dual isotope plots show characteristic slopes that are little affected by the presence of slow additional steps so that they provide a particularly robust indicator of the prevailing transformation mechanisms. Recent studies have demonstrated that hydrolysis [33, 34] and photolysis [35] of atrazine are associated with significant carbon, chlorine and nitrogen isotope fractionation, and that it is indeed possible to differentiate between the different modes of transformation due to their different dual-isotope pattern. Thus, it was a major aim of our study to investigate for the first time isotope fractionation of C and N associated with the oxidative dealkylation of atrazine. To this end we used the bacterial strain *Rhodococcus* sp. strain NI86/21 as model organism. It contains a single cytochrome P450 monooxygenase system responsible for the oxidation of atrazine to desethylatrazine (DEA) or desisopropylatrazine (DIP) [36] (scheme 4_2).

To address the first question – whether stable isotope measurements can present a new approach to trace degradation of atrazine in the environment – our main objectives were to investigate (i) whether biotic oxidative dealkylation is associated with significant isotope fractionation, and (ii)

4. Probing for Concurring Mechanisms of Oxidative Atrazine Dealkylation: A Combined Approach with Metabolite Identification and Dual Isotope (C and N) Fractionation Measurements

whether the dual isotope plot (carbon versus nitrogen) shows a slope different from previously investigated degradation pathways [33, 35]. To further constrain the nature of transformation products and intermediates, it was our aim to quantify known transformation products by HPLC-UV/VIS (high pressure liquid chromatography with UV/VIS detector) and to identify additional products for which no standards are available by LC-MS/MS (liquid chromatography coupled to tandem mass spectrometry). Simazine was included for comparison.

To address the second question – the mechanism of the underlying biochemical transformation – we explored the full potential of a combined approach: the use of compound specific isotope analysis together with quantification of compound concentrations by HPLC-UV/VIS and identification of metabolites by LC-MS/MS. In this approach we relied on two hypotheses. (i) The magnitude of nitrogen isotope fractionation is hypothesized to be indicative of the prevailing transformation mechanism, being greater for the oxidation of the nitrogen atom (mechanism a), and smaller for the homolytic C-H bond cleavage, since it does not directly involve the nitrogen atom (mechanism b). (ii) Also product formation is hypothesized to be indicative, because oxidation of the nitrogen atom (mechanism a) is expected to produce C-OH groups in the adjacent α -position only, whereas the radical reaction (mechanism b) may be more unspecific and lead to products with C-OH groups also in β -position. To test these hypotheses, we compared the results (stable isotope fractionation and product formation) of biotransformation to those of a reference transformation with selective C-H bond oxidation and where the reaction involves strictly a C-H bond so that no nitrogen isotope effects are expected. We chose permanganate as such a model reactant, since studies on the oxidation of ethers and primary amines have established a high selectivity and a direct attack at the C-H bond [37-39].

4.2 Experimental Section

4.2.1 Chemicals

Atrazine (1-chloro-3-ethylamino-5-isopropylamino-2,4,6-triazine, CAS: 1912-24-9) was purchased from Tropitzsch (97.7 %) and simazine (2-chloro-4,6-bis(ethylamino)-s-triazine, CAS: 122-34-9, 99,0%) from Dr. Ehrenstorfer GmbH (Augsburg, Germany). Ethyl acetate (99.8% Riedel-de Haën, supplied by Sigma Aldrich, Taufkirchen, Germany) was used as a solvent for standard solutions (GC-IRMS). Atrazine standards for GC-IRMS were adjusted to 300 and 600 mg/L. Aqueous HPLC standards contained atrazine, simazine, hydroxyatrazine (CAS: 2163-68-0), desethylatrazine (CAS: 6190-65-4), and desisopropylatrazine (CAS: 1007-28-9) (96.0%, 99.9%, and 96.3%,

4. Probing for Concurring Mechanisms of Oxidative Atrazine Dealkylation: A Combined Approach with Metabolite Identification and Dual Isotope (C and N) Fractionation Measurements

respectively; all Riedel de Haën, supplied by Sigma Aldrich, Seelze, Germany) and had concentrations of 4.7, 11.6, 23.3, 46.6 and 93.2 μM of the analytes. Potassium permanganate (99%) as oxidative agent was from Sigma Aldrich (Seelze, Germany). Acetonitrile used as HPLC eluent was from Roth (Karlsruhe, Germany), $\text{Na}_3\text{PO}_4 \cdot 12\text{H}_2\text{O}$ and $\text{Na}_2\text{HPO}_4 \cdot 2\text{H}_2\text{O}$ (for aqueous puffer solution), and dichloromethane for extraction were purchased from Merck (Darmstadt, Germany).

4.2.2 Bacterial strain and cultivation media

Rhodococcus sp. strain NI86/21 was purchased from the National Collection of Agricultural and Industrial Microorganisms (Budapest, Hungary). The strain was grown in nutrient broth (Roth, Karlsruhe, Germany) containing either atrazine (90 μM) or simazine (60 μM). For the degradation experiment 100 μL of cell suspension ($\text{OD}_{580\text{nm}}$: 1.2 – 1.5) was transferred to about 400 ml fresh nutrient broth solution containing atrazine or simazine with a concentration of between 60 μM and 80 μM . Experiments were carried out in triplicates at 21 °C. The pH of the nutrient broth was 6.9. Control experiments, carried out in the absence of the bacterial strain, did not show any degradation of simazine or atrazine (results not shown).

4.2.3 Oxidative degradation with potassium permanganate

Triplicate experiments were carried out in a phosphate-buffered (10 mM, pH: 7.1) aqueous (deionized water) solution (500 mL) at 21°C and in darkness. Concentrations of atrazine or simazine solutions were between 60 μM and 80 μM . Concentration of the oxidant KMnO_4 was 0.1 M.

4.2.4 Sampling for concentration measurements, identification of metabolites and isotope analysis

At each sampling event, samples were taken for quantification (150 μL), identification (150 μL , stored until analysis at -8°C in the freezer) and isotope analysis (15 mL – 200 mL) of atrazine or simazine and its metabolites. Quantification of atrazine, simazine, desethylatrazine, desisopropylatrazine (= desethylsimazine) and hydroxyatrazine was accomplished by HPLC UV/VIS analysis, whereas identification of unknown metabolites was done by LC-MS/MS analysis. In both cases aqueous samples were used directly. For isotope analysis, aqueous samples were extracted with 5-10 mL dichloromethane, which was subsequently dried at room temperature under the hood. Dried extracts were redissolved in ethyl acetate to final atrazine and simazine concentrations of about 900 μM . Tests with standards showed that fractionation introduced by the preparation steps was not detectable within the analytical uncertainty of the method.

4. Probing for Concurring Mechanisms of Oxidative Atrazine Dealkylation: A Combined Approach with Metabolite Identification and Dual Isotope (C and N) Fractionation Measurements

4.2.5 Quantification and identification of atrazine, simazine and its metabolites

For concentration measurements of atrazine and simazine and its degradation products a Shimadzu LC-10A series HPLC system was used. The column used was an ODS (30) (Ultracarb 5 μ M, 150 x 4.6 mm, Phenomenex, Aschaffenburg). Separation was performed using gradient elution at a flow rate of 0.8 mL/min. Initial conditions (15% acetonitrile and 85% buffer of KH₂PO₄ 0.001 M, pH 7.0) were maintained isocratic for 1 min followed by a linear gradient to 55% acetonitrile within 9 min and a gradient to 75 % acetonitrile within 14 min after which conditions remained 2 min isocratically; a subsequent gradient led to initial conditions within 2 min. The injection volume was 25 μ L, and the oven-temperature was set to 45°C. Compounds were detected by their UV absorbance at 220 nm and quantified by CLASS-VP V6.10 software (Shimadzu). Precision of atrazine, simazine, desethylatrazine, desisopropylatrazine and hydroxyatrazine quantification was high, with coefficients of variation less than 5 %. Concentrations of the other metabolites could not be determined accurately, since no standards were available. Their relative amounts are indicated by the ratio of their UV absorbance and the absorbance of atrazine or simazine, respectively, at time 0.

Identification (see also Appendix A3) of unknown peaks was performed on a Q-Trap MS/MS system (Applied Biosystems, Toronto, Canada) linked to an Agilent HP 1200 HPLC system. Mass spectrometry was carried out in the Enhanced Product Ion scan mode. Ionisation was accomplished by electron spray ionization (ESI) in the positive ion mode, with an ion spray voltage of 4600 V. Declustering potential (DP) was 46 V, entrance potential (EP) 4.5 V, collision energy (CE) 23 eV, and collision cell exit potential was 4 eV. Nitrogen was used as curtain gas, collision gas, turbo gas and nebulizer gas. Temperature of the turbo gas was 400 °C. Chromatographic separation was carried out by the same analytical column as used for HPLC UV/VIS analysis. Flow rate was 0.4 mL/min. Initial conditions were 15 % acetonitrile and 85 % acetic acid solution (0.1 M) for 1 min, followed by a linear gradient to 55 % acetonitrile within 18 min, a gradient to 75 % within 28 min after which conditions remained isocratic for 4 min; a subsequent gradient led to initial conditions within 3 min. To assign the obtained peaks by their retention time to the analysis of the HPLC UV/VIS we reanalyzed samples on the HPLC UV/VIS at flow and eluent conditions given as for the Q-Trap LC-MS/MS system. Retention times, precursor (M+H⁺) and MS/MS spectrum ions are shown in Table 3_1, 3_2 and Figure A3_1, A3_2, A3_3 and A3_4 of the Appendix A3.

4. Probing for Concurring Mechanisms of Oxidative Atrazine Dealkylation: A Combined Approach with Metabolite Identification and Dual Isotope (C and N) Fractionation Measurements

4.2.6 Isotope analysis

Isotope analyses were performed on a GC-C-IRMS (Thermo Fisher Scientific, Bremen, Germany). Briefly, samples were injected with a GC Pal autosampler (CTC, Zwingen, Switzerland). The split/splitless injector was operated for 1 min in splitless and then in split mode (split ratio 1:10) held at 250 °C, with a column flow of 1.4 mL min⁻¹. The analytical column was a DB-5 (60 m x 0,25 mm; 1 µm film; J&W Scientific, Folsom; CA, USA). The GC oven was programmed from 140 °C (hold: 1 min), ramp 18 °C/min to 155 °C, ramp 2 °C/min to 240 °C, ramp 30 °C/min to 260 °C (hold: 5 min). For carbon isotope analysis analytes were combusted to CO₂ in a GC IsoLink oven (Thermo Fisher Scientific, Bremen, Germany) at 1050 °C. Analytical uncertainty was with ± 0.7 ‰ the same as for the method described by Meyer et al. [40]. For N isotope analysis, analytes were converted to N₂ with the setup described in Hartenbach et al. [35].

The δ¹⁵N- and δ¹³C-values are reported in per mil relative to Vienna PeeDee Belemnite (V-PDB) and air respectively:

$$\delta^{13}\text{C} = \left[\left(\frac{^{13}\text{C}/^{12}\text{C}_{\text{Sample}}}{^{13}\text{C}/^{12}\text{C}_{\text{Standard}}} - 1 \right) \cdot 1000 \right] \text{‰} \quad (4_1)$$

$$\delta^{15}\text{N} = \left[\left(\frac{^{15}\text{N}/^{14}\text{N}_{\text{Sample}}}{^{15}\text{N}/^{14}\text{N}_{\text{Standard}}} - 1 \right) \cdot 1000 \right] \text{‰} \quad (4_2)$$

CO₂ and N₂ reference gas were calibrated to V-PDB and air, respectively, as described in Meyer et al. [40].

4.2.7 Evaluation of stable isotope fractionation

Isotope enrichment factors for carbon and nitrogen were determined as the slope of a linear regression according to the Rayleigh-equation:

$$\ln \frac{R_t}{R_0} = \ln \left(\frac{1 + \delta^h E_t}{1 + \delta^h E_0} \right) = \varepsilon \cdot \ln f \quad (4_3)$$

where R_t and R₀ are the compound-specific isotope ratios of heavy versus light isotopes at a given time and at the beginning of the reaction. δ^hE_t and δ^hE₀ are the isotopic signatures of the compound for the element E at times t and zero, respectively, while C_t/C₀ is the fraction f of the remaining compound. The enrichment factor ε is a measure for the isotopic enrichment as average over all positions in a molecule. ε has a negative value for normal kinetic isotope effects and is positive for inverse isotope effects. To correct for non-reacting positions and to obtain values of kinetic isotope effects specifically in the reacting bond, Elsner et al. [27] proposed a re-evaluation scheme. When isotope effects are small (e.g. for carbon and nitrogen) and when they occur in essentially only one

4. Probing for Concurring Mechanisms of Oxidative Atrazine Dealkylation: A Combined Approach with Metabolite Identification and Dual Isotope (C and N) Fractionation Measurements

position (i.e. with primary isotope effects in non-concerted reactions) this gives in good approximation

$$AKIE \approx \frac{1}{(n \cdot \varepsilon_{bulk} / 1000) + 1} \quad (4_4)$$

Here, n is the number of atoms of element E inside the molecule, and AKIE is the apparent kinetic isotope effect. The term “apparent” acknowledges the possibility that additional slow steps can mask the isotopic discrimination of the elementary reaction step so that the intrinsic KIE is not directly observable [27].

4.2.8 Dual isotope plots

In dual (“two-dimensional”) isotope plots, isotope values of two elements, e.g. C and N, are plotted against each other. The characteristic slope of this correlation was determined by linear regression of all triplicates. The error of the regression is the 95 % confidence interval calculated from the data set [38].

4.3 Results

4.3.1 Metabolite identification during biotic oxidation of simazine and atrazine

For a better understanding of the underlying transformation reactions during oxidation of atrazine and simazine either by *Rhodococcus* sp. NI86/21 or by permanganate, metabolites were characterized using HPLC-UV/VIS and LC-MS/MS.

Metabolites of Atrazine. During biotic degradation of atrazine five metabolites were formed: DEA, DIA, and three metabolites denoted according to their elution times as A1, A2 and A3. DEA and DIA and A2 accumulated during transformation as major products (Figure 4_1a, Figure A3_5a, b in Appendix A3). The retention time of A2 from HPLC-UV/VIS analysis corresponded to the peak characterized as a hydroxyethylatrazine (AETOH) by LC-MS/MS (Figure A3_1). Accumulation of AETOH (Figure 4_1a) indicates that it is not an intermediate of the desethylation pathway (scheme 4_3). The retention time of A3 matched that of a peak characterized by LC-MS/MS as AETOxo (atrazine with a keto, or aldehyde, functionality in the ethyl group Figure A3_1). Concentrations of AETOxo initially increased during atrazine dealkylation, but subsequently decreased again. We therefore hypothesize that AETOxo is an intermediate in the desethylation reaction (scheme 4_3).

4. Probing for Concurring Mechanisms of Oxidative Atrazine Dealkylation: A Combined Approach with Metabolite Identification and Dual Isotope (C and N) Fractionation Measurements

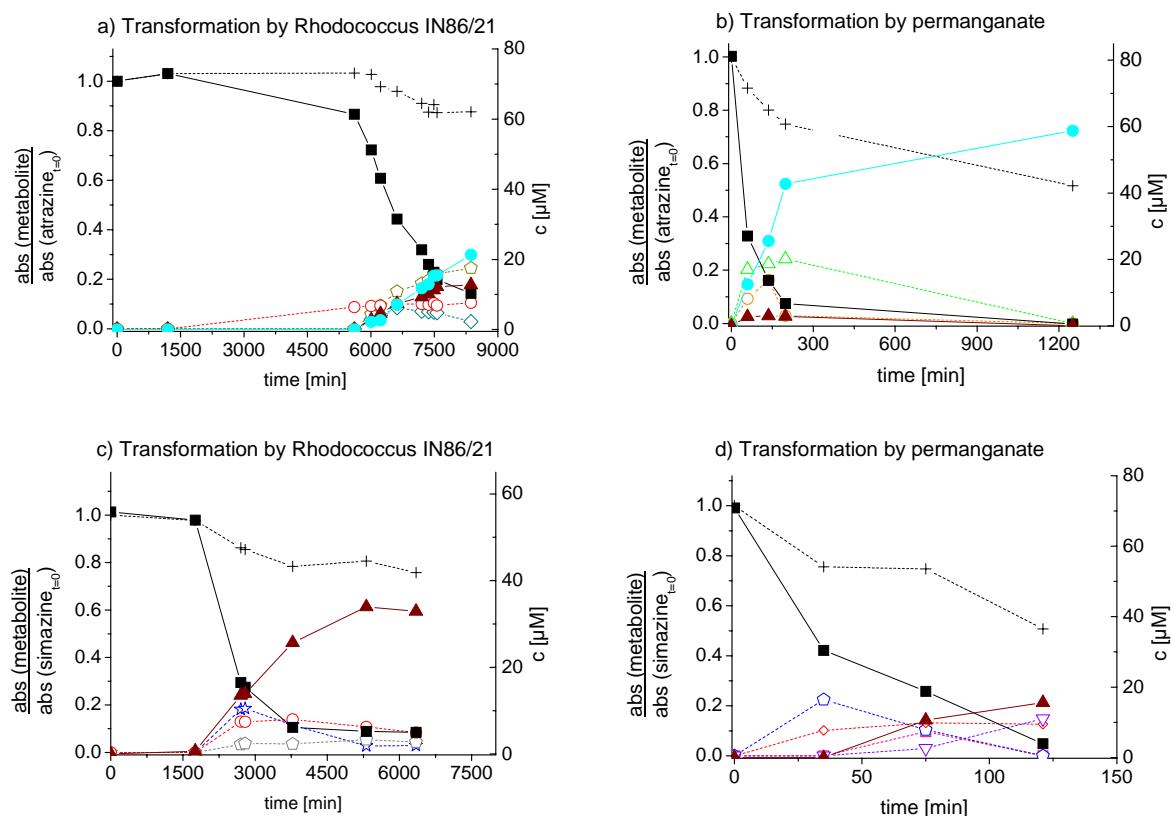


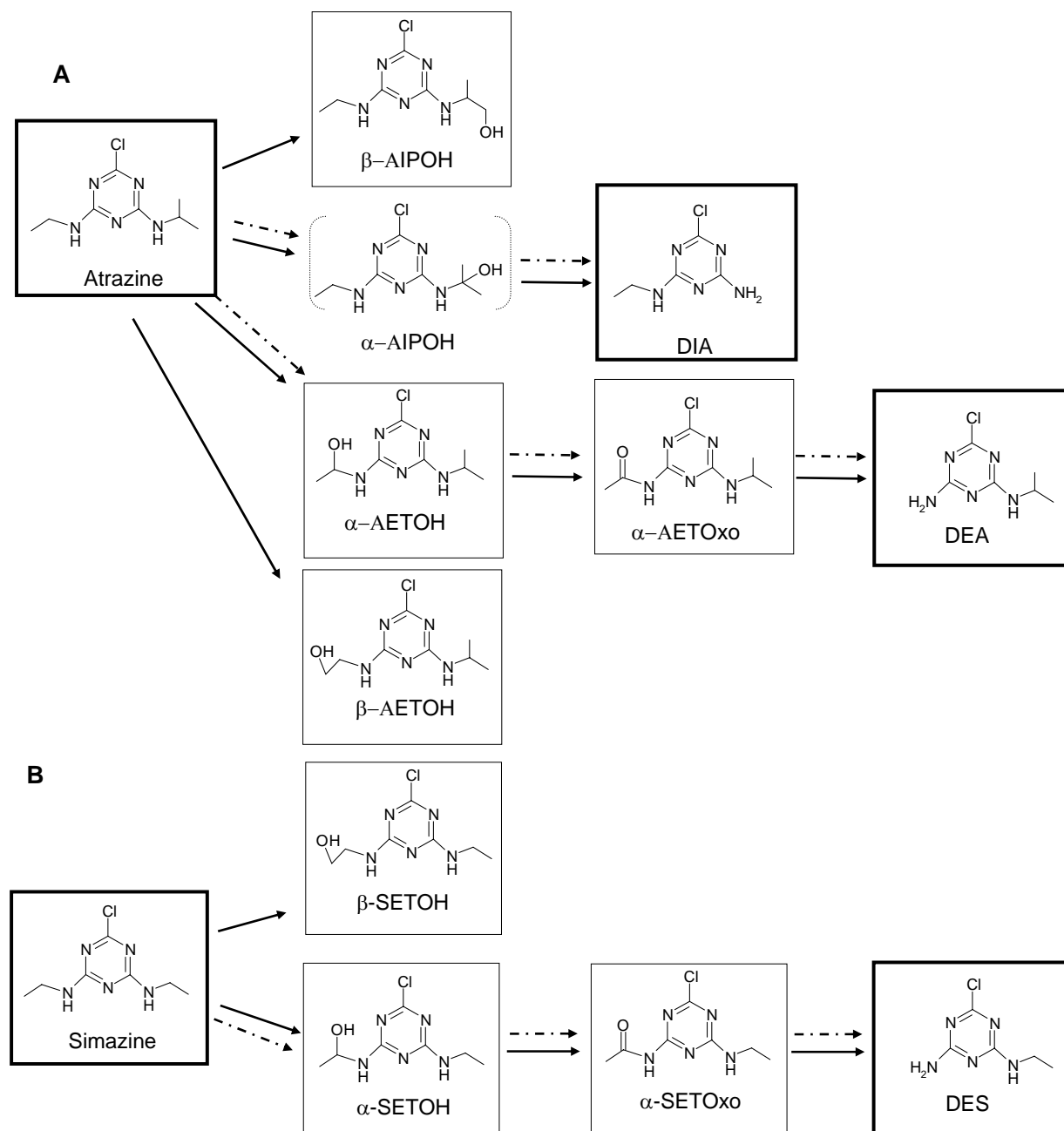
Figure 4_1. Time course of atrazine (a, b) and simazine (c, d) concentrations and formation of products during transformation by *Rhodococcus* sp. NI86/21 and by permanganate. Data with solid lines and solid symbols can be read on the right ordinate, giving the concentration of atrazine (black squares), DEA (cyan circles), DIA (brown triangles) and of simazine (black squares) and DES (brown triangles), respectively. Data with dashed lines and open symbols correspond to the left ordinate giving the relative amount by the ratio of UV/VIS absorbances at 220 nm, $(\text{abs}(\text{metabolite})_{220\text{nm}}/\text{abs}(\text{triazine}_{t=0})_{220\text{nm}})$. Crosses represent the molar balance based on the assumption that metabolites have the same UV absorbance as atrazine. In panel a, open red circles represent metabolite A1, open green pentagons A2 and open turquoise rhombs A3. In panel b, open orange circles give PA1 and open green triangles PA2. In panel c, open grey pentagons denote metabolite S1, open blue stars S2 and open red circles S3. In panel d, open pink squares represent metabolite PS1, open violet triangles PS2, open blue pentagons PS3 and open red rhombs PS4.

To our knowledge AETOH and AETOxo species were so far solely identified during abiotic transformation of atrazine with hydroxyl radicals [41-43]. An AETOxo species was also detected during catalytic conversion of atrazine in metalloporphyrin systems imitating cytochrome P450 enzymes ([44, 45]. Characterization of A1 by LC-MS/MS (Figure A3_1), finally, suggests that it is atrazine with a hydroxylated isopropyl group (AIPOH). This product was also found in the study of Nagy et al.[36] using the same bacterial strain, as well as during metabolism of atrazine by mammal

4. Probing for Concurring Mechanisms of Oxidative Atrazine Dealkylation: A Combined Approach with Metabolite Identification and Dual Isotope (C and N) Fractionation Measurements

hepatic cytochrome P450 enzymes [46]. The AIPOH was already formed during the initial phase of atrazine degradation and its concentration increased steadily, indicating that the product was not further converted (scheme 4_3). Finally, since no formation of hydroxyatrazine was observed and all identified products carried an oxygen substituent in either the ethyl or the isopropyl group (Table A3_2) we conclude that all products were formed by oxidation of one of the alkyl side chain C-atoms. To better pinpoint the molecular structure of metabolites detected during biotic oxidation, and to tell whether AETOH and AETOxo species were oxidized in the α - or the β -position, abiotic oxidation experiments with permanganate were conducted. Abiotic degradation of atrazine led to the formation of DEA and DIA in a proportion of about 30:1 (Figure 4_1b, Figure A3_6a, b) indicating a highly regioselective desalkylation of atrazine. In addition, two other unknown metabolites denoted as PA1 and PA2 were observed. According to LC-MS/MS analysis PA1 can be attributed to an AETOH species and PA2 to an AETOxo species (Figure A3_2). Importantly, AETOH (PA1) is not identical with the peak A2 (biotic experiment), which had the same mass for the molecular ion (232 m/z) and practically the same fragmentation pattern (188, 172, 146 m/z), but eluted at a later retention time. This demonstrates that A2 and PA1 are both hydroxyethylatrazine (AETOH) metabolites, one with the OH group in α -position of the ethyl amino chain (α -AETOH) and the other with the OH group in β -position (β -AETOH). A strong accumulation of A2 was observed in the biotic oxidation suggesting that further reaction of A2 was negligible. In contrast, an increase and subsequent decrease of concentrations was observed for PA1, which is the typical behaviour of an intermediate (Figure 4_1b). According to scheme 4_3, A2 is therefore attributable to β -AETOH, and PA1 to α -AETOH. In addition, permanganate oxidation formed PA2 as consecutive product of α -AETOH so that PA2 must be α -AETOxo. The observation that neither PA1 nor PA2 were observed at the end of the permanganate experiment confirms that both were intermediates of DEA formation. Permanganate oxidation therefore proved indeed highly stereoselective, not only with preference for the ethyl over the isopropyl group, but also for the α - over the β -position within a given alkyl group. The HPLC retention time of PA2 (AETOxo), finally, was comparable to that of A3 of the biotic experiment indicating that the missing structure of the intermediate in atrazine desethylation must also be α -AETOxo.

4. Probing for Concurring Mechanisms of Oxidative Atrazine Dealkylation: A Combined Approach with Metabolite Identification and Dual Isotope (C and N) Fractionation Measurements



Scheme 4_3. Proposed degradation pathway for atrazine (A) and simazine (B) with detected metabolites. Solid lines indicate degradation by *Rhodococcus* sp. NI86/21, dashed lines represent oxidation with permanganate. Product in bold lined boxes are identified by standards, product in thin lined boxes are identified by LC-MS/MS. Product α -AIPOH (in brackets) is proposed as intermediate of DIA formation, but could not be observed by LC-MS/MS.

4. Probing for Concurring Mechanisms of Oxidative Atrazine Dealkylation: A Combined Approach with Metabolite Identification and Dual Isotope (C and N) Fractionation Measurements

Metabolites of Simazine. Besides desethylsimazine (DES = DIA) three unknown metabolites denoted as S1, S2 and S3 (Figure 4_1c, Figure A3_3a, b, Figure A3_7a, b), were detected during degradation by *Rhodococcus* sp. NI86/21. LC-MS/MS analysis identified hydroxyethylsimazine (SETOH, Table S1), which we attribute to S1 because of comparable retention times in HPLC-UV/VIS and LC-MS/MS runs (Figure A3_3). S2 was not detectable in later analysis of all samples indicating that it is an unstable intermediate. Further identification of S3 was not possible. Monitoring characteristic masses of possible follow up products of DES such as desethylhydroxysimazine, 2,4-dihydroxy-6-(N'-ethyl)amino-1,3,5-s-triazine, 2-chloro-4-hydroxy-6-amino-1,3,5-s-triazine and 2-chloro-4,6-diamino-s-triazine did not match (Table A3_1). Also, we did not detect a peak which was related to the mass of hydroxysimazine, the product of the alternative hydrolytic pathway. Thus we suggest that S3 must be a product which is formed by oxidation. Since concentrations of S2 and S3 increased at the beginning of the reaction and subsequently decreased again, while DES continuously accumulated, we hypothesize that S2 and S3 are intermediates on the way to the dealkylation (scheme 4_3). In contrast, S1 was produced in small amounts and remained constant, suggesting that this product, supposedly a SETOH, accumulated besides DES during oxidation of simazine by *Rhodococcus* sp. NI86/21 (scheme 4_3).

Oxidation of simazine by permanganate gave the main product DES, together with several other products denoted as PS1, PS2, PS3 and PS4 (Figure 4_1d, Figure A3_8a, b). LC-MS/MS analysis identified mass spectra of SETOH and SETOxo, which corresponded most probably to PS3 and PS4 (Figure A 3_4), respectively. Considering the evolution of PS3 and PS4 concentrations with time and assuming the same regioselectivity as for atrazine, PS3 and PS4 can tentatively be attributed to α -SETOH and α -SETOxo as intermediates of simazine desethylation (Scheme 4_3). Since SETOH of the biotic experiment had a different retention time than the α -SETOH peak, we conclude that S1 is the hydroxylated product at the β -carbon of the ethyl moiety. On the other hand, S3 eluted at the same time as PS3 and PS4, indicating that it is a product oxidized at the α -carbon. PS1 and PS2 did not match any of the scanned mass spectra (see Table A3_2). Thus we expected them to be products of mixed oxidation in both ethyl groups. Table 4_1 gives a comprehensive summary of detected metabolites, attributed structures and the lines of evidence on which the attribution was based.

4. Probing for Concurring Mechanisms of Oxidative Atrazine Dealkylation: A Combined Approach with Metabolite Identification and Dual Isotope (C and N) Fractionation Measurements

Table 4_1. Identification of atrazine and simazine metabolites by different lines of evidence

Metabolite	Attributed structure	Evidence
A1	β -AIPOH	- mass spectrum in LC-MS/MS - no further degradation
A2	β -AETOH	- mass spectrum in LC-MS/MS (Table A3_1) - accumulation during biotic oxidation (Figure 4_1) - retention time different from PA1 (Figure A3_2, A3_3)
A3	α -AETOxo	- mass spectrum in LC-MS/MS - same retention time as PA2
PA1	α -AETOH	- mass spectrum in LC-MS/MS - intermediate of permanganate oxidation - retention time different from A2
PA2	α -AETOxo	- mass spectrum in LC-MS/MS - intermediate of permanganate oxidation - formed as product of PA1
S1	β -SETOH	- mass spectrum in LC-MS/MS - retention time different from PS3 - no further degradation
S3	α -SETOH or α -SETOxo	- retention time between PS3 and PS4 - unstable intermediate
PS3	α -SETOH	- mass spectrum in LC-MS/MS - intermediate of permanganate oxidation - retention time different from S1
PS4	α -SETOxo	- mass spectrum in LC-MS/MS - intermediate of permanganate oxidation

4.3.2 Quantitative estimates of concurring transformation reactions

The relative abundance of the concurring biotransformation reactions (oxidation at the α - versus β -position and in the ethyl versus isopropyl group) can be estimated assuming (a) that the response of

4. Probing for Concurring Mechanisms of Oxidative Atrazine Dealkylation: A Combined Approach with Metabolite Identification and Dual Isotope (C and N) Fractionation Measurements

the UV/VIS detector at 220 nm is similar for the different metabolites of Table 1 and (b) that the dealkylated products are formed exclusively from oxidation in the α -position. The first assumption is supported by good molar balances of the biodegradation experiments (crosses in the left panels of Figure 4_1), whereas the second assumption is in accordance with Scheme 4_2. Accordingly, the contribution of oxidation in the α -position of the ethyl group in atrazine is given as

$$\frac{\sum([\text{DEA}] + [\alpha - \text{AETOH}] + [\alpha - \text{AETOxo}])}{\sum[\text{all products}]} = \frac{\sum([\text{DEA}] + [\alpha - \text{AETOH}])}{\sum[\text{all products}]}$$
 (note that α -AETOxo was not

detected) whereas the contribution of oxidation in the β -position of the ethyl group is given as

$$\frac{\sum([\beta - \text{AETOH}])}{\sum[\text{all products}]}$$
 where square brackets indicate UV absorbances at 220 nm. This gives the

following estimates for position specific oxidation of atrazine:

- in the α -position of the ethyl group: 35%.
- in the β -position of the ethyl group: 34%.
- in the α -position of the isopropyl group: 17%.
- in the β -position of the isopropyl group: 14%.

Similarly, for simazine:

- in the α -position of the ethyl group: 85%.
- in the β -position of the ethyl group: 15%.

Therefore, the preference for oxidation in the ethyl over the isopropyl group of atrazine was 2.1:1. Likewise, the overall proportion of oxidation in α -positions of atrazine was 52%, whereas for simazine it was 85%. To compare these numbers, it must be considered that simazine has 4 C-H bonds in α -position and 6 C-H bonds in β -position, whereas in atrazine there are only 2 C-H bonds in α -ethyl position and 1 in α -isopropyl position and 3 C-H bonds in β -ethyl and 6 C-H bonds in β -isopropyl position. After normalizing for the number of C-H bonds, the selectivity for oxidation in α - over β -position was preferential in both compounds: 8.5:1 in the ethyl groups of simazine and 7.3:1 in the isopropyl group of atrazine, whereas it was just 1.5:1 in the ethyl group of atrazine. Presently we do not have an explanation for the different selectivity of oxidation in the ethyl groups of atrazine and simazine.

4. Probing for Concurring Mechanisms of Oxidative Atrazine Dealkylation: A Combined Approach with Metabolite Identification and Dual Isotope (C and N) Fractionation Measurements

4.3.3 Carbon and nitrogen isotope fractionation during biotic and abiotic oxidation of atrazine and simazine

Oxidation of atrazine and simazine catalyzed by *Rhodococcus* sp. IN86/21 was associated with a pronounced enrichment of ^{13}C and, to a smaller extent, of ^{15}N (Figure 4_2); no isotope fractionation was observed in sterile controls (data not shown).

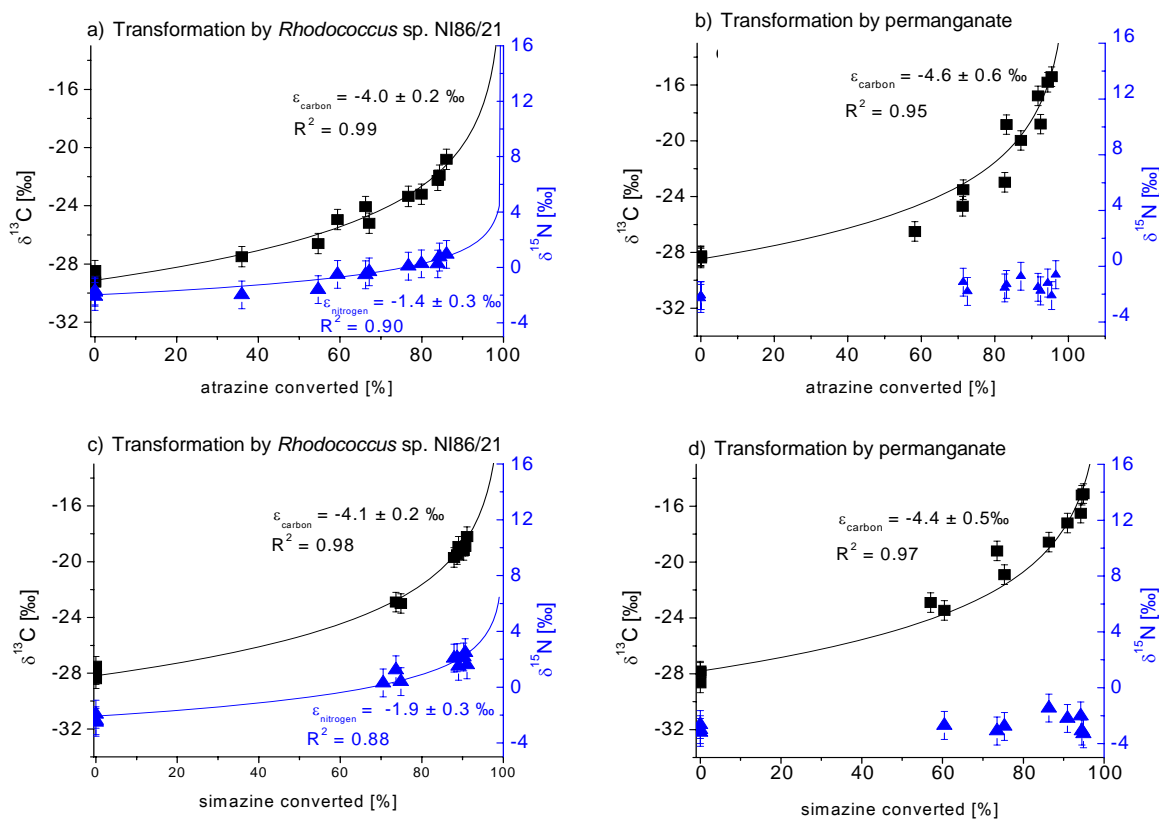


Figure 4_2. Panel a and b show change in carbon (left dark y-axis) and nitrogen (blue right y-axis) isotope ratio of atrazine and panel c and d show change in carbon (left dark y-axis) and nitrogen (blue right y-axis) isotope ratio of simazine during biotic and abiotic conversion. Rayleigh fits and corresponding enrichment factors ϵ are shown (see also Figure A3_9 and A3_10). Error bars indicate total uncertainty of carbon (± 0.7 ‰) and nitrogen isotope analysis (± 1.0 ‰).

Evaluation of experimental data according to the Rayleigh equation (eq. 4_3) resulted in enrichment factors of $\epsilon_{\text{carbon}} = -4.0\text{‰} \pm 0.2\text{‰}$ and $\epsilon_{\text{nitrogen}} = -1.4\text{‰} \pm 0.3\text{‰}$ for atrazine as well as of $\epsilon_{\text{carbon}} = -4.1\text{‰} \pm 0.3\text{‰}$ and $\epsilon_{\text{nitrogen}} = -1.9\text{‰} \pm 0.3\text{‰}$ for simazine. Using equation 4_4, this gives $\text{AKIE}_{\text{carbon}}$ values of 1.033 ± 0.002 for atrazine and 1.032 ± 0.002 for simazine. To calculate AKIE values also

4. Probing for Concurring Mechanisms of Oxidative Atrazine Dealkylation: A Combined Approach with Metabolite Identification and Dual Isotope (C and N) Fractionation Measurements

for nitrogen, there are two possibilities. (i) $AKIE_N$ values can simply be calculated according to equation 4_4 giving 1.007 ± 0.002 for atrazine and 1.009 ± 0.002 for simazine. We relied on the reasonable assumption that nitrogen isotope effects occurred primarily in the N atoms directly adjacent to a reacting carbon atom. This implies that nitrogen isotope fractionation took place if oxidation occurred in the α -position, but not when the side chain was oxidized in β -position. Therefore, the intrinsic N isotope fractionation of the oxidation in α -position was diluted by non-fractionating, simultaneous β -oxidation. To take this effect into account, the contribution of oxidation in α -position (52% for atrazine, 85% for simazine, see above) can be used to convert $\epsilon_{\text{nitrogen}}$ values into values specific for the α -oxidation pathway, giving $\epsilon_{\text{nitrogen}, \alpha\text{-oxidation}} = -2.7\text{‰} \pm 0.6\text{‰}$ for atrazine and $\epsilon_{\text{nitrogen}, \alpha\text{-oxidation}} = -2.6\text{‰} \pm 0.4\text{‰}$ for simazine. This gives $AKIE_{\text{nitrogen}, \alpha\text{-oxidation}}$ values of 1.013 ± 0.003 for atrazine and 1.011 ± 0.003 for simazine. Excellent agreement suggests that essentially the same transformation mechanisms occurred in atrazine and simazine and that our assumption of highly localized nitrogen isotope effects is most likely accurate.

Oxidation by permanganate. Similar to the catalysis by *Rhodococcus* sp. NI86/21, abiotic oxidation led to large enrichment of ^{13}C in atrazine and simazine expressed by ϵ_{carbon} of $-4.6 \pm 0.6\text{‰}$ and $-4.4 \pm 0.5\text{‰}$ (Figure 4_2c, d), respectively. Calculated $AKIE_{\text{carbon}}$ were 1.038 ± 0.005 for atrazine and 1.032 ± 0.004 for simazine. In contrast to the biotic transformation, significant N isotope fractionation was not observed.

Dual isotope plots. If an element shows a different extent of isotope fractionation in two transformation experiments, this can be caused by two different effects. Either a different reaction mechanism takes place that is associated with a different intrinsic isotope effect. Or alternatively, masking may occur meaning that additional slow steps prevent direct observation of the intrinsic fractionation in one of the experiments. The bias can be resolved when measuring isotope changes for two elements. Since masking generally affects isotopic changes of both elements to the same extent, dual isotope slopes typically do not change in the presence of masking. In contrast, if a different reaction mechanism prevails, this is typically reflected in different dual isotope slopes. Our results show that the slopes obtained from the reaction catalyzed by *Rhodococcus* sp. NI86/21 ($\Delta_{\text{atrazine}} = 0.36 \pm 0.06$; $\Delta_{\text{simazine}} = 0.46 \pm 0.08$) were significantly different from the slopes derived from oxidation with permanganate ($\Delta_{\text{atrazine}} = 0.06 \pm 0.06$; $\Delta_{\text{simazine}} = 0.01 \pm 0.06$) demonstrating that the two transformations involved indeed different reaction mechanisms.

4. Probing for Concurring Mechanisms of Oxidative Atrazine Dealkylation: A Combined Approach with Metabolite Identification and Dual Isotope (C and N) Fractionation Measurements

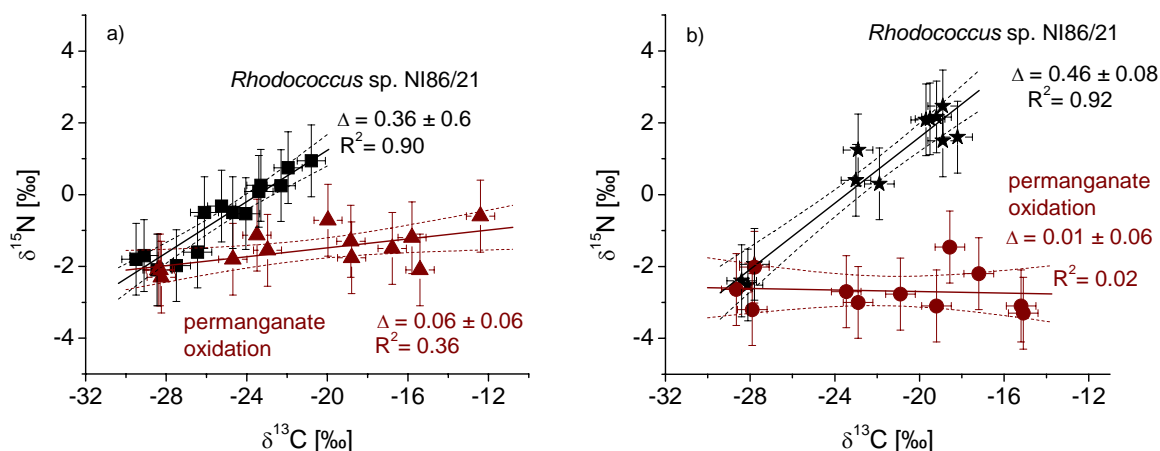


Figure 4_3. Two dimensional isotope plot of carbon and nitrogen ratios of atrazine (a) and simazine (b) for degradation by *Rhodococcus* sp. NI86/21 and permanganate. The slopes are given as Δ . Error bars indicate total uncertainty of carbon isotope ($\pm 0.7\text{‰}$) and nitrogen isotope ($\pm 1.0\text{‰}$) measurements. Dotted lines represent 95% confidence intervals of linear regression.

4.4 Discussion

4.4.1 Mechanistic elucidation

The mechanistic interpretation of our results is based on two hypotheses: (i) that nitrogen isotope fractionation may be used to probe for an initial single electron transfer (SET), since isotope effects at the nitrogen atom are expected to be greater for a SET than in the case of direct C-H bond cleavage; and (ii) that also the product distribution is indicative, since SET is expected to give oxidation primarily in α -position, whereas less selective radical reactions can give oxidation products in β -position.

Our results demonstrate that permanganate is well suited as a reference system to investigate these hypotheses. On the one hand, the absence of nitrogen isotope fractionation confirms that permanganate oxidation involves only C-H bond cleavage, most likely via hydride transfer [39]. On the other hand, our product identification by LC-MS/MS confirms that the oxidation occurs in a highly selective fashion, only in α -position and with preference of the ethyl over the isopropyl group.

A comparison of these results to those of the biotic transformation by *Rhodococcus* sp. NI86/21 gives intriguing pieces of evidence.

4. Probing for Concurring Mechanisms of Oxidative Atrazine Dealkylation: A Combined Approach with Metabolite Identification and Dual Isotope (C and N) Fractionation Measurements

- Dual isotope plots clearly demonstrate that, as expected, different mechanisms were at work.
- The magnitude of carbon isotope effects ($AKIE_{\text{carbon}} \approx 1.03$) in both reactions suggests that effects of masking were small and intrinsic KIE were directly observable.
- The significant nitrogen isotope fractionation for biotic oxidation in α -position ($AKIE_{\text{nitrogen/atrazine}} = 1.013$ and $AKIE_{\text{nitrogen/simazine}} = 1.011$) falls in the range of primary isotope effects and gives, therefore, proof of pronounced changes in bonding at the nitrogen atom. According to our working hypothesis this would indicate oxidation of the nitrogen atom according to a SET mechanism.
- The product distribution in biotic degradation, however, was much less selective than for permanganate, with a significant proportion of β -oxidation products that would argue *against* a SET mechanism,

This contradicting evidence suggests that the enzymes involved in the biotic transformation of atrazine were not very selective: a range of different products was obtained and our results suggest that different mechanisms (SET and hydrogen abstraction) may even have been occurring simultaneously. This ambivalent evidence is also consistent with insight from past studies where both mechanisms were postulated for transformation of different amines. Our combined approach with dual isotope plots and careful metabolite analysis therefore confirms results of these past investigations. However, to our knowledge the simultaneous occurrence of both mechanisms associated with the same cytochrome P450 system and occurring within the same substance has not been described so far. An alternative explanation may be that the investigated bacterial strain contained also other oxidative enzymes (monoamine oxidase, heme proteins) that were capable of converting atrazine and simazine giving rise to the concurring pathways. Finally, it cannot be completely excluded that also radical reactions may cause nitrogen isotope effects (by radical stabilization through the adjacent N center) which would be incorrectly interpreted as evidence of SET. This is supported by the possibility of small secondary nitrogen isotope effects in reaction of atrazine with OH radicals where isotope variations were within the uncertainty of the method[35]. Further C and N isotope fractionation studies on the pure cytochrome P450 systems of *Rhodococcus* sp. IN86/21, studies with model systems for hydrogen abstraction and SET, respectively, and computational approaches may therefore help to further distinguish the different possible mechanisms.

4. Probing for Concurring Mechanisms of Oxidative Atrazine Dealkylation: A Combined Approach with Metabolite Identification and Dual Isotope (C and N) Fractionation Measurements

4.4.2 Environmental Significance

The significant changes in isotope values observed in this study demonstrate that CSIA bears indeed potential to trace oxidative dealkylation of triazines in natural systems. Importantly, isotope fractionation trends are distinctly different from those of biotic hydrolysis. While in our study enrichment of ^{13}C and ^{15}N occurred in atrazine (i.e., normal isotope effects for both elements) biotic hydrolysis (chapter 3, [33]) lead to enrichment of ^{13}C , but depletion of ^{15}N (inverse isotope effect). Such differences in degradation pathways are most visibly represented in the different slopes Δ of the dual isotope plot of atrazine. With $\Delta = 0.36 \pm 0.06$ (figure) biotic oxidation is significantly different from the slope obtained for biotic hydrolysis ($\Delta = -0.62 \pm 0.06$, [32]).

Thus we demonstrate that CSIA can indeed be a valuable tool to identify oxidative dealkylation of triazines, without the need to identify its associated metabolites. Also quantification of degradation according to the Rayleigh equation approach [47] appears possible, since fractionation was strongly expressed and calculated $\text{AKIE}_{\text{carbon}}$ values were of similar magnitude as expected for intrinsic isotope effects. Future studies with different microorganisms capable of atrazine dealkylation may help to obtain more knowledge about a possible variability and to further confirm this magnitude of observable fractionation.

Supporting Information Available in Appendix A3

4.5. References

1. Rohr, J. R.; Schotthoefer, A. M.; Raffel, T. R.; Carrick, H. J.; Halstead, N.; Hoverman, J. T.; Johnson, C. M.; Johnson, L. B.; Lieske, C.; Piwoni, M. D.; Schoff, P. K.; Beasley, V. R., Agrochemicals increase trematode infections in a declining amphibian species. *Nature* 2008, 455, 1235-1239.
2. Pang, L.; Close, M.; Flintoft, M., Degradation and sorption of atrazine, hexazinone and procymidone in coastal sand aquifer media. *Pest. Manag. Sci.* 2005, 61, 133-143.
3. Ellis, L.; Wackett, L.; Li, C.; Gao, J.; Turnbull, M., Biocatalysis/Biodegradation Database. In University of Minnesota: 2006.
4. Mandelbaum, R. T.; Allan, D. L.; Wackett, L. P., Isolation and characterization of a *Pseudomonas* sp. that mineralizes the s-triazine herbicide atrazine. *Appl. Environ. Microbiol.* 1995, 61, (4), 1451-1457.

4. Probing for Concurring Mechanisms of Oxidative Atrazine Dealkylation: A Combined Approach with Metabolite Identification and Dual Isotope (C and N) Fractionation Measurements

5. Radosevich, M.; Traina, S. J.; Hao, Y. L.; Tuovinen, O. H., Degradation and mineralization of atrazine by a soil bacterial isolate. *Appl. Environ. Microbiol.* 1995, 61, (1), 297-302.
6. Wackett, L.; Sadowsky, M.; Martinez, B.; Shapir, N., Biodegradation of atrazine and related s-triazine compounds: from enzymes to field studies. *Appl. Microbiol. Biotechnol* 2002, V58, (1), 39-45.
7. Graymore, M.; Stagnitti, F.; Allinson, G., Impacts of atrazine in aquatic ecosystems. *Environ. Int.* 2001, 26, (7-8), 483-495.
8. Erickson, L. E., Degradation of atrazine and related s-triazines. *Crit. Rev. Env. Con.* 1989, 19, 1-14.
9. Strandberg, M. T.; Scott-Fordsmand, J. J., Field effects of simazine at lower trophic levels-a review. *Sci. Total. Environ.* 2002, 296, (1-3), 117-137.
10. Spalding, R. F.; Snow, D. D.; Cassada, D. A.; Burbach, M. E., Study of pesticide occurrence in two closely spaced lakes in northeastern Nebraska. *J. Environ. Qual.* 1994, 23, 571-578.
11. Thurman, E. M.; Meyer, M.; Pomes, M.; Perry, C. A.; Schwab, P. A., Enzyme-linked immunosorbent assay compared with gas chromatography/mass spectrometry for the determination of triazine herbicides in water. *Anal. Chem.* 1990, 62, 2043 - 2048.
12. Tappe, W.; Groeneweg, J.; Jantsch, B., Diffuse atrazine pollution in German aquifers. *Biodegradation* 2002, 13, (1), 3-10.
13. Guengerich, F. P., Common and uncommon cytochrome P450 reactions related to metabolism and chemical toxicity. *Chem. Res. Toxicol.* 2001, 14, (6), 611-650.
14. Karki, S. B.; Dinnocenzo, J. P.; Jones, J. P.; Korzekwa, K. R., Mechanism of oxidative amine dealkylation of substituted N,N-dimethylanilines by cytochrome P-450: application of isotope effect profiles. *J. Am. Chem. Soc.* 1995, 117, (13), 3657-3664.
15. Sono, M.; Roach, M. P.; Coulter, E. D.; Dawson, J. H., Heme-containing oxygenases. *Chem. Rev.* 1996, 96, (7), 2841-2888.
16. Miwa, G. T.; Walsh, J. S.; Kedderis, G. L.; Hollenberg, P. F., The use of intramolecular isotope effects to distinguish between deprotonation and hydrogen atom abstraction mechanisms in cytochrome P-450- and peroxidase-catalyzed N-demethylation reactions. *J. Biol. Chem.* 1983, 258, (23), 14445-14449.
17. Hall, L. R.; Hanzlik, R. P., N-Dealkylation of tertiary amides by cytochrome P-450. *Xenobiotica* 1991, 21, (9), 1127-1138.

4. Probing for Concurring Mechanisms of Oxidative Atrazine Dealkylation: A Combined Approach with Metabolite Identification and Dual Isotope (C and N) Fractionation Measurements

18. Wang, Y.; Kumar, D.; Yang, C.; Han, K.; Shaik, S., Theoretical study of N-demethylation of substituted N,N-dimethylanilines by cytochrome P450: the mechanistic significance of kinetic isotope effect profiles. *J. Phys. Chem. B* 2007, *111*, (26), 7700-7710.
19. Dinnocenzo, J. P.; Karki, S. B.; Jones, J. P., On isotope effects for the cytochrome P-450 oxidation of substituted N,N-dimethylanilines. *J. Am. Chem. Soc.* 1993, *115*, (16), 7111-7116.
20. Guengerich, F. P.; Okazaki, O.; Seto, Y.; Macdonald, T. L., Radical cation intermediates in N-dealkylation reactions. *Xenobiotica* 1995, *25*, (7), 689-709.
21. Brown, C. M.; Reisfeld, B.; Mayeno, A. N., Cytochromes P450: a structure-based summary of biotransformations using representative substrates. *Drug Metab. Rev.* 2008, *40*, (1), 1-100.
22. Burka, L. T.; Guengerich, F. P.; Willard, R. J.; Macdonald, T. L., Mechanism of cytochrome P-450 catalysis. Mechanism of N-dealkylation and amine oxide deoxygenation. *J. Am. Chem. Soc.* 1985, *107*, (8), 2549-2551.
23. Galliani, G.; Nali, M.; Rindone, B.; Tollari, S.; Rocchetti, M.; Salmona, M., The rate of N-demethylation of N,N-dimethylanilines and N-methylanilines by rat-liver microsomes is related to their first ionization potential, their lipophilicity and to a steric bulk factor. *Xenobiotica* 1986, *16*, 511-517.
24. Hall, L. R.; Hanzlik, R. P., Kinetic deuterium isotope effects on the N-demethylation of tertiary amides by cytochrome P-450. *J. Biol. Chem.* 1990, *265*, (21), 12349-12355.
25. Manchester, J. I.; Dinnocenzo, J. P.; Higgins, L. A.; Jones, J. P., A new mechanistic probe for cytochrome P450: an application of isotope effect profiles. *J. Am. Chem. Soc.* 1997, *119*, (21), 5069-5070.
26. Kuder, T.; Wilson, J. T.; Kaiser, P.; Kolhatkar, R.; Philp, P.; Allen, J., Enrichment of stable carbon and hydrogen isotopes during anaerobic biodegradation of MTBE: Microcosm and field evidence. *Environ. Sci. Technol.* 2005, *39*, (1), 213-220.
27. Elsner, M.; Zwank, L.; Hunkeler, D.; Schwarzenbach, R. P., A new concept linking observable stable isotope fractionation to transformation pathways of organic pollutants. *Environ. Sci. Technol.* 2005, *39*, (18), 6896-6916.
28. Fischer, A.; Bauer, J.; Meckenstock, R. U.; Stichler, W.; Griebler, C.; Maloszewski, P.; Kastner, M.; Richnow, H. H., A multitracer test proving the reliability of Rayleigh equation-based approach for assessing biodegradation in a BTEX contaminated aquifer. *Environ. Sci. Technol.* 2006, *40*, (13), 4245-4252.
29. Morasch, B.; Richnow, H. H.; Schink, B.; Meckenstock, R. U., Stable hydrogen and carbon isotope fractionation during microbial toluene degradation: mechanistic and environmental aspects. *Appl. Environ. Microbiol.* 2001, *67*, (10), 4842-4849.

4. Probing for Concurring Mechanisms of Oxidative Atrazine Dealkylation: A Combined Approach with Metabolite Identification and Dual Isotope (C and N) Fractionation Measurements

30. Hofstetter, T. B.; Schwarzenbach, R. P.; Bernasconi, S. M., Assessing transformation processes of organic compounds using stable isotope fractionation. *Environ. Sci. Technol.* 2008, 42, (21), 7737-7743.
31. Zwank, L.; Berg, M.; Elsner, M.; Schmidt, T. C.; Schwarzenbach, R. P.; Haderlein, S. B., New evaluation scheme for two-dimensional isotope analysis to decipher biodegradation processes: Application to groundwater contamination by MTBE. *Environ. Sci. Technol.* 2005, 39, (4), 1018-1029.
32. Schmidt, T. C.; Zwank, L.; Elsner, M.; Berg, M.; Meckenstock, R. U.; Haderlein, S. B., Compound-specific stable isotope analysis of organic contaminants in natural environments: a critical review of the state of the art, prospects, and future challenges. *Anal. Bioanal. Chem.* 2004, 378, (2), 283-300.
33. Meyer, A. H.; Penning, H.; Elsner, M., C and N isotope fractionation suggests similar mechanisms of microbial atrazine transformation despite involvement of different Enzymes (AtzA and TrzN). *Environ. Sci. Technol.* 2009, 43, (21), 8079-8085.
34. Dybala-Defratyka, A.; Szatkowski, L.; Kaminski, R.; Wujec, M.; Siwek, A.; Paneth, P., Kinetic isotope effects on dehalogenations at an aromatic carbon. *Environ. Sci. Technol.* 2008, 42, (21), 7744-7750.
35. Hartenbach, A. E.; Hofstetter, T. B.; Tentscher, P. R.; Canonica, S.; Berg, M.; Schwarzenbach, R. P., Carbon, hydrogen, and nitrogen isotope fractionation during light-Induced transformations of atrazine. *Environ. Sci. Technol.* 2008, 42, (21), 7751-7756.
36. Nagy, I.; Compennolle, F.; Ghys, K.; Vanderleyden, J.; De Mot, R., A single cytochrome P-450 system is involved in degradation of the herbicides EPTC (S-ethyl dipropylthiocarbamate) and atrazine by *Rhodococcus* sp. strain NI86/21. *Appl. Environ. Microbiol.* 1995, 61, (5), 2056-2060.
37. Wei, M. M.; Steward, R., The mechanisms of permanganate oxidation. VIII. Substituted benzylamines. *J. Am. Chem. Soc.* 1966, 88, 1974-1979.
38. Elsner, M.; McKelvie, J.; LacrampeCouloume, G.; SherwoodLollar, B., Insight into methyl tert-butyl ether (MTBE) stable isotope fractionation from abiotic reference experiments. *Environ. Sci. Technol.* 2007, 41, (16), 5693-5700.
39. Gardner, K. A.; Mayer, J. M., Understanding C-H bond oxidations: H. and H- transfer in the oxidation of toluene by permanganate *Science* 1995, 269, (5232), 1849-1851.
40. Meyer, A. H.; Penning, H.; Lowag, H.; Elsner, M., Precise and accurate compound specific carbon and nitrogen isotope analysis of atrazine: critical role of combustion oven conditions. *Environ. Sci. Technol.* 2008, 42, (21), 7757-7763.

4. Probing for Concurring Mechanisms of Oxidative Atrazine Dealkylation: A Combined Approach with Metabolite Identification and Dual Isotope (C and N) Fractionation Measurements

41. Arnold, S. M.; Hickey, W. J.; Harris, R. F., Degradation of atrazine by fenton's reagent: condition optimization and product quantification. *Environ. Sci. Technol.* 1995, 29, (8), 2083-2089.
42. Chan, G. Y. S.; Hudson, M. J.; Isaacs, N. S., Degradation of atrazine by hydrolysis and by hydroxyl radicals. *J. Phys. Org. Chem.* 1992, 5, (9), 600-608.
43. McMurray, T. A.; Dunlop, P. S. M.; Byrne, J. A., The photocatalytic degradation of atrazine on nanoparticulate TiO₂ films. *J. Photoch. Photobio. A* 2006, 182, (1), 43-51.
44. Gotardo, M. C. A. F.; Moraes de, L. A. B.; Assis, M. D., Metalloporphyrins as biomimetic models for cytochrome P-450 in the oxidation of atrazine. *J. Agric. Food Chem.* 2006, 54, (26), 10011-10018.
45. Rebelo, S. L. H.; Pereira, M. M.; Monsanto, P. V.; Burrows, H. D., Catalytic oxidative degradation of s-triazine and phenoxyalkanoic acid based herbicides with metalloporphyrins and hydrogen peroxide: Identification of two distinct reaction schemes. *J. Mol. Catal. A-Chem.* 2009, 297, (1), 35-43.
46. Hanioka, N.; Tanaka-Kagawa, T.; Nishimura, T.; Ando, M., In vitro metabolism of simazine, atrazine and propazine by hepatic cytochrome P450 enzymes of rat, mouse and guinea pig, and oestrogenic activity of chlorotriazines and their main metabolites. *Xenobiotica* 1999, 29, (12), 1213-1226.
47. Meckenstock, R. U.; Morasch, B.; Griebler, C.; Richnow, H. H., Stable isotope fractionation analysis as a tool to monitor biodegradation in contaminated aquifers. *J. Contam. Hydrol.* 2004, 75, (3-4), 215-255.

5.

Conclusions and Outlook

5.1 Conclusions and Outlook

In the years of their application and also afterwards, atrazine and its primary metabolites hydroxyatrazine, desethylatrazine and desisopropylatrazine have led to worldwide contamination of groundwater. Despite much research, however, it is still difficult to adequately assess atrazine transformation in the environment by conventional methods. The reason is that from measuring contaminant concentrations in aqueous solution alone conclusions about predominant degradation pathways may be biased. Specifically, hydroxyatrazine, the product of biotic hydrolysis, tends to sorb to the soil matrix so that its importance is often underestimated in comparison to the more mobile desethyl- and desisopropylatrazine, which are formed by biotic oxidative dealkylation. Further, mass balances are difficult to establish so that decreasing concentrations alone cannot give conclusive evidence whether degradation occurs or whether concentration decreases are caused by sorption or dilution.

This work evaluates for the first time the potential of compound specific isotope analysis (CSIA) as an alternative, complementary way of assessing atrazine degradation in the environment. Further it was investigated if isotope fractionation measurements can shed light on the underlying reaction mechanisms of atrazine biodegradation. This new approach is pioneered all the way, starting from fundamental method development and leading up to the first investigations of isotope fractionation for the two most important natural biodegradation pathways of atrazine: biotic hydrolysis and oxidative dealkylation.

Specifically, chapter 2 of this thesis demonstrates that careful method evaluation is a prerequisite for isotope measurements by GC-C-IRMS (gas chromatography combustion isotope ratio mass spectrometry). In particular, for atrazine isotope analysis combustion to the analyte gases CO₂ and N₂ played a critical role. Even though advertised by the manufacturer and used for many other compounds, the use of a conventional combustion oven at 960°C did not give accurate and precise measurements. Careful validation of different combustion reactors showed that reactor tubes containing Ni/NiO and operated at 1150°C gave the best precision (analytical uncertainty of ± 0.7 ‰ for C and ± 0.9 ‰ for N) and accuracy (mean deviation of $\Delta\delta^{13}\text{C}$ and $\Delta\delta^{15}\text{N}$ from dual inlet measurements of 0.2‰). These findings clearly emphasize the general need of evaluating the performance of GC-C-IRMS conditions when addressing new target compounds.

With the analytical method in place, carbon and nitrogen isotope fractionation of atrazine were investigated for the first time during biotic hydrolysis (chapter 3) and oxidation (chapter 4). Both degradation pathways were found to produce an enrichment of ¹³C in the remaining atrazine. A different picture was obtained for N. Hydrolytic reaction led to a depletion of ¹⁵N (inverse nitrogen isotope effect) whereas oxidation caused an enrichment of the heavier isotope (normal isotope

effect) in the residual atrazine. Such differences are most clearly illustrated in dual isotope plots, where isotope shifts for carbon are plotted against the shift for nitrogen atoms (see Figure 5-1). These trends alone give already a visible indication of different reaction mechanisms [1-4]. However, through a careful analysis of underlying kinetic isotope effects, through comparison with abiotic reference experiments and by complementary identification of metabolites it even became possible to pinpoint the chemical nature of these reaction mechanisms.

To start with, during biotic hydrolysis similar dual isotope plots were obtained for microorganisms containing the chlorohydrolases AtzA and TrzN indicating that despite their different evolutionary origin, these hydrolyzing enzymes involved essentially the same biochemical reaction mechanism. Further, these plots fell together with the plot for acidic atrazine hydrolysis, and they were clearly different from the plot obtained for alkaline hydrolysis in abiotic reference reactions. These results give the first mechanistic evidence that both chlorohydrolases mostly likely activated atrazine by protonation of one of its nitrogen atoms prior to the nucleophilic aromatic substitution (chapter 3).

An even more powerful approach was used to investigate the mechanism of biotic oxidative dealkylation of atrazine by *Rhodococcus* sp. NI86/21 (chapter 4): the combination of stable isotope fractionation measurements – to test for changes in bonding at the carbon and nitrogen centers – and product identification – to test for the selectivity of oxidation (α - versus β -position) in the alkyl side chains of atrazine. Dealkylation of atrazine by *Rhodococcus* sp. NI86/21 is hypothesized to involve a cytochrome P450 system [5]. For this enzymatic reaction, two putative mechanisms have been postulated: single electron transfer (SET) oxidation of the nitrogen atom versus direct H radical abstraction in the side chain. The results obtained in chapter 4 are at first sight contradictory. Pronounced N isotope effects indicated the occurrence of a SET oxidation of the nitrogen center in the alkyl side chain. Metabolite analysis, in contrast, gave evidence of non-selective oxidation suggesting that rather hydrogen atom abstraction took place in the initial oxidation step. In both cases, again abiotic oxidation experiments with permanganate provided crucial reference data: on the one hand, for identification of metabolites, and on the other hand to verify the absence of N isotope fractionation during a permanganate oxidation, a reaction involving purely C-H cleavage. Taken together, the results of this work therefore suggest that oxidation of atrazine by *Rhodococcus* sp. NI86/21 was facilitated by both, single electron transfer and hydrogen atom abstraction, and that both mechanisms were *occurring simultaneously*. This finding consolidates for the first time seemingly contradictory pieces of evidence from past studies [6-9] and gives a telling indication of the power of stable isotope fractionation as additional line of evidence in mechanistic studies.

The potential of CSIA for environmental assessments – that is, to identify degradation of atrazine in nature - is most illustrated shown in Figure 5-1. The simple occurrence of changes in carbon and nitrogen isotope values during biotic hydrolysis (chapter 3), biooxidation (chapter 4) and photolytic degradation of atrazine [10] clearly demonstrates that these changes may indeed serve to detect transformation of atrazine in the environment. Even better, Figure 5-1 shows that the characteristic differences in slopes Δ of dual isotope plots make it possible to identify different transformation pathways of atrazine. With $\Delta = 0.36 \pm 0.06$ biotic oxidation is significantly different from the slope obtained by biotic hydrolysis ($\Delta = -0.62 \pm 0.06$, chapter 3) and direct photolysis ($\Delta = 1.05 \pm 0.14$ [10]). On the other hand, slopes for photooxidation with OH radicals or mediated by the excited triplet state of 4-carboxybenzophenone (${}^34\text{-CBBP}^*$) [10] are in the same range as for biooxidation. With DEA and DIA, all three transformation pathways produce the same products, however, so that risk assessments with respect to generated products are not expected to be biased.

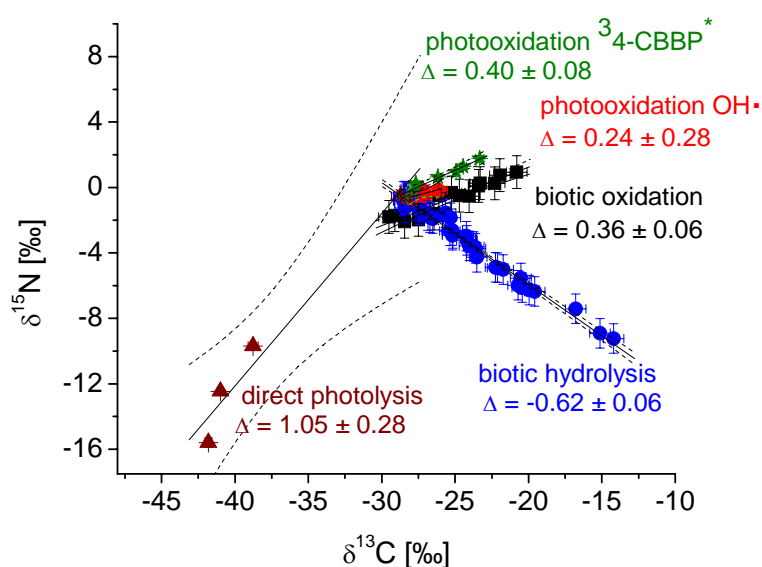


Figure 5-1. Dual isotope plots of carbon and nitrogen ratios obtained in lab experiments addressing different natural degradation processes of atrazine. Original isotope data for degradation by photolysis and photooxidation was kindly provided by A. Hartenbach and T. Hofstetter (EAWAG / ETH Zürich, Switzerland). For biotic experiments the total uncertainty is $\pm 0.7\text{‰}$ for carbon isotope and $\pm 1.0\text{‰}$ for nitrogen isotope measurements. For photodegradation error bars indicate one standard deviation of triplicate measurements [1]. Dotted lines represent 95% confidence intervals of the linear regression.

When attempting to use isotope measurements also for quantification of atrazine degradation according to the Rayleigh equation (Chapter 1, eq. 9), the identification of predominant pathways by dual isotope patterns clearly helps to select an appropriate enrichment factor. On the other hand, the results from biotic hydrolysis of atrazine in chapter 3 demonstrate that enrichment factors can

vary even for the same pathway leading to an uncertainty in the assessment of the actual degradation [4]. Therefore, we recommend to apply conservative quantification where the enrichment factor corresponding to the highest fractionation should be used [11]. To evaluate also the variability of isotope enrichment factors related to the oxidative dealkylation pathway, further lab experiments with other dealkylating microorganisms will be helpful.

In summary, the results of this thesis clearly demonstrate the potential of CSIA as a new, complementary approach for a better understanding of the fate of atrazine in the environment. The work illustrates that carbon and nitrogen isotope fractionation associated with degradation processes of atrazine can be measured by GC-C-IRMS, that the fractionation can serve to identify and distinguish different degradation pathways of atrazine and that it may even help to elucidate underlying reaction mechanisms. Nonetheless, important challenges remain to be addressed in the future.

One important research gap concerns possible fractionation associated with sorption, the main non-degradative process of atrazine in soils and groundwater aquifers. The extent of isotopic fractionation associated with reversible sorption has been discussed with controversy. One-step sorption experiments conducted with PCE, TCE, benzene and toluene [12], [13] did not show significant isotopic fractionation within the analytical error. On the other hand, multiple-step sorption experiments gave evidence that sorption may have a small, but non-negligible effect on isotopic composition of carbon and hydrogen [14, 15]. In contrast, Meckenstock *et al.* [16] did not observe significant changes in aromatic hydrocarbons when they were passing through a column filled with aquifer material. In the case of atrazine even irreversible sorption has been postulated [17-19], by electron transfer between the triazine ring or the amino groups and quinone-like moieties in humic substances. It has been reasoned that such complexes would be stabilized as semiquinone species by the complex molecular structure of humic substances [20-22]. In such a case the process would represent an actual chemical reaction, which may be associated with specific isotope fractionation of as yet unknown magnitude, which would need to be taken into account when conducting assessments analogous to Figure 5-1.

A major analytical challenge, finally, is to provide approaches which make it possible to analyze triazines in low concentrations as encountered in the environment (down to 0,1 µg/L). Different enrichment methods will have to be tested in order to increase analyte concentration by a factor of about 1000 without altering the isotope composition of the compound. Since also non target compounds of the surrounding matrix may be enriched, in addition further purification may be necessary prior to precise and accurate isotope analysis [23].

5.2 References

1. Zwank, L.; Berg, M.; Elsner, M.; Schmidt, T. C.; Schwarzenbach, R. P.; Haderlein, S. B., New evaluation scheme for two-dimensional isotope analysis to decipher biodegradation processes: Application to groundwater contamination by MTBE. *Environ. Sci. Technol.* 2005, *39*, (4), 1018-1029.
2. Elsner, M.; McKelvie, J.; LacrampeCouloume, G.; SherwoodLollar, B., Insight into methyl tert-butyl ether (MTBE) stable isotope fractionation from abiotic reference experiments. *Environ. Sci. Technol.* 2007, *41*, (16), 5693-5700.
3. Vogt, C.; Cyrus, E.; Herklotz, I.; Schlosser, D.; Bahr, A.; Herrmann, S.; Richnow, H.-H.; Fischer, A., Evaluation of toluene degradation pathways by two-dimensional stable isotope fractionation. *Environ. Sci. Technol.* 2008, *42*, (21), 7793-7800.
4. Fischer, A.; Herklotz, I.; Herrmann, S.; Thullner, M.; Weelink, S. A. B.; Stams, A. J. M.; Schlömann, M.; Richnow, H.-H.; Vogt, C., Combined carbon and hydrogen isotope fractionation investigations for elucidating benzene biodegradation pathways. *Environ. Sci. Technol.* 2008, *42*, (12), 4356-4363.
5. Nagy, I.; Compennolle, F.; Ghys, K.; Vanderleyden, J.; De Mot, R., A single cytochrome P-450 system is involved in degradation of the herbicides EPTC (S-ethyl dipropylthiocarbamate) and atrazine by *Rhodococcus* sp. strain NI86/21. *Appl. Environ. Microbiol.* 1995, *61*, (5), 2056-2060.
6. Dinnocenzo, J. P.; Karki, S. B.; Jones, J. P., On isotope effects for the cytochrome P-450 oxidation of substituted N,N-dimethylanilines. *J. Am. Chem. Soc.* 1993, *115*, (16), 7111-7116.
7. Guengerich, F. P.; Yun, C. H.; MacDonald, T. L., Evidence for a 1-electron oxidation mechanism in N-dealkylation of N,N-dialkylanilines by cytochrome P450 2B1. *The Journal of Biological Chemistry* 1996, *271*, (44), 27321-27329.
8. Karki, S. B.; Dinnocenzo, J. P.; Jones, J. P.; Korzekwa, K. R., Mechanism of oxidative amine dealkylation of substituted N,N-dimethylanilines by cytochrome P-450: application of isotope effect profiles. *J. Am. Chem. Soc.* 1995, *117*, (13), 3657-3664.
9. Miwa, G. T.; Walsh, J. S.; Kedderis, G. L.; Hollenberg, P. F., The use of intramolecular isotope effects to distinguish between deprotonation and hydrogen atom abstraction mechanisms in cytochrome P-450- and peroxidase-catalyzed N-demethylation reactions. *J. Biol. Chem.* 1983, *258*, (23), 14445-14449.
10. Hartenbach, A. E.; Hofstetter, T. B.; Tentscher, P. R.; Canonica, S.; Berg, M.; Schwarzenbach, R. P., Carbon, hydrogen, and nitrogen isotope fractionation during light-Induced transformations of atrazine. *Environ. Sci. Technol.* 2008, *42*, (21), 7751-7756.
11. Meckenstock, R. U.; Safinowski, M.; Griebler, C., Anaerobic degradation of polycyclic aromatic hydrocarbons. *Fems Microbiology Ecology* 2004, *49*, (1), 27-36.
12. Harrington, R. R.; Poulson, S. R.; Drever, J. I.; Colberg, P. J. S.; Kelly, E. F., Carbon isotope systematics of monoaromatic hydrocarbons: vaporization and adsorption experiments. *Org. Geochem.* 1999, *30*, 765-775.

13. Slater, G. F.; Ahad, J. M. E.; Sherwood Lollar, B.; Allen-King, R.; Sleep, B., Carbon isotope effects resulting from equilibrium sorption of dissolved VOCs. *Analytical Chemistry* 2000, 72, (22), 5669-5672.
14. Caimi, R. J.; Brenna, J. T., Quantitative evaluation of carbon isotopic fractionation during reversed-phase high-performance liquid chromatography. *J. Chrom. A* 1997, 757, 307-310.
15. Kopinke, F. D.; Georgi, A.; Voskamp, M.; Richnow, H. H., Carbon isotope fractionation of organic contaminants due to retardation on humic substances: Implications for natural attenuation studies in aquifers. *Environ. Sci. Technol.* 2005, 39, (16), 6052-6062.
16. Meckenstock, R. U.; Morasch, B.; Warthmann, R.; Schink, B.; Annweiler, E.; Michaelis, W.; Richnow, H. H., $^{13}\text{C}/^{12}\text{C}$ isotope fractionation of aromatic hydrocarbons during microbial degradation. *Environ. Microbiol.* 1999, 1, (5), 409-414.
17. Ma, L.; Selim, H. M., Atrazine retention and transport in soils. *Rev. Environ. Contam. T.* 1996, 145, 129-162.
18. Moreau-Kervevan, C.; Mouvet, C., Adsorption and desorption of atrazine, deethylatrazine, and hydroxyatrazine by soil components. *J. Environ. Qual.* 1998, 27, 46-53.
19. Senesi, N.; D'Orazio, V.; Miano, T. M., Adsorption mechanisms of s-triazine and bipyridylum herbicides on humic acids from hop field soils. *Geoderma* 1995, 66, (3-4), 273-283.
20. Martin-Neto, L.; Tragheta, D. G.; Vaz, C. M. P.; Crestana, S.; Sposito, G., On the interaction mechanisms of atrazine and hydroxyatrazine with humic substances. *J. Environ. Qual.* 2001, 30, (2), 520-525.
21. Senesi, N., Binding mechanisms of pesticides to soil humic substances. *Sci. Total. Environ.* 1992, 123/124, 63-76.
22. Sposito, G.; Martin-Neto, L.; Yang, A., Atrazine complexation by soil humic acids. *J. Environ. Qual.* 1996, 25, 1203-1209.
23. Blessing, M.; Jochmann, M.; Schmidt, T., Pitfalls in compound-specific isotope analysis of environmental samples. *Analytical and Bioanalytical Chemistry* 2008, 390, (2), 591-603.

APPENDIX A1

(Supporting Information of Chapter 2- Precise and Accurate Compound Specific Carbon and Nitrogen Isotope Analyses of the Herbicide Atrazine: Critical Role of Combustion Oven Conditions)

A1.1 Results and Discussion

Table A1_1. Mean isotope ratios determined for different atrazine batches using either GC-IRMS operating with different combustion reagents and temperatures, EA-IRMS or dual-inlet-IRMS. Values are reported in permil.

Combustion reagent Temperature	GC-IRMS					EA-IRMS			dual-inlet-IRMS		
	CuO 800°C		Ni/NiO 1150°C		TU	WO ₃ +O ₂ 1000°C		TU	CuO 960°C		TU
Carbon	$\delta^{13}\text{C}$	SD	$\delta^{13}\text{C}$	SD	TU	$\delta^{13}\text{C}$	SD	TU	$\delta^{13}\text{C}$	SD	TU
Tropitzsch	-	-	-28.5	0.3	0.7	-28.73	0.03	0.20	-28.75	0.02	0.10
Chem Service	-30.2	0.4	-28.7	0.4	0.7	-28.60	0.10	0.20	-28.90	0.01	0.10
Riedel-de Haën	-	-	-27.1	0.3		-27.03	0.06	0.20	-26.95	0.04	0.10
Nitrogen			$\delta^{15}\text{N}$	SD	TU	$\delta^{15}\text{N}$	SD	TU			
Tropitzsch			-1.7	0.3	0.9	-1.48	0.03	0.2			
Chem Service			-0.1	0.1	0.9	-0.25	0.05	0.2			

SD: standard deviation

TU: Total uncertainty of measurement as indicated in figure 1c) for the Ni/NiO oven. For the CuO oven the total uncertainty is not given as values are systematically in error (see figure 1 b)).

A1_1.1 Hydrolysis of atrazine at pH 12 and 20°C. Quality control of the GC-IRMS performance during analyses of samples.

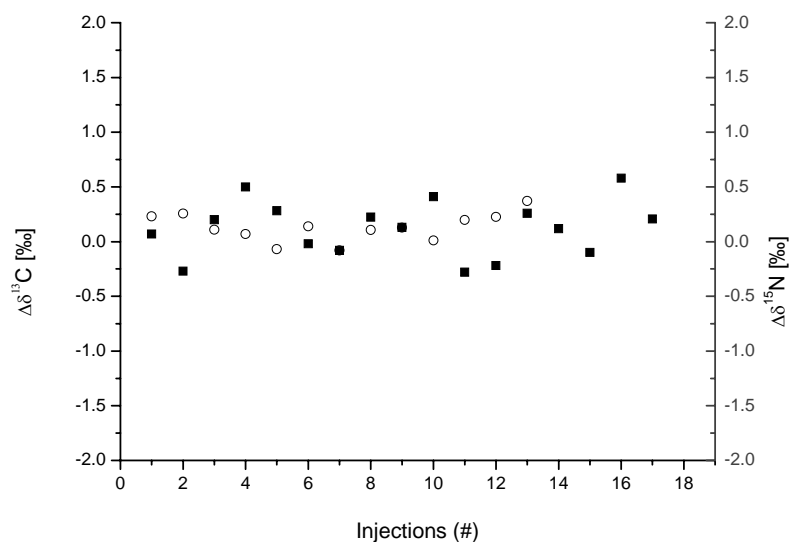


Figure A1_1. Carbon (squares) and nitrogen (circles) isotope values of atrazine standards during measurements of samples from the hydrolysis experiment. Injected amount for carbon and nitrogen was 3.7 nmol and 4.7 nmol, respectively. $\Delta\delta^{13}\text{C}$ and $\Delta\delta^{15}\text{N}$ values are reported as deviations from the values measured on the dual-inlet and the elemental analyzer, respectively.

APPENDIX A2

(Supporting Information of chapter 3 - C and N isotope fractionation suggests similar mechanisms of microbial atrazine transformation despite involvement of different enzymes (AtzA and TrzN))

A 2_1 Material and Methods

a) Bacterial growth and cultivation media

All strains were grown in mineral salt medium, containing $1.78 \text{ g L}^{-1} \text{ Na}_2\text{HPO}_2 \cdot 2\text{H}_2\text{O}$; $1.36 \text{ g L}^{-1} \text{ KH}_2\text{PO}_4$; $0.05 \text{ g L}^{-1} \text{ MgSO}_4 \cdot 7\text{H}_2\text{O}$; $0.0132 \text{ g L}^{-1} \text{ CaCl}_2 \cdot 2\text{H}_2\text{O}$; $2.86 \text{ g L}^{-1} \text{ H}_3\text{BO}_3$; $1.54 \text{ g L}^{-1} \text{ MnSO}_4 \cdot \text{H}_2\text{O}$; $0.039 \text{ g L}^{-1} \text{ CuSO}_4 \cdot 5\text{H}_2\text{O}$; $0.021 \text{ g L}^{-1} \text{ ZnCl}_2$; $0.041 \text{ g L}^{-1} \text{ CoCl}_2 \cdot 6\text{H}_2\text{O}$; $0.025 \text{ g L}^{-1} \text{ Na}_2\text{MoO}_4 \cdot 2\text{H}_2\text{O}$, $5.14 \text{ g L}^{-1} \text{ FeCl}_3 \cdot 6\text{H}_2\text{O}$ supplemented with 100 mg L^{-1} of glucose and 100 mg L^{-1} fructose (?) and 20 mg L^{-1} atrazine. pH was adjusted to 7.2.

A2_2 Results and Discussion

a) Biotic hydrolysis of atrazine. Temporal course of decrease of atrazine and formation of the metabolite hydroxyatrazine.

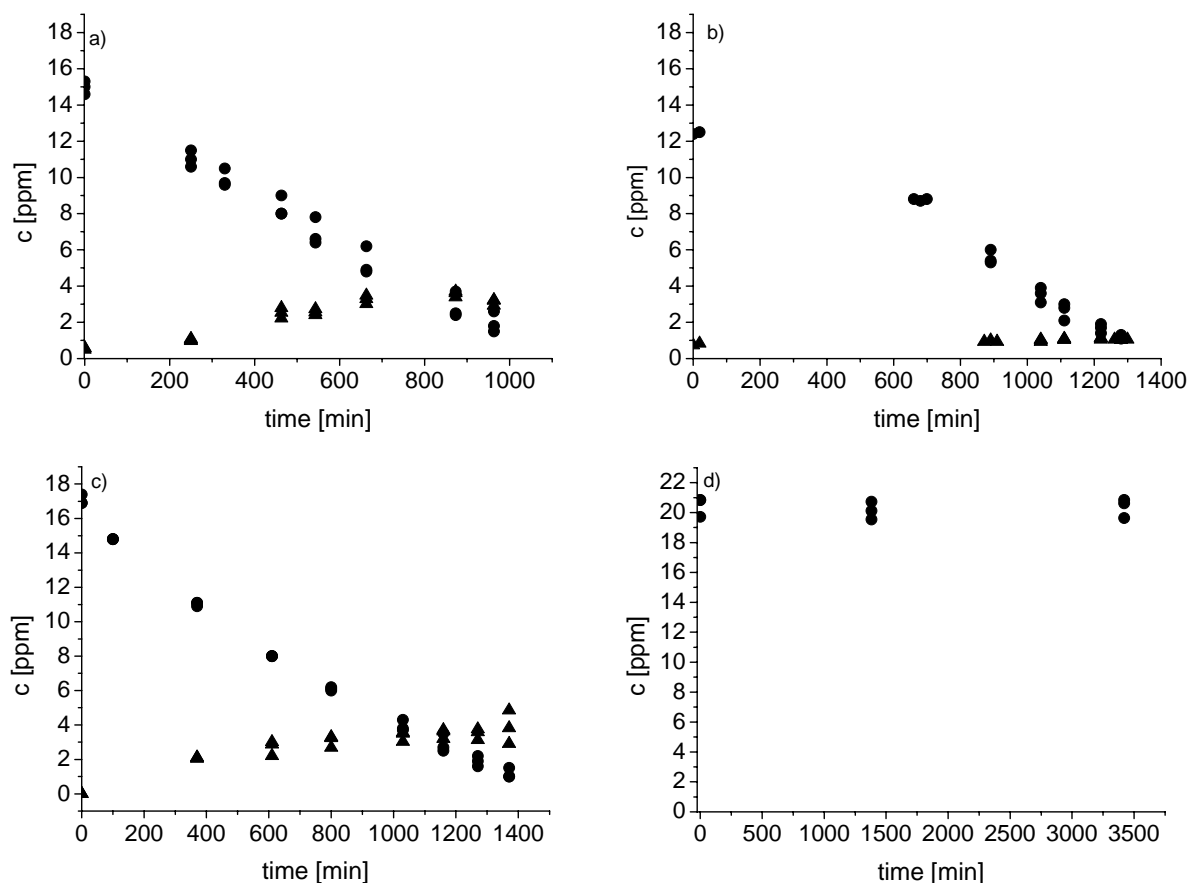


Figure A2_1. Biotic hydrolysis of atrazine. Concentrations of atrazine (filled dots) and of the direct degradation product hydroxyatrazine (filled triangles) over time for *Chelatobacter heintzii* (a), *Pseudomonas sp. ADP* (b) and *Arthrobacter aureescens TC1* (c) and sterile control (d)

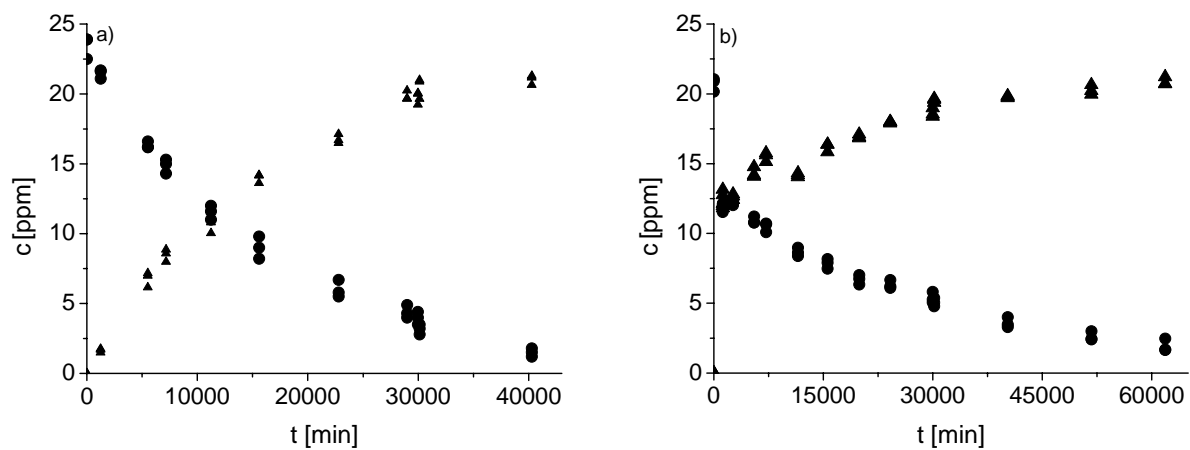


Figure A2_2. Abiotic hydrolysis of atrazine at pH 3 (a) and pH 12 (b) at 60°C. concentrations of atrazine (filled dots) and of the direct degradation product hydroxyatrazine (filled triangles) over time.

APPENDIX A3

(Supporting Information of Chapter 4 - Probing for Concurring Mechanisms of Oxidative Atrazine Dealkylation: A combined Approach with Metabolite Identification and Dual Isotope Fractionation (C and N) Measurements)

A3.1 MATERIAL AND METHODS

A3.1.1 Identification of atrazine, simazine and its metabolites

To identify unknown peaks of the biotic and abiotic degradation experiments we analysed aqueous samples on a Q-Trap MS/MS system (Applied Biosystems, Toronto, Canada). Scan type was Enhanced Ion Product Scan, where analytes are scanned and characterized for their molecular ion and for generated fragment ions (Table S1, S2). To link the products identified by LC-MS/MS (Figure S1, S2, S3, S4) to the peaks of the HPLC-UV/VIS runs in which quantification over time had been determined (i.e., the data of Figure 1 of Chapter 4), we re-run selected samples on the HPLC-UV/VIS system using the eluents and gradient program of the LC_MS/MS runs.

For oxidation with permanganate such retrospective analysis on the HPLC-UV/VIS was not possible since after a second rethawing samples showed precipitation of MnO₂, which could not be separated from solution within the sample volume of just about 50 uL. In this case peak identification was accomplished using relative RT differences obtained by comparing RT of the initial HPLC-UV/VIS analysis of known standards with the RT of the LC-MS/MS run of the corresponding masses.

A3.2 RESULTS

Table A3_1: Identification of biotic and abiotic simazine degradation products by LC-MS/MS. Scan was done for target molecule-ion. Target molecule ions with no successful hit are in brackets. n.d. = not detected.

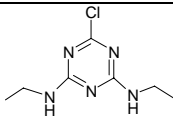
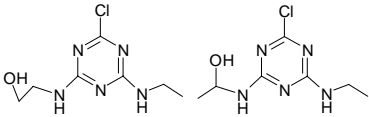
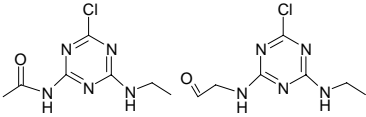
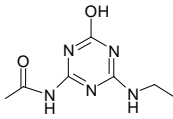
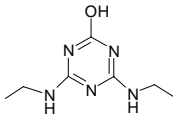
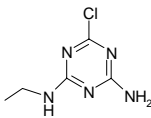
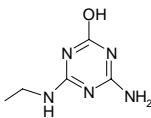
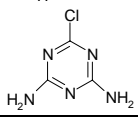
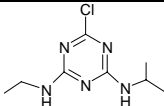
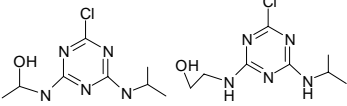
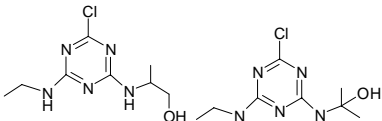
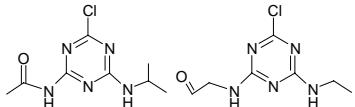
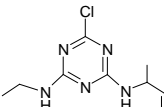
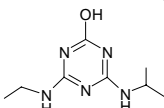
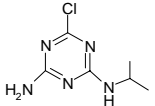
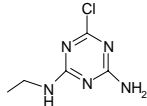
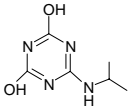
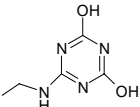
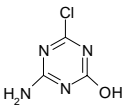
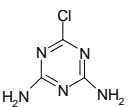
Name/abbreviation	structure	target molecule-ion [m/z]	fragment-ions [m/z]	Matches retention time of
Simazine		202	174, 132, 104	Standard
SETOH		218	200, 174, 146, 104	S1, PS4
SETO _{oxo}		216	174, 146, 104	PS5
ODET		(198)	n.d.	
OEET		(184)	n.d.	
DES		174	146, 132, 104	Standard
OEAT		(154)	n.d.	
CAAT		(146)	n.d.	

Table A3_2: Identification of biotic and abiotic atrazine degradation products by LC-MS/MS. Scan was done for target molecule-ion. Target molecule ions with no successful hit are in brackets. N.d. = not detected.

Name/abbreviation	structure	target molecule-ion [m/z]	fragment-ions [m/z]	Matches retention time of
Atrazine		216	174, 146, 104	Standard
AETOH		232	214, 188, 172, 146	A2, PA1
AIPOH		232	214, 174, 146	A1
AETOxo		230	188, 146	PA2,A3
AIPOxo		(230)	n.d.	
HAT		(198)	n.d.	
DEA		188	146, 104	Standard
DIA		174	146, 132, 104	Standard
2,6-Dihydroxy-4-(N'-isopropylamino)-1,3,5-triazine		(170)	n.d.	
2,4-Dihydroxy-6-(N'-ethylamino)-1,3,5-triazine		(157)	n.d.	
2-Chloro-4-hydroxy-6-amino-1,3,5-triazine		(147)	n.d.	
2-Chloro-4,6-diamino-1,3,5-triazine		(146)	n.d.	

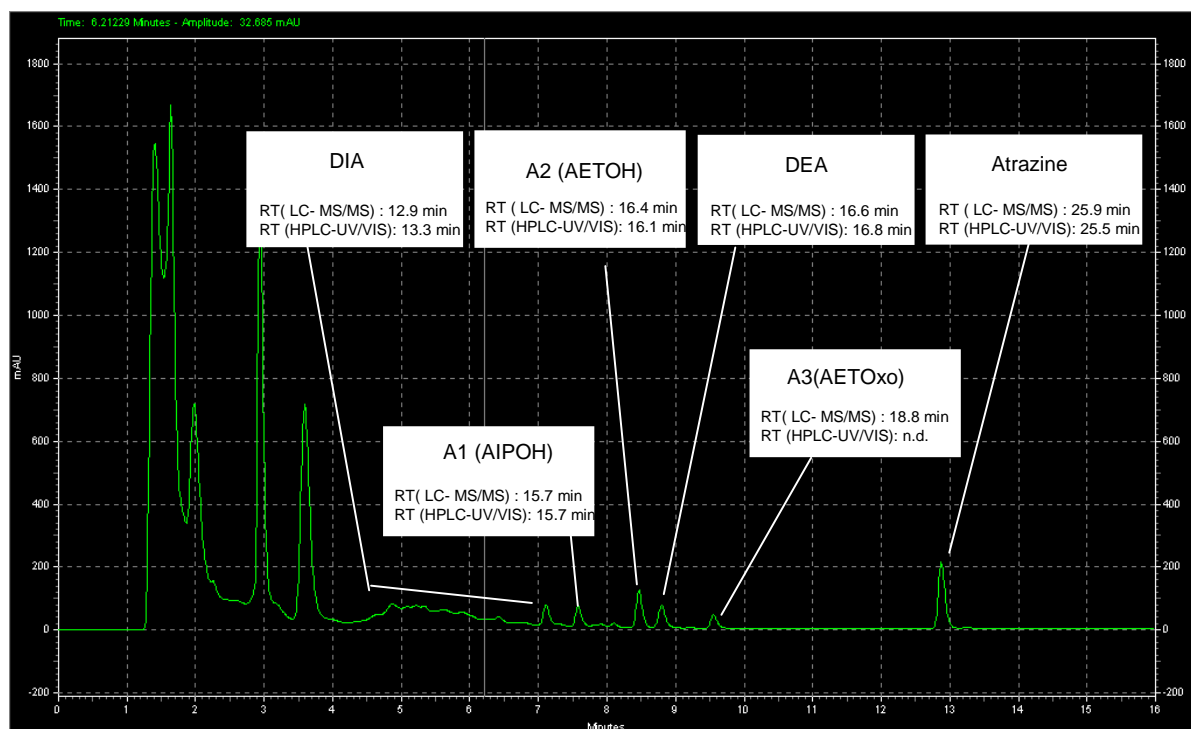


Figure A3_1. HPLC chromatograms at 220 nm of initial HPLC-UV/VIS analysis at about 77 % atrazine degradation by *Rhodococcus* sp. NI86/21. Boxes contain products obtained by standards or mass spectrometry (in brackets), and corresponding retention times of LC MS/MS and of second HPLC UV/VIS analysis. Peaks at the beginning (1-4min) of chromatogram are identical to control samples.

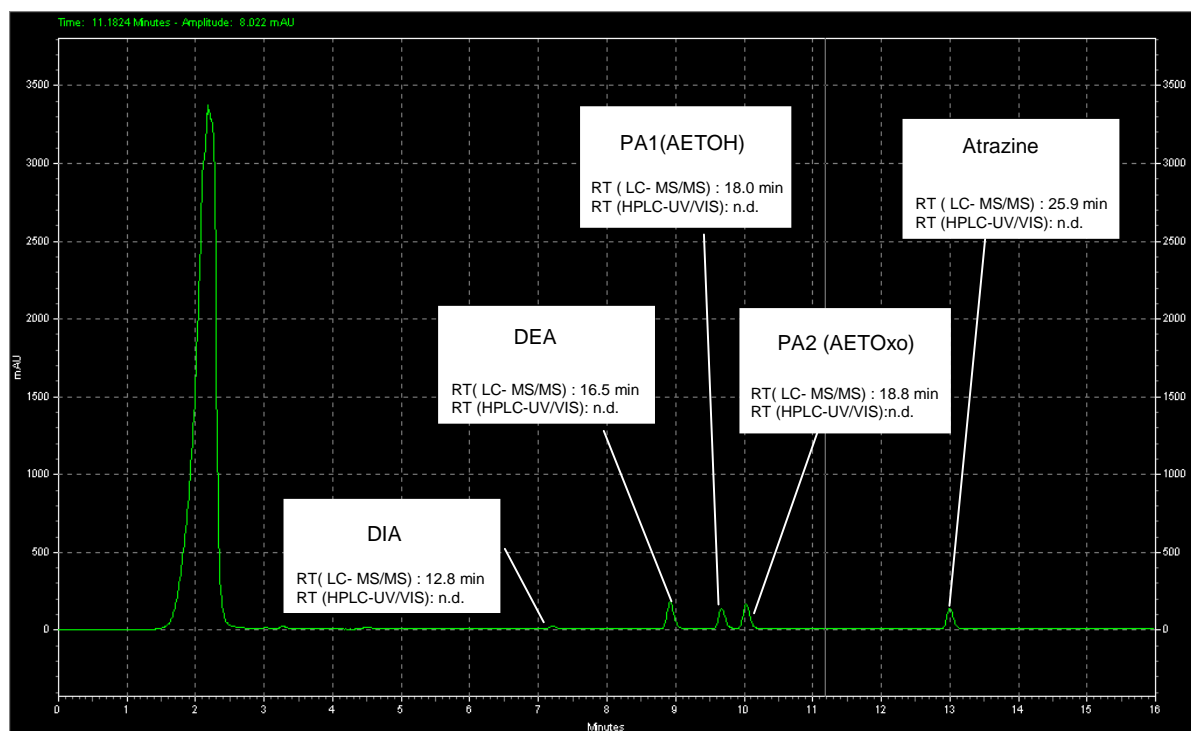


Figure A3_2. HPLC chromatograms at 220 nm of initial HPLC-UV/VIS analysis at about 90 % atrazine degradation by permanganate oxidation. Boxes contain products obtained by standards or mass spectrometry (in brackets), and corresponding retention times of LC MS/MS analysis. Peaks with RT of 2 min is identical to control samples.

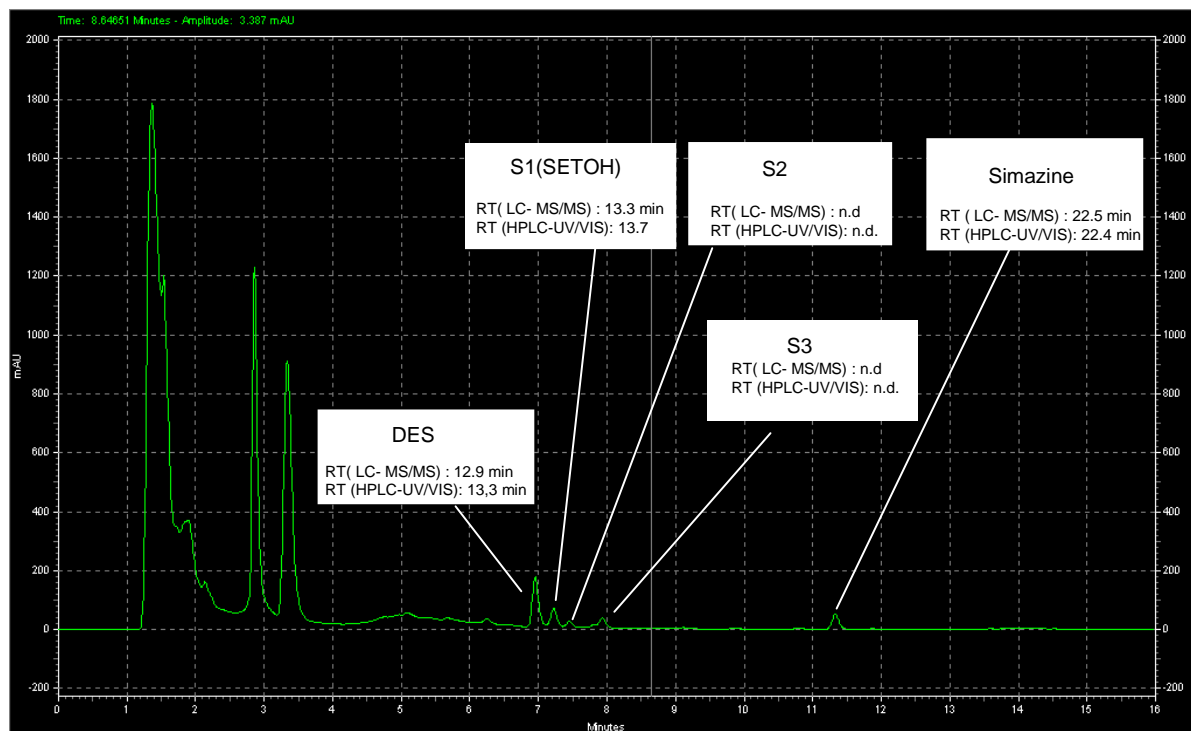


Figure A3_3. HPLC chromatograms at 220 nm of initial HPLC-UV/VIS analysis at about 90 % simazine degradation by *Rhodococcus* sp. NI86/21. Boxes contain products obtained by standards or mass spectrometry (in brackets), and corresponding retention times of LC MS/MS and of second HPLC UV/VIS analysis. S2 and S3 were no detected in later analysis. Peaks at the beginning of chromatogram (1-4min) are identical to control samples.

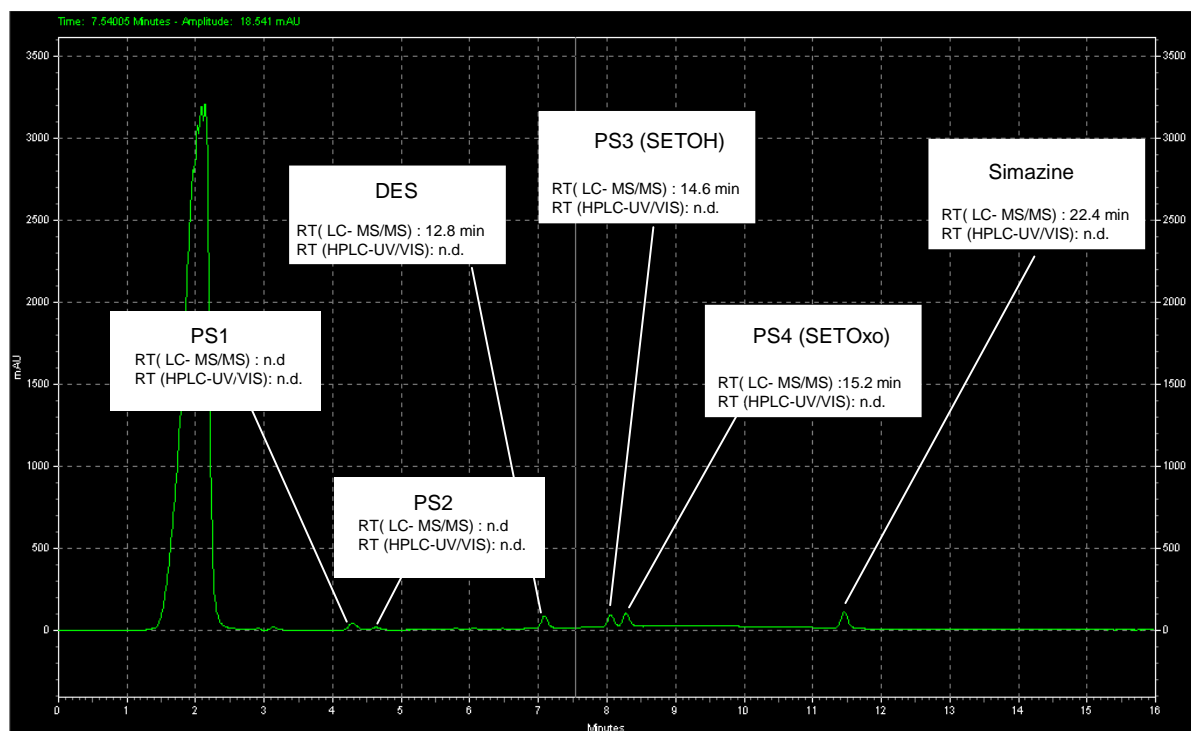


Figure A3_4. HPLC chromatograms at 220 nm of initial HPLC-UV/VIS analysis at about 75 % simazine degradation by permanganate oxidation. Boxes contain products obtained by standards or mass spectrometry (in brackets), and corresponding retention times of LC MS/MS analysis. For L1 and L2 none of the investigated target ion masses matched. Peaks with RT of 2 min is identical to control samples.

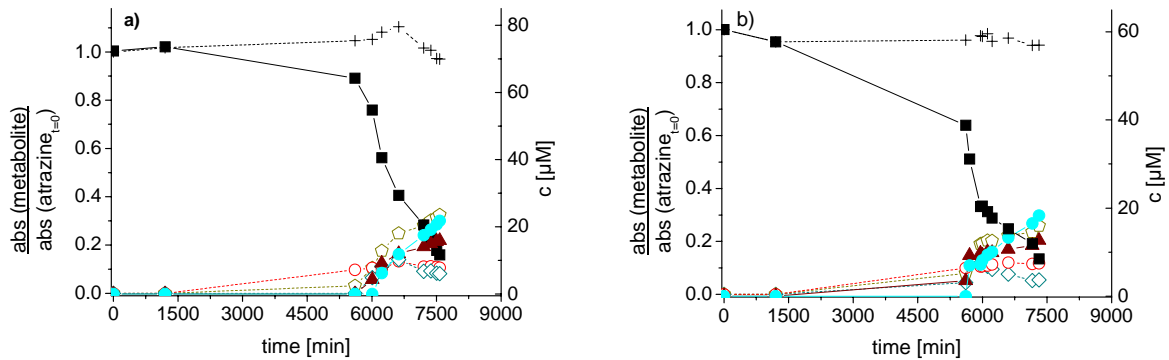


Figure A3_5. Time course of atrazine concentration and formation of products for replicates (a,b) of atrazine degradation by *Rhodococcus* sp. NI86/21. The right y-axis shows concentration of atrazine (solid black squares) and DEA (solid cyan circles) and DIA (solid brown triangles). The left y-axis illustrates relative amount of metabolites A1 (open red circles), A2 (open green pentagons), A3 (open teal blue rhombs) and the molar balance of transformation (crosses, sum) expressed by the ratio $(\text{abs}(\text{metabolite})_{220\text{nm}}/\text{abs}(\text{triazine}_{t=0})_{220\text{nm}})$.

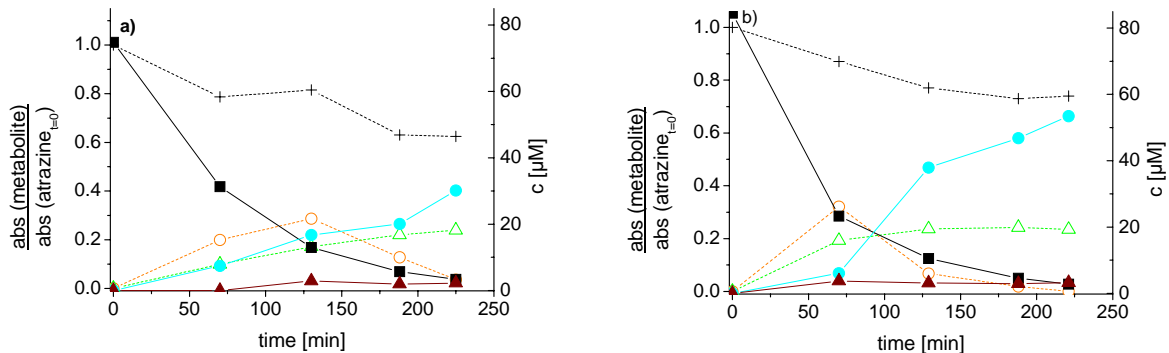


Figure A3_6. Time course of atrazine concentration and formation of products for replicates (a,b) of atrazine degradation by permanganate. NI86/21. The right y-axis shows concentration of atrazine (solid black squares) and DEA (solid cyan circles) and DIA (solid brown triangles). The left y-axis illustrates the relative amount of metabolites PA1 (open orange circles), PA2 (open green triangles), A3 (open teal blue rhombs) and molar balance of transformation (crosses, sum) expressed by the ratio $(\text{abs}(\text{metabolite})_{220\text{nm}}/\text{abs}(\text{triazine}_{t=0})_{220\text{nm}})$.

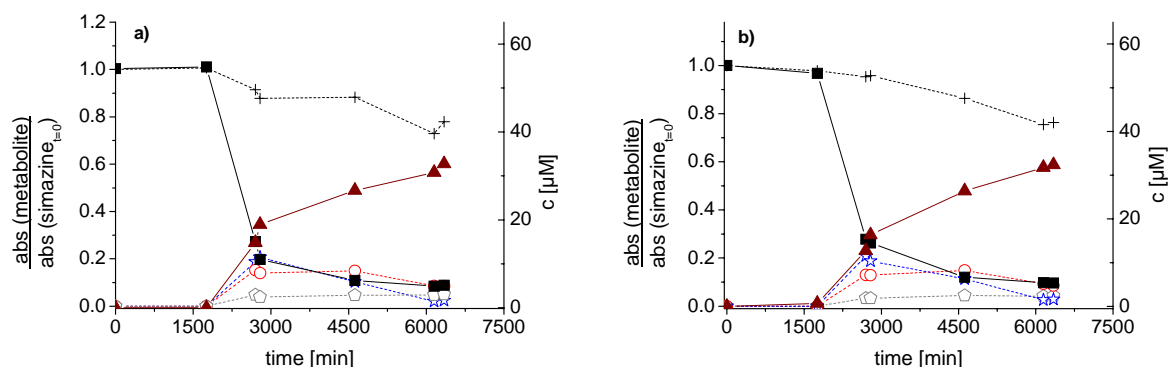


Figure A3_7. Time course of simazine concentration and formation of products for replicates (a,b) of simazine degradation by *Rhodococcus* sp. NI86/21. The right y-axis shows concentration of simazine (solid black squares) and DES (solid brown triangles). The left y-axis illustrates the relative amount of metabolites S1 (open grey pentagons), S2 (open blue stars), S3 (open red circles) and molar balance of transformation (crosses, sum) by the ratio $\frac{\text{abs (metabolite)}_{220\text{nm}}}{\text{abs (triazine}_{t=0})_{220\text{nm}}}$.

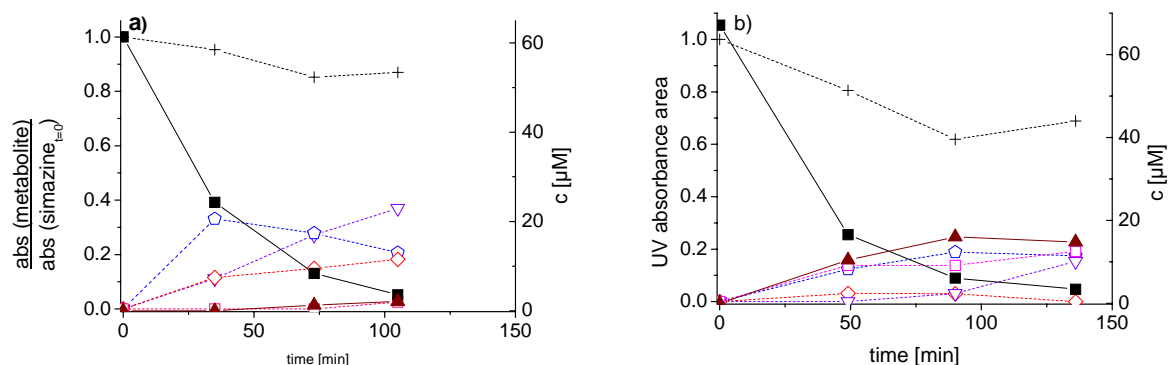


Figure A3_8. Time course of simazine concentration and formation of products for replicates (a,b) of simazine degradation by permanganate. The right y-axis shows concentration of simazine (solid black squares) and DES (solid brown triangles). The left y-axis illustrates relative amount of metabolites PS1 (open pink squares), PS2 (open violet triangles), PS3 (open blue pentagons), PS4 (open red rhombs) and molar balance of transformation (crosses, sum) expressed by the ratio $\frac{\text{abs (metabolite)}_{220\text{nm}}}{\text{abs (triazine}_{t=0})_{220\text{nm}}}$.

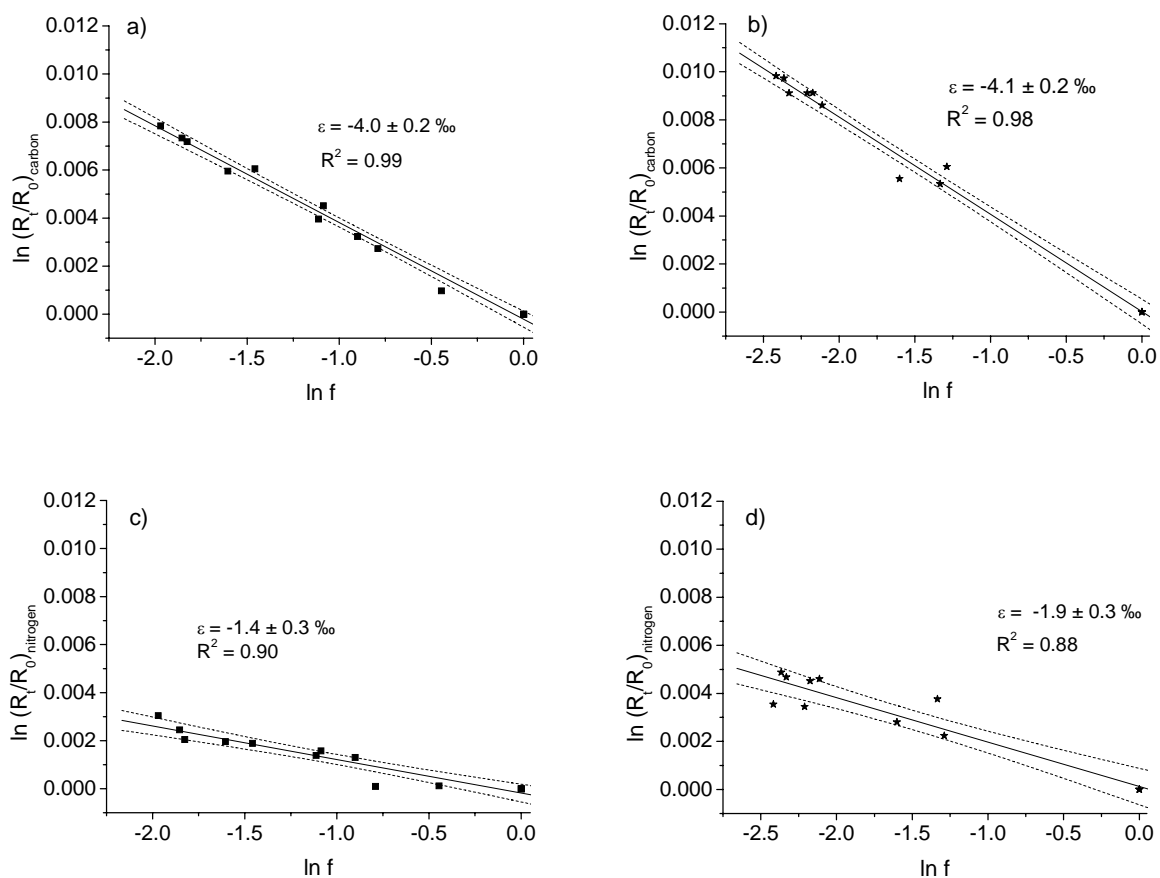


Figure A3_9. Logarithmic plots of isotope ratios according to the Rayleigh equation (eq. 3, Chapter 3) determined for degradation of atrazine (squares) and simazine (stars) by *Rhodococcus* sp. IN86/21. Rayleigh plot for carbon of atrazine (a) and simazine (b) and for nitrogen of atrazine (c) and simazine (d), respectively. Dotted lines represent 95% confidence interval of linear regression.

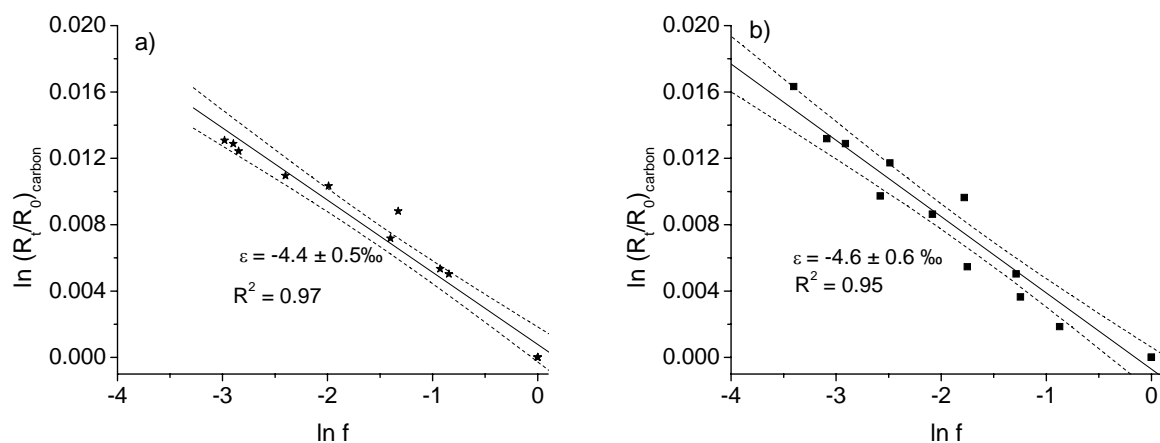


Figure A3_10. Logarithmic plots of isotope ratios according to the Rayleigh equation (eq. 1) determined for degradation of simazine (stars) and atrazine (squares) by permanganate. (a) Rayleigh plot for carbon of simazine (a) and atrazine (b). As for nitrogen no isotope fractionation was observed, no Rayleigh plots were defined. Dotted lines represent 95% confidence interval of linear regression.

PhD candidate contributions to the published chapter 2 and 3 and the unpublished chapter 4

Chapter 2: “Precise and accurate compound specific carbon and nitrogen isotope analysis of atrazine: critical role of combustion oven conditions.” *Environ. Sci. Technol.* 2008, 42, (21), 7757-7763.

The contributions of the PhD candidate to this work were the following:

Experimental design for the development of the analysis of compound specific isotope analysis of atrazine at the GC-IRMS and for alkaline hydrolysis of atrazine was elaborated in accordance with the supervisor Dr Martin Elsner. Sampling, preparation, and measurements by GC-IRMS and HPLC UV/VIS analyses of the experiments were done by the PhD candidate. Also statistical data analyses and their graphical illustration were done independently. Interpretation and discussion of the results were done in cooperation with the other co-authors leading to autonomous compilation of the draft of the manuscript. Comments of the co-authors were included. Manuscript was submitted by the corresponding author Dr Martin Elsner to the ACS Journal *Environmental Science and Technology*. Comments and recommendations of the peer-reviewer of the journal were addressed in consultation to the co-authors and successfully resubmitted.

Chapter 3: “C and N isotope fractionation suggests similar mechanisms of microbial atrazine transformation despite involvement of different enzymes (AtzA and TrzN).” *Environ. Sci. Technol.* 2009, 43, (21), 8079-8085.

The contributions of the PhD candidate to this work were the following:

The concept and setup of the experiment was conceived by the PhD candidate and discussed and refined with the supervisor. Cultivation of bacteria, sample preparation, and measurements (GC-IRMS, HPLC UV/VIS) of the biotic and abiotic degradation experiments were performed by the PhD candidate as well as statistical data analyses and graphical illustrations. The results were discussed with the co-authors and combined to a manuscript by the PhD candidate. Proof reading was done by the co-authors. Manuscript was submitted by the corresponding author Dr Martin Elsner to the ACS Journal *Environmental Science and Technology*. In accordance with the co-authors, comments and recommendations of the reviewers were included to the manuscript by the PhD candidate and resubmitted successfully to the journal.

Chapter 4: “Probing for Concurring Mechanisms of Oxidative Atrazine Dealkylation: A combined Approach with Metabolite Identification and Dual Isotope Fractionation (C and N) Measurements”.

The contributions of the PhD candidate to this work were the following:

The experimental design was carried out in agreement with the supervisor Dr Martin Elsner. Cultivation of bacteria for the biotic oxidation experiments, preparation of the abiotic reference experiments as well as concentration measurements (HPLC UV/VIS), isotope analyses (GC-IRMS), and metabolite identifications (LC-MS/MS) were done by the PhD candidate. All statistical data analyses and graphical illustrations were performed by the PhD candidate. After discussion with the supervisor chapter 4 was written by the PhD candidate.

Publications:

Peer-reviewed journals

Meyer, A. H.; Penning, H.; Lowag, H.; Elsner, M., Precise and accurate compound specific carbon and nitrogen isotope analysis of atrazine: critical role of combustion oven conditions. *Environ. Sci. Technol.* 2008, 42, (21), 7757-7763.

Meyer, A. H.; Penning, H.; Elsner, M., C and N isotope fractionation suggests similar mechanisms of microbial atrazine transformation despite involvement of different enzymes (AtzA and TrzN). *Environ. Sci. Technol.* 2009, 43, (21), 8079-8085.

Penning, H.; Meyer A. H.; Sørensen S. R.; Aamand J.; Elsner, M., C, N and H isotope fractionation of the herbicide isoproturon reflects different microbial transformation pathways. 2010. *Environ. Sci. Technol. accepted.*

Selected Conference contributions

Meyer, A. H.; Penning, H.; Elsner, M., Compound-specific isotope analysis of atrazine. 2007. International workshop on stable isotopes, Ascona, Switzerland. Poster presentation.

Meyer, A.H.; Penning, H.; Elsner M., Variability in carbon and nitrogen isotope fractionation associated with bacterial hydrolysis of atrazine. 2009. Jahrestreffen der VAAM, Bochum, Germany. Poster Presentation.

Meyer, A.H.; Penning, H.; Lowag, H.; Elsner M., Präzise und akkurate Substanz-spezifische Isotopenanalytik von Kohlenstoff und Stickstoff für die Risikobewertung des Herbizides Atrazin in der aquatischen Umwelt. 2009. Jahrestagung der Wasserchemischen Gesellschaft-GDCh, Stralsund, Germany. Oral presentation.

Danksagung

Damit meine Arbeit ein fruchtvolles Ende finden konnte, gebührt vielen Personen sehr großer Dank, da sie mich auf diesem Weg begleitet und auf verschiedenste Weise unterstützt haben. Der größte Dank richtet sich an meinen Betreuer Dr. Martin Elsner. Zum einen natürlich, dass er sich entschlossen hatte, mich für diese Arbeit auszuwählen. Zum anderen aber vor allem, dass ich bei ihm eine hervorragende Betreuung genießen durfte, die maßgeblich zum Gelingen dieser Arbeit beigetragen hatte. Ich danke dir Martin, für die große Freiheit, die du mir gegeben hast, Ideen und Lösungen zu entwickeln, aber gleichzeitig bei aufkommenden Fragestellungen oder Problemen immer Zeit für mich gefunden hast, mir zu helfen. Die Diskussionen, die immer von einer sehr freundschaftlichen Atmosphäre geprägt gewesen waren, sind für mich immer äußerst spannend und zugleich höchst motivierend gewesen und das betraf neben dem wissenschaftlichen auch den alltäglichen Bereich, wie z.B. unsere Kinder und den Sport. Martin dafür vielen, vielen Dank!!

Großen Dank möchte ich auch meinem Doktorvater und Institutsleiter Prof. Dr. Meckenstock entgegenbringen. Er ermöglichte mir jegliche fachliche, konzeptionelle und finanzielle Unterstützung damit diese Forschung erfolgreich gestaltet werden konnte und ich die Möglichkeit erhielt, den Doktorgrad erlangen zu können.

Außerdem möchte ich sehr Holger Penning, Harald Lowag, Nadja Kadlec und Martina Höche danken, die mir im Labor (und nicht nur da) immer mit Rat und Tat zur Seite standen. In diesem Zusammenhang möchte ich auch Akane Hartenbach und Thomas Hofstetter von der EAWAG (Zürich, Schweiz) für ihre Hilfsbereitschaft und Kooperativität danken.

Ein spezieller Dank gilt Sandra, Claudia, Franz (die Container-Enklave), Giovanni (Grazie 'mbare!) Holger, Heini und Draženka. Die Zeit, die ich mit euch an vielen Tagen aber auch an so manchen Abenden verbringen durfte, wird mir unvergesslich bleiben.

Dankbar bin ich aber auch allen anderen IGÖ'lern, die dafür sorgten, dass immer eine freundschaftlich produktive Atmosphäre am Institut herrschte.

An dieser Stelle möchte ich aber auch die Gelegenheit wahrnehmen und meiner ganzen Familie danken ohne deren mentale und auch finanzielle Unterstützung und Hilfe ich niemals so weit gekommen wäre. Ich danke meinen Eltern, meiner Großmutter, Guido, Adele, Helmut und Ursel. Und natürlich Gritta und Carlo, ohne deren Zuneigung, Geduld und Freude diese Arbeit niemals gelungen wäre.

Curriculum Vitae:

Armin Meyer

- 20.07.1979 geboren in Ansbach
- 1989-1995 Besuch des Platen-Gymnasiums, Ansbach (Deutschland)
- 1995-1998 Besuch des Laurentius-Gymnasiums, Neuendettelsau (Deutschland)
- 1999-2006 Absolvierung des Diplomstudienganges der Geoökologie an der Universität Bayreuth (Deutschland)
- 2004-2005 Austauschstudent an der Universität Catania (Università di Catania, Facoltà di Matematica, Fisica e Scienze Naturali) (Italien)
- 2006-2010 wissenschaftliche Promotion am Institut für Grundwasserökologie, Helmholtz Zentrum München, unter der Betreuung von Prof. Dr R. Meckenstock und Dr. M. Elsner